

4 Andean magmatism

MIGUEL A. PARADA (coordinator), LEOPOLDO LÓPEZ-ESCOBAR, VERÓNICA OLIVEROS, FRANCISCO FUENTES, DIEGO MORATA, MAURICIO CALDERÓN, LUIS AGUIRRE, GILBERT FÉRAUD, FELIPE ESPINOZA, HUGO MORENO, OSCAR FIGUEROA, JORGE MUÑOZ BRAVO, ROSA TRONCOSO VÁSQUEZ & CHARLES R. STERN

Magmatism in the Chilean Andes has taken place since about 300 Ma as a consequence of protracted subduction, although with significant spatial and temporal variations due to changes in ocean-floor geodynamics controlling distinct large-scale magmatic events. Early subduction along the Chilean segment of the Gondwana active margin took place during Late Palaeozoic times and generated typical arc magmatism and a subduction complex in the forearc environment. This tectonomagmatic regime was interrupted by mid-Permian contractional tectonics (collisional?) giving rise to a thickening of the crust that allowed deep crustal melt generation. Following this the entire Mesozoic history of the area became dominated by subduction-related extensional tectonics with mostly bimodal magmatism reflecting the involvement, to different degrees, of both crust and mantle as magma sources. Mesozoic volcanism and plutonism appear to have been independent of each other. Subsequent Cenozoic magmatism records changing geodynamic conditions from Palaeogene–early Neogene extension to late Neogene compression. The Neogene magmatic episodes are interpreted as an indirect consequence of oceanic ridge subduction: the Juan Fernández Ridge along the north-central Chilean margin, and the Chile Ridge along the southernmost Chilean border. Modern volcanism is also influenced by these ridge subductions, either by generating gaps in the Quaternary volcanic chain, or adakitic volcanism derived from slab melting.

Despite the essentially tectonic control outlined above, this chapter is subdivided geographically into four Andean segments, each of which exhibits distinct magmatic features. These segments are: 18–28°S, 28–38°S, 40–47°S and 47–55°S. The exception to this approach is the section on Quaternary volcanism, which is treated as a whole and acts as an introduction to Chapter 5, which deals with recent Chilean volcanism and associated hazards. The amount of information available for each segment, as well as for the Quaternary volcanism, is quite variable and has been obtained mainly during the last fifteen years. Consequently, the inferences presented here are supported by information of different weight and reliability. We do not attempt to produce an exhaustive description of the magmatic rocks of the Chilean Andes: emphasis is put on those aspects and units where available information is most relevant to the understanding of the magmatic evolution.

Magmatism in northern Chile (18–28°S): the Jurassic extensional volcanism of La Negra Formation (V.O., L.A. & G.F.)

La Negra Formation (and its stratigraphic equivalents, the Oficina Viz and Camaraca formations near Iquique and Arica

respectively) is a thick sequence of volcanic extrusive rocks which crops out in several locations for c.1000 km along the Coastal Cordillera of northern Chile (Fig. 4.1). The volcanic rocks from this unit, together with huge plutons and other, smaller intrusive bodies, are interpreted as representing magmatic arc activity in the first stages of the Andean cycle (Suárez *et al.* 1985; Dallmeyer *et al.* 1996; Scheuber & González 1999). Near the type locality of La Negra Formation (Quebrada La Negra south of Antofagasta), the volcanic pile reaches 10 km in thickness and rocks belonging to this unit are found up to 1200 m above sea level. Although many faults cross the volcanic sequence it is unlikely that its thickness could be the result of tectonic events (Buchelt & Tellez 1988). Sequences up to 4 km thick crop out in the Coastal Cordillera (e.g. south of Antofagasta) where they consist of lava flows, pyroclastic rocks and minor volcanoclastic sediments, with thicknesses ranging from 5 to 40 m, lying conformably and dipping (20–55°) north, west or east depending on the area. In the outcrops which consist mainly of lava flows, thickness variations or lateral unconformities are rarely observed and eruptive centres have not been identified (Buchelt & Tellez 1988), suggesting fissure eruption as the most probably mechanism for their emplacement (Losert 1974; Rogers & Hawkesworth 1989). In some localities, interbedded shallow-level sediments with marine fossils, and pillow structures, indicate that the volcanic materials were emplaced into a shallow sea level environment (Tobar *et al.* 1968; Suárez *et al.* 1985, Muñoz *et al.* 1988b).

Based on their lithological characteristics, Hildebrandt *et al.* (2000) divided the Jurassic deposits of northern Chile into three segments: (1) 26°20'–25°20'S, basic lavas and pyroclastic rocks with intercalations of volcanoclastic terrestrial sediments, followed by ignimbrites and acid to intermediate lavas; (2) 25–21°40'S, intermediate lava flows with interbedded epiclastic sandstones; (3) 21–18°30'S, amphibole-bearing intermediate lava flows, followed by bimodal explosive volcanic rocks and intermediate to acid lava flows, subordinate ignimbrites, tuffs and volcanoclastic sediments, and finally intermediate composition lava flows (Kossler 1998).

With regard to stratigraphic ages, in the areas where the base of this unit is exposed (27–26° and 23°S) the volcanic rocks overlie Hettangian–Sinemurian sediments and are interbedded with red sedimentary rocks which contain marine fossils of Aalenian–Bajocian and Pliensbachian age (Suárez *et al.* 1985, Naranjo *et al.* 1982) or Sinemurian age (Buchelt & Tellez 1988). The top of the formation is mainly in contact with Lower Cretaceous units (24°S; Charrier & Muñoz 1994) except between 21°30' and 18°30'S, where the lavas from the Oficina Viz Formation are overlain by middle Bajocian sedimentary rocks (Thomas 1970). More explosive volcanism is recorded in this area until Callovian times and, south of Arica (18°30') there is evidence of andesitic lava flows of Oxfordian age (Kossler

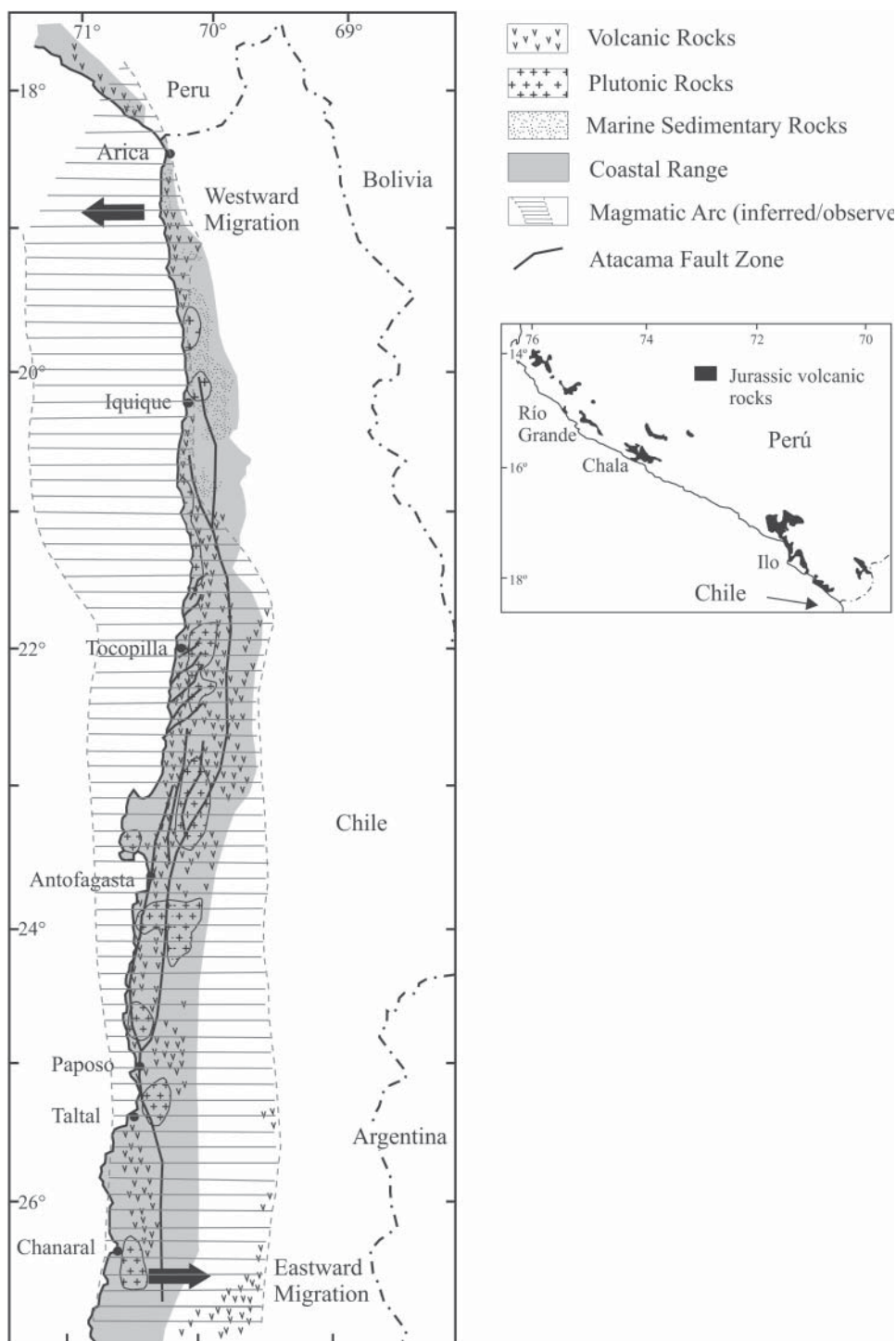


Fig. 4.1. Simplified map of northern Chile (left) and southern Peru (right) showing the distribution of Jurassic volcanic, plutonic and sedimentary rocks, and the approximate position of the volcanic arc (only for northern Chile). Insert shows distribution of Jurassic volcanic rocks of southern Peru. Modified after Romeuf *et al.* (1995) and Hildebrandt *et al.* (2000).

1998). The magmatic foci of the volcanic rocks are thought to have migrated eastward between 22°S and 27°S from Jurassic to Early Cretaceous times (Dallmeyer *et al.* 1996). In northernmost Chile, between 18°S and 21°S, a Late Jurassic transgression from the east of the backarc sea, coupled with the development of explosive volcanism to the west of the older volcanic arc (Oficina Viz Formation), indicates a westward migration of the arc (Fig. 4.1, Hildebrandt *et al.* 2000; Kramer *et al.* 2005).

The Coastal Batholith consists of numerous plutonic complexes, mainly hornblende–biotite gabbros, diorites, tonalites/granodiorites and minor granites, which intrude the Jurassic volcanic sequences. The emplacement of huge plutonic bodies was largely controlled by NS and NW–SE faults, with both sinistral strike-slip and normal dip-slip movements (Scheuber *et al.* 1995; González 1996; Dallmeyer *et al.* 1996). Long-lasting cooling of high T–low P metabasites related to plutonic emplacement during Early Jurassic times records a long

residence period of accreted magmatic intrusive rocks at mid-crustal levels and a high thermal gradient in the arc (Lucassen & Thirlwall 1998).

At least two generations of dykes and other small intrusive bodies can be identified (Dallmeyer *et al.* 1996; Scheuber & González 1999) and are associated with Cu–(Au) stratabound deposits hosted in Jurassic volcanic rocks. Some authors have interpreted these minor intrusive rocks as feeder conduits of the volcanism (Palacios & Definis 1981b; Pichowiak *et al.* 1990; Grocott *et al.* 1994; Espinoza *et al.* 1996).

Widespread low-grade alteration events affected both volcanic and, to a minor extent, plutonic rocks. The common mineral products of these events are epidote, chlorite, albite, white mica, clays, quartz, calcite, prehnite, pumpellyite, potassic feldspar, actinolite and zeolites. These secondary minerals occur mainly in the porous tops of the lava flows, breccia and tuff matrix, and as cement in sedimentary rocks (Losert 1974; Oliveros 2002). On a local scale, hydrothermal alteration events are associated with the formation of the Cu–Ag stratabound deposits.

Petrology

The products of the Jurassic volcanism in northern Chile are mainly porphyritic lavas with up to 20% phenocrysts. Volcanic breccias, tuffs and sedimentary rocks, and epiclastic sandstone lenses also occur but are less abundant. Basaltic andesites and andesites are by far the main compositional types, but basalts, dacites and rhyolites (ignimbrites) have been reported. At 23°30'S in the Mantos Blancos mining area, a sequence thought to be Jurassic consists mostly of intermediate and acid rocks such as andesites and rhyolites as along with dacitic dykes (Boric *et al.* 1990). Hillebrandt *et al.* (2000) proposed a bimodal magmatism based on the occurrence of acid volcanic rocks within the main intermediate lava flow succession at 25–21°S.

The lava flows have a basal zone with aphanitic texture and flattened amygdaloids, a more massive central part where phenocrysts are often large, and an upper part which is brecciated and highly amygdaloidal. Commonly, the contact surface with the overlying flow is glassy, very oxidized, and contains oriented amygdaloids or flux textures. Epiclastic sandstone lenses, from a few centimetres to more than one metre thick, often finely laminated, can be observed between flows. Plagioclase is the most frequent phenocryst with crystals commonly normally zoned (with An_{30} rims), reaching up to 1 cm in size and with a labradoritic composition, although bytownite is present in basalts and andesine–oligoclase in more silicic rocks (Buchelt & Tellez 1988; Rogers 1985). Ferromagnesian minerals are rare as phenocrysts and are commonly altered, augite and minor diopside being the commonest phases among them. Enstatite and olivine occur in basaltic andesites but they are completely altered to mafic phyllosilicates. Hornblende and rare Fe-rich biotite occur in andesites and dacites.

The groundmass comprises plagioclase microlites, clinopyroxene, magnetite or titanomagnetite, glass, sanidine and quartz in more silicic rocks. Microlites are not generally orientated except in the flow tops where fluid textures are frequent and an increase in glass content is observed. The explosive rocks such as breccias and tuffs have high lithic contents and their main mineral phases are Na- and K-feldspars.

Low-grade alteration minerals occur replacing primary crystal phases and glass in the groundmass. They are also found filling amygdaloids and veins. The degree of alteration varies from one area to another, albitization of Ca-plagioclase and total/partial chloritization of mafic minerals being the commonest expression. As a whole, alteration was pervasive making unaltered outcrops extremely rare, with the products of explosive volcanicity, the epiclastic sandstones, and the brecciated tops of lava flows normally being the most altered lithologies.

Geochemistry

The volcanic rocks of La Negra Formation are predominantly mantle-derived, with their major and trace element signatures showing a subduction pattern largely unaffected by crustal contamination (Rogers & Hawkesworth 1989; Kramer *et al.* 2005). Major element compositions show that they have mainly high-K to calcalkaline affinities (Buchelt & Tellez 1988; Lucassen & Franz 1994), although tholeiitic affinities have been found in rocks representing initial stages in the arc evolution (Palacios 1978; Pichowiak *et al.* 1990). Fe, Mg, Cr, Ni, V and Ti contents, as well as Eu anomalies, clearly indicate that fractional crystallization of plagioclase was the main process in the generation of these rocks from the parental magma, whereas clinopyroxene, olivine and titanomagnetite crystallization had only a secondary influence in the magma evolution except during the initial stages (Rogers 1985; Buchelt & Tellez 1988).

It should be pointed out that, in many samples, Ca, K or Na contents are highly variable over a small silica range (Rogers 1985). Large-scale alteration processes affecting the igneous rocks are interpreted as mobilizing Ca, K, Na, Fe, Rb and Cu (Losert 1974; Oliveros 2002). Thus, many of the observed variations in chemical composition are likely due to alteration events.

Rare earth element (REE) patterns are uniform for the flows and dykes and coincide with those for the plutonic rocks suggesting a similar source region (Lucassen & Franz 1994). Enrichment in light REE relative to chondrite composition, La/Yb normalized ratios of 3–5 and Eu negative anomalies are striking features. Their trace-element compositions are typical of subduction-related rocks with depletion in high-field-strength elements (HFSE) with respect to mid-ocean-ridge-basalts (MORB) and no significant variations in large-ion lithosphere elements (LILE). Contents of Sr, Rb, K, Ba and Th are much higher than in MORB but published data show large variations for samples from the same locality. High Th/Ta ratios and Ta/Nb > 1 are typical for these volcanic rocks together with depletion in Nb, Ti and P (Rogers 1985; Rogers & Hawkesworth 1989; Lucassen & Franz 1994; Pichowiak 1994; Kramer & Ehrlichmann, 1996).

Initial $^{87}\text{Sr}/^{86}\text{Sr}$ ratios for these volcanic rocks and dykes range from 0.7030 to 0.7040 and show no significant correlation with differentiation degree or stratigraphical position. ϵNd values range between 0.512850 and 0.512950, so that the samples plot on the mantle array near the depleted mantle field (Rogers & Hawkesworth 1989; Pichowiak 1994; Lucassen & Thirlwall 1998). Pb isotopic contents show only small variations, with most being in the following ranges: $^{206}\text{Pb}/^{204}\text{Pb}$, 17.96–18.42; $^{207}\text{Pb}/^{204}\text{Pb}$, 15.55–15.63; $^{208}\text{Pb}/^{204}\text{Pb}$, 37.99–39.73. They plot closer to average Pacific MORB than to average Palaeozoic crust. Isotopic compositions for volcanic rocks, dykes and some plutons are reasonably uniform and reflect a common source. Assimilation of Palaeozoic crust is unlikely as Sr–Nd–Pb isotopic compositions clearly indicate a mantle source (Lucassen *et al.* 2002).

Geochronology

Geochronological age data are scarce for the volcanic rocks, but the ages of the plutonic rocks and dykes, as well as sinistral shear zones associated with the Atacama Fault Zone, are well documented (Table 4.1, Fig. 4.2). Rb–Sr ages from the volcanic rocks are known from three localities, with all rocks having similar chemical compositions and trace element trends. Rogers & Hawkesworth (1989) obtained a whole-rock isochron of 186.5 ± 13.6 Ma for a thick succession of lava flows along an east–west profile at 22°S; Venegas *et al.* (1991) reported a Rb–Sr ‘errorchron’ age of 173 ± 19 Ma for andesitic lava flows from a copper deposit in the Michilla mining area; and finally Pichowiak (1994) obtained a whole-rock isochron of

Table 4.1. Radiometric age data for volcanic rocks of La Negra, Camaraca and Chala formations, intrusives from coastal batholith and dykes intruding both

Region	Location		Rock type	Material	Method	Age (Ma)	Reference
	Lat.	Long.					
Peru	14°58'S	75°27,0'W	Lava flow	Whole rock	K-Ar	164 ± 4	Aguirre 1988
	15°51,5'S	74°14,8'W	Lava flow	Whole rock	⁴⁰ Ar/ ³⁹ Ar	177.1 ± 2.2	Roperch & Carlier 1992
	15°51,5'S	74°09,8'W	Dyke	Whole rock	⁴⁰ Ar/ ³⁹ Ar	157.3 ± 2.2	Roperch & Carlier 1992
	15°51,8'S	74°14,9'W	Lava flow	Plagioclase	⁴⁰ Ar/ ³⁹ Ar	165.8 ± 0.5	Romeuf <i>et al.</i> 1995
Arica	18°01,0'S	70°50,0'W (approx.)	Dyke	Plagioclase	⁴⁰ Ar/ ³⁹ Ar	157.2 ± 0.4	Romeuf <i>et al.</i> 1995
	18°46,0'S	70°21,0'W	Lava flow	Whole rock	K-Ar (isochron)	157 ± 4	Palmer <i>et al.</i> 1980
	18°37,0'S	70°16,0'W (approx.)	Intrusive	Biotite	K-Ar	165 ± 5	García <i>et al.</i> 2004
	18°51,0'S	70°10,1'W (approx.)	Intrusive	Biotite	K-Ar	164 ± 4	García <i>et al.</i> 2004
Tocopilla	18°28,7'S	70°19,5'W	Lava flow	Plagioclase	⁴⁰ Ar/ ³⁹ Ar	157.9 ± 0.8	Oliveros <i>et al.</i> 2004
	18°32,7'S	70°19,5'W	Lava flow	Plagioclase	⁴⁰ Ar/ ³⁹ Ar	159.4 ± 0.6	Oliveros <i>et al.</i> 2004
	22°21,1'S	70°15,3'W	Lava flow	Whole rock	Rb-Sr	186.5 ± 13.6	Rogers & Hawkesworth 1989
	22°27,5'S	70°14,5'W (approx.)	Intrusive	Whole rock	Rb-Sr	158.3 ± 5.8	Rogers & Hawkesworth 1989
	22°04,5'S	70°07,5'W (approx.)	Intrusive	Whole rock	Rb-Sr	154.7 ± 13.4	Rogers & Hawkesworth 1989
	22°09,8'S	70°13,0'W	Small intrusive	Plagioclase	K-Ar	168 ± 5	Maksaev <i>et al.</i> 1988a
	22°28,0'S	70°14,0'W (approx.)	Intrusive	Biotite	⁴⁰ Ar/ ³⁹ Ar	158.8 ± 0.7	Maksaev <i>et al.</i> 1988a
	22°40,0'S	70°10,0'W (approx.)	Intrusive	Biotite	⁴⁰ Ar/ ³⁹ Ar	159.9 ± 0.7	Maksaev <i>et al.</i> 1988a
	23°14,7'S	70°18,8'W	Dyke	Hornblende	⁴⁰ Ar/ ³⁹ Ar	148.5 ± 1.0	Maksaev 1990
	22°20,7'S	70°14,8'W	Lava flow	Plagioclase	⁴⁰ Ar/ ³⁹ Ar	161.6 ± 1.2	Oliveros <i>et al.</i> 2004
	22°08,7'S	70°13,1'W	Lava flow	Plagioclase	⁴⁰ Ar/ ³⁹ Ar	164.9 ± 1.7	Oliveros <i>et al.</i> 2004
	22°40,2'S	70°09,8'W (approx.)	Small intrusive	Whole rock	K-Ar	154 ± 8	Astudillo 1984
Michilla	22°40,2'S	70°09,8'W (approx.)	Lava flows	Whole rock	Rb-Sr	173 ± 19	Venegas <i>et al.</i> 1991
	22°40,2'S	70°09,8'W (approx.)	Small intrusive	Whole rock	K-Ar	146 ± 13	Venegas <i>et al.</i> 1991
	22°40,2'S	70°09,8'W (approx.)	Dyke	Hornblende	⁴⁰ Ar/ ³⁹ Ar	112.0 ± 4.0	Venegas <i>et al.</i> 1991
	23°24,2'S	70°05,0'W (approx.)	Intrusive	Biotite	K-Ar	147 ± 4	Chávez 1985
Mantos	23°24,2'S	70°05,5'W (approx.)	Intrusive	Biotite	K-Ar	147 ± 1	Chávez 1985
Blancos	23°25,2'S	70°35,3'W (approx.)	Intrusive	Whole rock	Rb-Sr	200 ± 10	Díaz <i>et al.</i> 1985
Antofagasta-Mejillones	23°25,0'S	70°35,0'W (approx.)	Intrusive	Zircon	U-Pb	196 ± 4	Damm <i>et al.</i> 1986
	23°28,0'S	70°34,0'S (approx.)	Intrusive	Zircon	U-Pb	191 ± 6	Damm <i>et al.</i> 1986
	23°14,1'S	70°17,5'W	Small intrusive	Hornblende	⁴⁰ Ar/ ³⁹ Ar	137.0 ± 2.2	Maksaev 1990
	24°10,1'S	70°30,1'W (approx.)	Lava fl + intrusive	Whole rock	Rb-Sr	183.0 ± 3.5	Pichowiak 1994
	23°06,5'S	70°30,1'W	Intrusive	Hornblende	K-Ar	169.0 ± 6.0	Scheuber & González 1999
	23°14,1'S	70°16,0'W	Intrusive	Biotite	K-Ar	152.0 ± 3.0	Scheuber & González 1999
	23°14,1'S	70°18,3'W	Intrusive	Hornblende	K-Ar	140.0 ± 5.0	Scheuber & González 1999
	23°14,1'S	70°18,3'W	Intrusive	Biotite	K-Ar	141.0 ± 3.0	Scheuber & González 1999
	23°12,8'S	70°17,1'W	Dyke	Hornblende	K-Ar	147.0 ± 6.0	Scheuber & González 1999
	23°41,8'S	70°23,8'W	Lava flow	Plagioclase	⁴⁰ Ar/ ³⁹ Ar	153.0 ± 2.0	Oliveros <i>et al.</i> 2004
	23°42,3'S	70°23,9'W	Lava flow	Plagioclase	⁴⁰ Ar/ ³⁹ Ar	151.0 ± 1.0	Oliveros <i>et al.</i> 2004
	23°43,0'S	70°22,8'W	Lava flow	Plagioclase	⁴⁰ Ar/ ³⁹ Ar	150.9 ± 1.8	Oliveros <i>et al.</i> 2004
Paposo	24°05,0'S	70°10,3'W	Intrusive	Biotite	K-Ar	192 ± 5	Hervé & Marinovic 1989
	24°01,2'S	70°14,0'W	Intrusive	Whole rock	Rb-Sr	170 ± 28	Hervé & Marinovic 1989
	24°29,6'S	70°33,7'W	Intrusive	Biotite	K-Ar	160 ± 4	Hervé & Marinovic 1989
	24°24,4'S	70°32,0'W	Intrusive	Biotite	K-Ar	157 ± 4	Hervé & Marinovic 1989
	24°17,9'S	70°21,5'W	Intrusive	Biotite	K-Ar	149 ± 4	Hervé & Marinovic 1989
	24°07,5'S	70°21,4'W	Intrusive	Whole rock	Rb-Sr	145 ± 10	Hervé & Marinovic 1989
	24°38,8'S	70°16,8'W	Intrusive	Biotite	K-Ar	133 ± 3	Hervé & Marinovic 1989
	24°56,6'S	70°25,2'W	Intrusive	Hornblende	K-Ar	131 ± 5	Hervé & Marinovic 1989
	24°58,2'S	70°25,5'W	Intrusive	Biotite	K-Ar	129 ± 3	Hervé & Marinovic 1989
	24°52,4'S	70°22,9'W	Intrusive	Biotite	K-Ar	128 ± 3	Hervé & Marinovic 1989
	24°38,7'S	70°19,5'W	Intrusive	Whole rock	Rb-Sr	131 ± 1	Hervé & Marinovic 1989
	24°52,8'S	70°03,1'W	Intrusive	Biotite	K-Ar	108 ± 4	Hervé & Marinovic 1989
	24°04,9'S	70°03,1'W	Intrusive	Biotite	K-Ar	107 ± 3	Hervé & Marinovic 1989
	24°06,2'S	69°58,0'W	Intrusive	Biotite	K-Ar	100 ± 3	Hervé & Marinovic 1989
	24°04,5'S	69°58,6'W	Intrusive	Biotite	K-Ar	98 ± 3	Hervé & Marinovic 1989
	24°23,3'S	70°26,9'W	Dyke	Biotite	K-Ar	131 ± 5	Hervé & Marinovic 1989
	24°44,8'S	70°28,9'W	Dyke	Biotite	K-Ar	122 ± 3	Hervé & Marinovic 1989
	24°58,4'S	70°24,9'W	Dyke	Whole rock	K-Ar	123 ± 4	Hervé & Marinovic 1989
	23°40,7'S	70°21,8'W	Dyke	Plagioclase	K-Ar	110 ± 4	Hervé & Marinovic 1989
	24°57,7'S	70°28,7'W	Dyke	Whole rock	Rb-Sr	131 ± 6	Hervé & Marinovic 1989
	25°05,5'S	70°29,1'W	Dyke	Plagioclase	K-Ar	139 ± 5	Maksaev 1990
	24°11,5'S	70°20,6'W	Intrusive	Hornblende	⁴⁰ Ar/ ³⁹ Ar	138.0 ± 1.7	Scheuber <i>et al.</i> 1995
	24°38,3'S	70°20,6'W	Intrusive	Hornblende	⁴⁰ Ar/ ³⁹ Ar	152.9 ± 2.4	Scheuber <i>et al.</i> 1995
	23°49,0'S	70°29,0'W	Intrusive	WR, pl, hb.	Sm-Nd	160 ± 23	Lucassen & Thirlwall 1998
	25°28,1'S	70°19,8'W	Intrusive	Hornblende	K-Ar	133 ± 5	Scheuber & González 1999
	25°31,3'S	70°19,3'W	Intrusive	Hornblende	K-Ar	136 ± 5	Scheuber & González 1999

Table 4.1. (Continued)

Region	Location		Rock type	Material	Method	Age (Ma)	Reference
	Lat.	Long.					
Taltal- Chañaral	25°38,2'S	70°33,5'W	Dyke	Hornblende	K-Ar	155 ± 5	Scheuber & González 1999
	25°38,8'S	70°31,7'W	Intrusive	Hornblende	K-Ar	164 ± 6	Scheuber & González 1999
	25°44,0'S	70°33,4'W	Intrusive	Hornblende	K-Ar	172 ± 8	Scheuber & González 1999
	27°20,4'S	70°54,9'W	Intrusive	Hornblende	⁴⁰ Ar/ ³⁹ Ar	192.4 ± 0.8	Dallmeyer <i>et al.</i> 1996
	27°07,1'S	70°55,2'W	Intrusive	Hornblende	⁴⁰ Ar/ ³⁹ Ar	188.8 ± 1.2	Dallmeyer <i>et al.</i> 1996
	26°52,7'S	70°44,2'W	Intrusive	Hornblende	⁴⁰ Ar/ ³⁹ Ar	193.4 ± 0.7	Dallmeyer <i>et al.</i> 1996
	26°48,5'S	70°47,0'W	Intrusive	Hornblende	⁴⁰ Ar/ ³⁹ Ar	192.7 ± 0.8	Dallmeyer <i>et al.</i> 1996
	26°52,3'S	70°39,4'W	Intrusive	Hornblende	⁴⁰ Ar/ ³⁹ Ar	190.2 ± 0.6	Dallmeyer <i>et al.</i> 1996
	26°33,4'S	70°35,5'W	Intrusive	Hornblende	⁴⁰ Ar/ ³⁹ Ar	190.2 ± 1.4	Dallmeyer <i>et al.</i> 1996
	26°30,2'S	70°41,9'W	Intrusive	Hornblende	⁴⁰ Ar/ ³⁹ Ar	199.3 ± 0.6	Dallmeyer <i>et al.</i> 1996
	26°33,0'S	70°27,0'W	Intrusive	Hornblende	⁴⁰ Ar/ ³⁹ Ar	153.0 ± 1.0	Dallmeyer <i>et al.</i> 1996
	27°21,8'S	70°36,0'W	Intrusive	Hornblende	⁴⁰ Ar/ ³⁹ Ar	138.4 ± 0.9	Dallmeyer <i>et al.</i> 1996
	26°48,0'S	70°27,0'W	Intrusive	Hornblende	⁴⁰ Ar/ ³⁹ Ar	140.1 ± 0.8	Dallmeyer <i>et al.</i> 1996
	26°35,1'S	70°16,0'W	Intrusive	Hornblende	⁴⁰ Ar/ ³⁹ Ar	129.2 ± 1.5	Dallmeyer <i>et al.</i> 1996
	26°55,6'S	70°22,2'W	Intrusive	Hornblende	⁴⁰ Ar/ ³⁹ Ar	127.2 ± 1.0	Dallmeyer <i>et al.</i> 1996
	26°50,4'S	70°21,6'W	Intrusive	Hornblende	⁴⁰ Ar/ ³⁹ Ar	107.1 ± 0.5	Dallmeyer <i>et al.</i> 1996
	26°33,8'S	70°39,4'W	Dyke	Whole rock	⁴⁰ Ar/ ³⁹ Ar	155.5 ± 0.6	Dallmeyer <i>et al.</i> 1996
	26°22,4'S	70°26,5'W	Dyke	Whole rock	⁴⁰ Ar/ ³⁹ Ar	153.7 ± 0.7	Dallmeyer <i>et al.</i> 1996

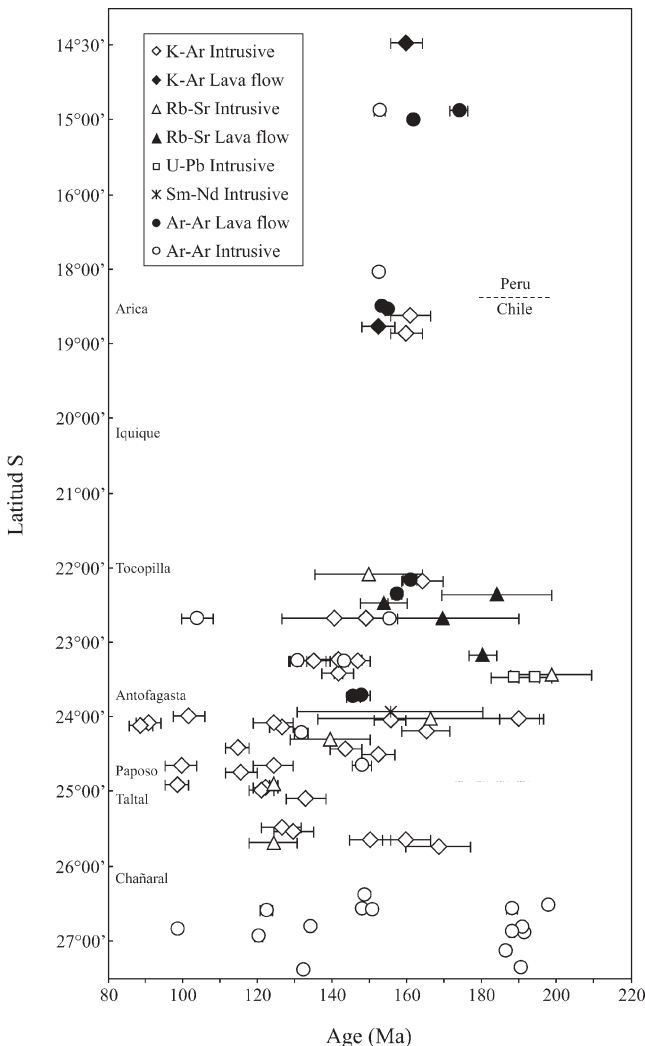
P, ⁴⁰Ar/³⁹Ar plateau age

Fig. 4.2. Radiometric ages for plutonic and volcanic rocks between 14°30'S and 26°S. References are given in Table 4.1.

186 ± 3.5 Ma for a suite of lavas from the La Negra Formation and plutonic rocks of the Coloso Gabbro Complex at around 24°S. Two K–Ar ages of 164 and 157 Ma are known for whole-rock samples from lava flows between latitudes 14°30'S and 19°S (Table 4.1, Fig. 4.2). ⁴⁰Ar/³⁹Ar plateau ages (2 sigma) have been obtained from unaltered plagioclase in Jurassic volcanic rocks from several localities with the following results: 157.9 ± 0.8 and 159.4 ± 0.6 Ma at 18°30'S (Arica), 161.2 ± 1.5 and 164.9 ± 1.7 Ma at 22°S (Tocopilla), and 150.9 ± 1.8 to 152.9 ± 2.02 Ma at 23°40'S (Antofagasta). These ages are significantly younger than those obtained using Rb–Sr methods, consistent with Jurassic volcanic activity lasting for only a short time (Oliveros *et al.* 2004).

Plutonic rocks belonging to the Coastal Batholith have been dated by Rb–Sr, ⁴⁰Ar/³⁹Ar, K–Ar and Sm–Nd methods. The ages obtained indicate that they were emplaced between *c.* 98 and 199 Ma (Table 4.1, Fig. 4.2). Rather than there having been continuous magmatic activity, pulses of plutonic intrusions appear to have occurred. Dallmeyer *et al.* (1996) obtained ⁴⁰Ar/³⁹Ar plateau and isochron correlation ages in hornblende of *c.* 199.3 ± 0.6 to 188.8 ± 1.2 Ma, 153.0 ± 1.0, 140.1 ± 0.8, 129.2 ± 1.0, 127.2 ± 1.0 and 107.1 ± 0.5 Ma for different plutonic complexes at 26–27°30'S, which suggests a magmatic gap between *c.* 190 and 150 Ma. Hervé & Marinovic (1989) obtained Rb–Sr and K–Ar ages ranging from 192 to 98 Ma for several plutonic complexes between 24 and 25°S. These ages indicate that successive pulses of magmatic activity occurred from Early Jurassic to Early Cretaceous times. These pulses record an eastward migration for the plutonic rocks. Several plutonic bodies have been dated between 23 and 25°S yielding ages of 172 ± 8 Ma to 164 ± 6 Ma, 147 ± 4 Ma, 140 ± 5 Ma, 136 ± 5 Ma (K–Ar; Chávez 1985, Scheuber & González 1999), 160 ± 23 Ma (Sm–Nd; Lucassen & Thirlwall 1998) and 137.0 ± 2.2 Ma and 138.0 ± 1.7 Ma (⁴⁰Ar/³⁹Ar plateau ages; Maksiyev 1990; Scheuber & González 1999). Rb–Sr ages of 155 ± 13 Ma and 158 ± 6 Ma and ⁴⁰Ar/³⁹Ar plateau ages of 159.9 ± 0.7 Ma and 158.8 ± 0.7 Ma have been reported for plutonic rocks between 22 and 22°30'S (Rogers & Hawkesworth 1989, Maksiyev 1990). South of Arica (19°S) two K–Ar biotite samples from plutonic rocks have yielded ages of 164 ± 5 Ma and 164 ± 4 Ma (García *et al.* 2004). Finally, dykes intruding both plutonic and volcanic rocks have been dated by various

methods (K–Ar, $^{40}\text{Ar}/^{39}\text{Ar}$, Rb–Sr) and have yielded ages between *c.* 155 and 120 Ma (Table 4.1, Fig. 4.2).

Concerning the alteration of these rocks, recent $^{40}\text{Ar}/^{39}\text{Ar}$ analyses on secondary mineral phases such as sericite, K-feldspar and actinolite yielded plateau ages at *c.* 105, 138, 140, 145, 150 and 156 Ma, in five localities between 18°30'S and 24°S. By comparison with volcanic and plutonic events, most of these ages appear valid, because (1) they are mostly duplicated on different rock samples, and (2) they often correspond to precisely dated magmatic events (Oliveros *et al.* 2004). Whether these alteration events are related to burial metamorphism or to hydrothermal activity generated by the intrusion of large plutons is not always clear.

Tectonic setting

The magmatic activity described is believed to have depended strongly on the rate of subduction and type of convergence. High-angle oblique subduction is thought to have been responsible for an extensional–transtensional tectonic regime along the whole arc (Dallmeyer *et al.* 1996; Taylor *et al.* 1998; Scheuber & González 1999; Grocott & Taylor 2002); this agrees with plate configurations for South America during the Mesozoic era (Zonenshayn *et al.* 1984; Jaillard *et al.* 1990).

The volcanic rocks of La Negra Formation were emplaced in an intra-arc basin setting related to an oblique convergent margin. They are thought to have extruded either during (1) a sinistral relative movement between the forearc sliver and the backarc when the forearc moved with the same sense as the convergence obliquity (Fig. 4.3a; Scheuber & González 1999); and/or (2) in an extensional fault system linked to a retreating subduction boundary (Fig. 4.3b; Grocott *et al.* 1994; Taylor *et al.* 1998). The fact that the thick volcanic sequence was entirely deposited close to sea level implies that subsidence (extension) and crustal growth were well balanced (Lucassen & Franz 1994). Tilting of the volcanic sequence is likely to have taken place during arc-normal extension (between *c.* 150 and 160 Ma; Fig. 4.3a) after the deposition of the whole sequence

and prior to Kimmeridge times as suggested by angular unconformity with the overlying sedimentary rocks of this age (Scheuber *et al.* 1995; Scheuber & González 1999).

A trench-linked structure in the arc also controlled the emplacement of plutons in different episodes from Jurassic to Early Cretaceous times as recorded by the brittle and ductile deformation that affected these rocks (Dallmeyer *et al.* 1996; González 1996; Scheuber & González 1999). Early Jurassic (or older) plutons were emplaced at mid-crustal levels and some had very slow cooling rates (50 Ma for K–Ar and Sm–Nd systems) while the Middle Jurassic to Early Cretaceous intrusions would have been emplaced and cooled at shallower levels. A late phase of cooling and later uplift of the Coastal Cordillera in the region started around 120 Ma (Maksaev 1990, 2000; Scheuber *et al.* 1994), coincident with the beginning of major sinistral strike-slip motion along the 1000-km-long Atacama Fault Zone at *c.* 125 Ma.

Crustal block rotations, partly affecting the Mesozoic igneous rocks, took place in post-Early Cretaceous time (Taylor *et al.* 1998) and/or during the Incaic orogenic event (Late Eocene–Early Oligocene) (Arriagada *et al.* 2003). Since Neogene times, the whole forearc has behaved as one tectonic block (Arriagada *et al.* 2003).

The Jurassic volcanosedimentary units of southern Peru: equivalents of La Negra Formation

In southern coastal Peru, between latitudes 14°S and 18°S, volcanic rocks of Jurassic age directly correlated with La Negra Formation are well displayed (Fig. 4.1). The main successions present there correspond to the Río Grande and the Chala formations.

In its type locality, the Río Grande Formation consists of two units separated by a slight angular unconformity. The lower unit, *c.* 500 m thick, consists of red agglomerates, conglomerates and fine- to medium-grained red volcanogenic sandstones accompanied by brecciated silicic lava flows, silicic ignimbrites, fossiliferous limestones, calcareous sandstones and greenish tuffs. The upper unit, *c.* 2000 m thick, largely consists

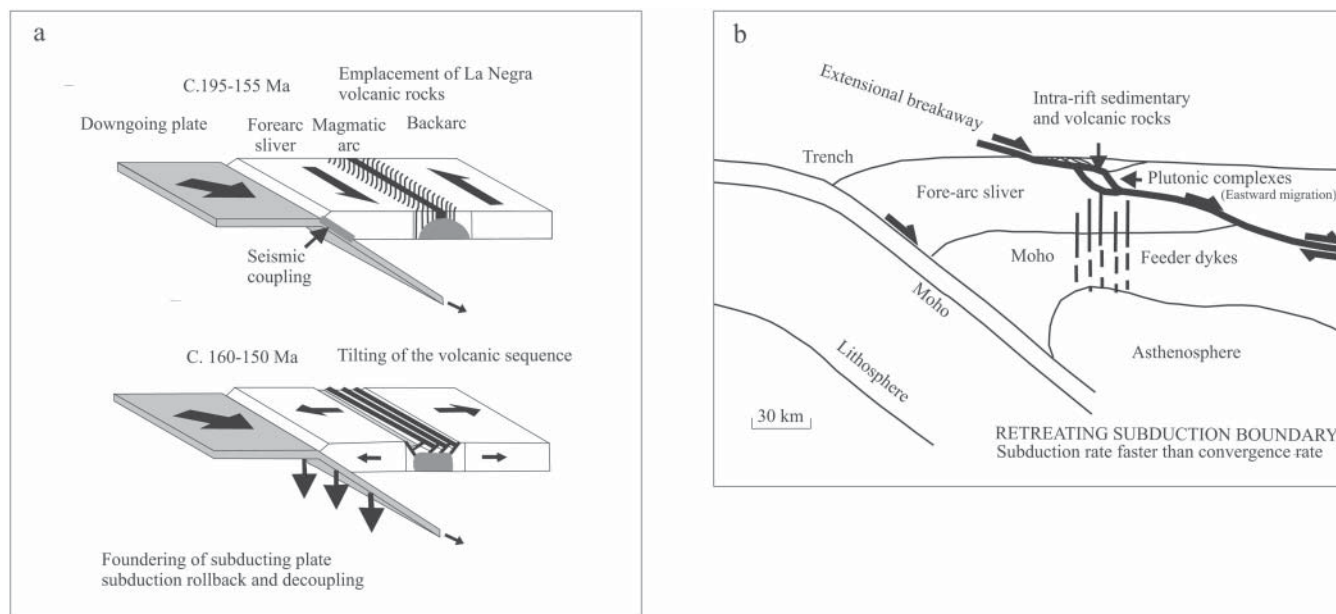


Fig. 4.3. Models for the Jurassic tectonic evolution of the Andean arc. (a) Sinistral movement in a high-stress regime, volcanism and deep-seated plutons at *c.* 195–155 Ma, followed by shallow level plutonism without volcanism, magmatic crustal growth and arc-normal extension due to low convergence rate in a low-stress subduction regime at *c.* 160–150 Ma. Modified after Scheuber & González (1999). (b) In a retreating subduction boundary, a breakaway zone is generated which acts as the locus of magma ascent. Changes in convergence rate would favour either volcanism or plutonism, leading to an eastward migration of plutonic complexes. Modified after Grocott *et al.* (1994).

of highly porphyritic, partly pillowed, basaltic andesites composed of large labradoritic plagioclase phenocrysts, augite, olivine ghosts, and iron–titanium oxides. Minor intercalations of reddish conglomerates and brick-red, cross-laminated, volcanogenic sandstones exist (Aguirre & Offler 1985; Aguirre 1988). The whole succession was affected by very low-grade metamorphism of the hydrothermal-burial type. A Middle Jurassic (Dogger) age was assigned to the Río Grande Formation by Ruegg (1956, 1961) based on fossil fauna and flora representing the Aalenian–Bajocian interval (175–168 Ma; 2004 Geologic Time Scale, ISC). A K–Ar (whole-rock) analysis on a weakly altered sample from the central part of a lava flow of the Río Grande upper unit gave an age of 164 ± 4 Ma which corresponds to the Bathonian–Callovian boundary, and a $^{87}\text{Sr}/^{86}\text{Sr}$ ratio of 0.70516 (at 160 Ma BP) (Aguirre 1988).

The Chala Formation at its type locality ($15^\circ 52'\text{S}$), is characterized by a basal sedimentary level consisting of sandstones and lutites and a thick upper section, *c.* 1500 m, made up of reddish-grey, strongly porphyritic flows of basalts and andesites with centimetric phenocrysts of labradoritic plagioclase plus augite and altered olivine. The formation is locally intruded by sills and porphyritic dykes petrographically akin to the flows (Romeuf 1994). As in the case of the Río Grande Formation, the rocks of the Chala Formation show a widespread metamorphic alteration. Roperch & Carlier (1992) obtained $^{40}\text{Ar}/^{39}\text{Ar}$ ages (whole rock) of 177.0 ± 2.0 Ma for a Chala basaltic flow and of 157.0 ± 1.0 Ma for two basaltic flows of the Chala Formation. Romeuf (1994) used $^{40}\text{Ar}/^{39}\text{Ar}$ on plagioclase bulk samples to date a basaltic andesite flow from the Chala Formation and a porphyritic basaltic dyke cross-cutting rocks of the Guaneros Formation, an equivalent of the Chala Formation. A high-temperature mini-plateau age of 165.8 ± 0.9 Ma (14 steps corresponding to 51% of ^{39}Ar released) was obtained on the lava flow whereas the dyke gave a high-temperature mini-plateau age of 157.2 ± 0.9 Ma (12 steps, 48% of ^{39}Ar released; Romeuf *et al.* 1995). These ages are probably valid when compared to the corresponding $^{37}\text{Ar}/^{39}\text{Ar}_{\text{Ca}}$ ratios, and are close to those obtained in northern Chile (Oliveros *et al.* 2004).

The chemical composition of the Río Grande and Chala lavas correspond to the K-rich calcalkaline series typical of volcanic arcs emplaced at a continental margin. Their REE patterns show a strong light REE (LREE) enrichment compared with heavy REEC to (HREE) (La/Yb chondrite-normalized ratios of 5.6–8.3), low TiO_2 (<1%) and Nb (5–6 ppm) and high Al_2O_3 (16.8–17.6) and Zr (150–180 ppm) contents. Compared with lavas from La Negra Formation they are poorer in MnO, TiO_2 , Y, Zr, V, Sm, Nd, Yb, Hf, Ta, Th and Sc, richer in K_2O , MgO , Al_2O_3 , Sr and Ba, and similar in FeO content (Romeuf 1994; Romeuf *et al.* 1995).

The presence of calcalkaline volcanism of arc type and Middle Jurassic age in southern coastal Peru has been interpreted as the result of WNW–ESE orientated subduction of the Phoenix oceanic plate along this segment of the South American Pacific margin at that time (Romeuf *et al.* 1995).

Concluding remarks

The thick, subaerial to shallow marine volcanic and sedimentary sequences in the Coastal Cordillera of northern Chile define intra-arc basins that existed during Jurassic–Early Cretaceous times. The change from marine conditions in some localities, e.g. southern Peru (Río Grande Formation volcanic and marine sedimentary rocks of the Aalenian–Bajocian interval) and northernmost Chile (e.g. volcanic and marine sedimentary rocks of Callovian age at Arica and Iquique), contrasting with the continental conditions in some other localities (e.g. Tocopilla and Quebrada La Negra in the Antofagasta area), suggests the existence of passages connecting the

backarc basin and the forearc sea, breaking through the arc barrier (Hildebrandt *et al.* 2000).

Volcanic and sedimentary successions, together with huge plutons and other, smaller intrusive bodies contributed to crustal growth despite the extensional–transtensional regime and the thinning of the continental crust that dominated during Jurassic–Early Cretaceous arc construction (Taylor *et al.* 1998). This extensional–transtensional tectonic setting is reflected in the geochemistry which indicates little or no crustal contamination.

The hypothesis of long-lasting, broadly continuous Jurassic to Early Cretaceous magmatism in northern Chile involving extension, large-scale crustal thinning, basin subsidence, and extrusion of huge volumes of magma covering large segments of the continental margin, seems to be strongly supported by the geological record. The existence of discrete pulses of magmatic activity, however, cannot be dismissed as it is implied by the $^{40}\text{Ar}/^{39}\text{Ar}$ ages on both volcanic and plutonic rocks.

Magmatism in central Chile (28–38°S) (M.A.P. & F.F.)

Magmatism within the central segment of the Chilean Pacific margin involved numerous and discrete intensive episodes of intrusion and volcanic emissions from Late Palaeozoic to Holocene times that gave rise to the north–south trending belts that occupy about 90% of the Coastal Cordillera and High Andes. The onset and duration of the magmatic episodes are poorly constrained and have been estimated by a limited number of reliable age determinations. On a broad scale, pre-Cenozoic magmatism took place during three main stages that started with a Carboniferous–Early Permian subduction regime along the western margin of Gondwana. This initial phase was followed by Late Permian–Early Jurassic period of arrested subduction associated with extensional tectonics, large-scale crustal partial melting (e.g. Kay *et al.* 1989; Parada *et al.* 1991; Martin *et al.* 1999) and production of only minor volumes of mantle-derived rocks. From Middle Jurassic to Early Cretaceous times, bimodal volcanism and calcalkaline plutonic activity, with progressively more mantle participation, took place along a rifted continental margin, generating an igneous belt about 1200 km long. After a period of magmatic quiescence that followed mid-Cretaceous contractional deformation (Mpodozis & Ramos 1989; see summary in Ramos & Aleman 2000), a new stage of extensional arc magmatism developed during the Oligocene–middle Miocene interval (Nyström *et al.* 2003). After this (i.e. post-20 Ma) arc magmatism progressively decreased in intensity, as a consequence of shallowing of the subducting slab (cf. Kay & Mpodozis 2002), and ended at about 5 Ma. The subduction of the Juan Fernández Ridge caused extreme shallowing of the oceanic slab beneath the continental margin of central Chile and the development of a modern volcanic gap between 27°S and 34°S . Today, active volcanoes are restricted to the High Andes, forming part of the northern segment of the Southern Volcanic Zone (SVZ), which extends from 33°S to 46°S .

One of the most striking features of the central Chilean Andes is the Meso-Cenozoic distribution of the plutonic belts characterized by an eastward decreasing age (Parada *et al.* 1988). The origin of this distribution remains poorly understood, although the lateral (westward) displacement of the continental margin due to successive plutonic–volcanic belt emplacement, analogous to oceanic spreading, has been invoked (Åberg *et al.* 1984). This ensialic spreading would explain the *c.* 100 km separating the pre-Middle Jurassic plutonic components of the Elqui–Limarí Batholith, in the High Andes, and the coeval plutonic rocks of the Coastal Batholith. Both batholiths and associated volcanic rocks are examined below.

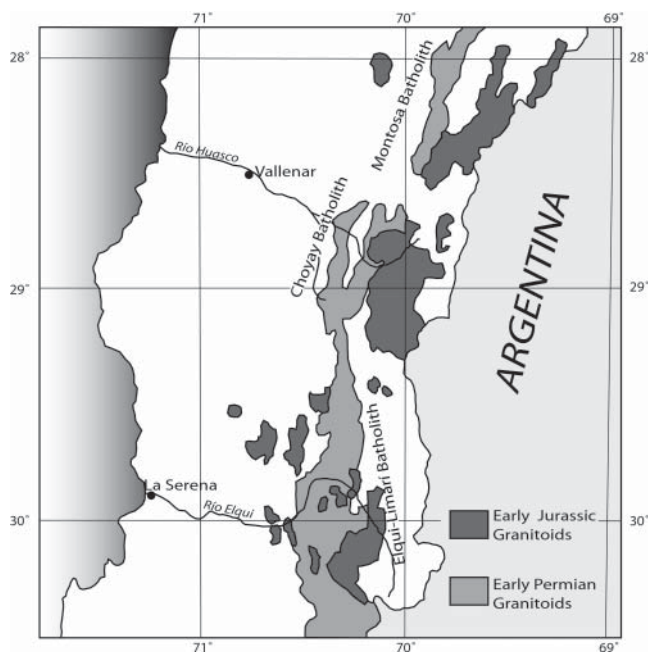


Fig. 4.4. Distribution of the High Andes Batholith between 28°S and 31°S.

The High Andes Batholith (28°–31°S)

The High Andes Batholith (HAB) extends from 28°S to 31°S along the Chilean Andes (Fig. 4.4) and continues to the south, along the Frontal Cordillera in the San Juan and Mendoza provinces of Argentina, to complete a length of about 800 km. In the Chilean Andes the HAB is represented by the Montosa, Choyay and Elqui–Limari intrusions (Mpodozis & Kay 1992). The batholith was assembled during three discrete events (Martin *et al.* 1999) represented by the Early Permian Elqui Complex, the Early Triassic El León–Chollay Complex and the Late Triassic–Early Jurassic Hacienda Vieja Complex (Parada *et al.* 1991). A mafic dyke swarm, hosted in all the complexes, is the last magmatic event of the HAB. The Early Permian event represents a subduction-related magmatism that followed the accretion of the Chilenia terrane in the Late Devonian to Early Carboniferous interval (Mpodozis & Kay 1992), whereas the other two events are post-orogenic to anorogenic developed during Early Mesozoic extension. The volcanic rocks associated with the HAB have been assembled within the Pastos Blancos Group, which includes two diachronous volcanic–sedimentary successions of Permian and Middle Triassic–Early Jurassic age, respectively. Compositionally, the volcanic rocks are similar to their plutonic counterpart.

Subduction-related Early Permian Elqui Complex

This complex occupies the western belt of the High Andes Batholith and comprises coarse-grained hornblende–biotite tonalites (Guanta unit) and two-mica granodiorites (Cochiguás unit). The Guanta tonalites, emplaced at a depth equivalent to a pressure of 4.5–5.0 kbar (Sial *et al.* 1999), exhibit foliated fabric and locally contain abundant mafic enclaves. A reliable U–Pb zircon age of 285.7 ± 1.5 Ma has been obtained in a Guanta tonalite sample A. Rb–Sr whole-rock isochron yielded an age of 256 ± 10 Ma for the Cochiguás unit some 180 km further south (Pankhurst *et al.* 1996).

The Guanta tonalites have *c.* 60% SiO₂ contents and exhibit the typical calcalkaline characteristics of arc plutons (Parada 1990). The Cochiguás granodiorites are slightly peraluminous and, unlike the Guanta tonalites, they exhibit steep HREE

patterns, small Eu anomalies and high La/Yb ratios, suggesting the presence of residual garnet in the source rocks (Mpodozis & Kay 1992). Both units are isotopically (Sr–Nd) radiogenic, with ϵ_{Nd} in the range of -3.1 to -5.8 and initial $^{87}\text{Sr}/^{86}\text{Sr}$ ratios between 0.70603 and 0.70965 indicating either a provenance from an enriched lithospheric mantle and crust or an origin by contamination of a depleted mantle by radiogenic crust (Mpodozis & Kay 1992). Because no magmatic event older than Late Carboniferous–Early Permian has been identified in central-north Chile, the existence of an enriched lithospheric mantle before the onset of the Elqui Complex plutonism is tenable.

This complex resulted from subduction beneath the continental margin of Gondwana after the docking of the Chilenia terrane during Devonian times (Ramos *et al.* 1986). The shift from the metaluminous Guanta unit to the peraluminous Cochiguás unit is explained by a mid-Permian plutonic thickening attributable to a contractional (collisional?) event (the San Rafael event of Polanski 1970; Azcuy & Caminos 1987; Llambías & Sato 1990), that allowed deep crustal melting and the formation of the Cochiguás intrusives.

Post-orogenic Early Triassic El León–Chollay Complex (ELCC)

Coarse-grained biotite granites and felsic porphyries of the ELCC intruded the Permian volcanic sequence of the Pastos Blancos Group and crop out along the axis and eastern flank of the Andes. U–Pb zircon ages of 249.7 ± 3.2 and 242.5 ± 1.5 Ma (Martin *et al.* 1999) indicate an Early Triassic plutonic event, partially coeval with the Cochiguás unit and the 267–247 Ma Colangüil Batholith (Llambías & Sato 1990) located further east in the Frontal Cordillera of Argentina (29–31°S), although an older biotite K–Ar age of 276 ± 4.0 Ma has also been obtained (Nasi *et al.* 1985). This complex includes typical calcalkaline metaluminous I-type granites, although S-type and A-type granites are also present. The REE patterns are commonly flat with large negative Eu anomalies consistent with a low-pressure, garnet-free source region (Mpodozis & Kay 1992). Like the Colangüil Batholith, this complex developed during the tectonic relaxation that followed the mid-Permian San Rafael deformational event.

Late Triassic–Early Jurassic bimodal intrusions

These intrusions represent the youngest event in the construction of the Elqui–Limari Batholith and include isolated bodies epizonally emplaced into the Elqui Complex. They comprise metaluminous to alkaline granites (A-type granites) and slightly peraluminous cordierite-bearing two-mica granodiorites and granites (S-type granitoids), that previously were assigned to the Monte Grande and Hacienda Vieja suites, respectively (Parada 1988). Los Colorados brick-red felsic porphyries and some plutons previously assigned to the El León unit (Mpodozis & Kay 1992) also belong to this intrusive complex. Small gabbro intrusions are also recognized, providing a bimodal character to the complex similar to that recognized in its volcanic counterpart, the youngest succession of the Pastos Blancos Group. The Hacienda Vieja bimodal intrusions were generated during an extensional regime, attributed to arrested subduction, which promoted partial melting and emplacement of crustal-derived and mantle-derived magmas.

K–Ar ages in biotite and muscovite of about 220 Ma and one imprecise Rb–Sr isochron age of 197 ± 5 Ma have been obtained from these rocks (Mpodozis & Kay 1992; Parada *et al.* 1981). The metaluminous and alkaline granites are high-SiO₂, low-CaO A-type granites, with moderately fractionated REE patterns and large negative Eu anomalies. On the contrary, the peraluminous granitoids have highly fractionated REE patterns with small or no Eu negative anomalies, suggesting a crustal source with residual garnet. Contrasting Sr–Nd isotopic features are recognized among both the A-type and S-type

components. A metaluminous sample has an initial $^{87}\text{Sr}/^{86}\text{Sr}$ ratio of 0.70692 and ϵNd of 0.0, whereas a peraluminous sample provided values of 0.71450 and -4 for the same isotopic parameters. Granitic and metapelitic source rocks have been invoked to explain the contrasting geochemical features between the A- and S-type granitoids, respectively (Parada *et al.* 1991).

Mafic dyke swarm

Mafic dykes (and minor felsic dykes) are widely distributed within the Elqui–Limarí Batholith, intruding both it and the overlying Triassic to Jurassic sedimentary cover successions. Mutual cross-cutting relationships with some Triassic–Early Jurassic granites are locally observed. The mafic dykes are basaltic (45–47% SiO_2) to andesitic (54–64% SiO_2) in composition and have high K_2O (shoshonitic affinity). In terms of Zr/TiO_2 and Nb/Y (Winchester & Floyd 1977), some lamprophyric dykes have alkaline affinities (Parada *et al.* 1991). The dyke swarm represents a protracted bimodal event precursor of the Mesozoic ensialic expansion. A similar bimodal dyke swarm has been recognized hosted in the Colangüil Batholith (Llambías & Sato 1990).

The Coastal Batholith and Mesozoic volcanic rocks between 28°S and 38°S

This segment of the Coastal Batholith is made up of four north–south trending belts with eastward decreasing age: Late Palaeozoic, Late Triassic–Early Jurassic, Middle Jurassic and Early Cretaceous. Between 28°S and 33°S, the batholith includes only the Mesozoic granitoids, whereas south of 33°S Late Palaeozoic granitoids constitute its main component (Fig. 4.5). Most of the information given below (and in Table 4.2) comes from studies carried out between 31°S and 33°S and at 37–38°S.

Late Palaeozoic plutonic component

Rock exposures of Late Palaeozoic granitoids form a north–south trending belt more than 750 km long from 33°S to 38°S (Fig. 4.5) and are usually continuous along the coastline, but limited inland. These granitoids appear to be the southern segment of a once-continuous Late Palaeozoic belt, now displaced c. 100 km west as a consequence of Mesozoic crustal spreading. Most of the studies on the coastal Late Palaeozoic granitoid belt are restricted to its northern and southern extremes, where the Santo Domingo Complex and Nahuelbuta Complex crop out, respectively.

Santo Domingo Complex. Exposed along the coastline from 33°S to 34°S approximately, this unit includes coarse-grained hornblende–biotite-bearing granodiorites and tonalites and minor amounts of granites with 1–4-cm-long microcline megacrysts. Tonalites commonly have ovoidal and lens-shaped mafic enclaves (gabbroic to dioritic compositions), schlieren and synplutonic dykes, all of them attributed to a process of mingling between two contrasting magmas represented by the enclave-free granites and the more mafic enclaves and synplutonic dykes (Parada *et al.* 1999). The northern and southern exposures of this complex consist of very coarse-grained tonalites and granodiorites with a NW-trending foliation and deformed fabrics that were generated during or soon after emplacement. Al-in-hornblende geobarometry obtained from the Santo Domingo tonalites gave a depth of emplacement equivalent to a pressure of about 4.5 kbar (Sial *et al.* 1999). Like the Elqui–Limarí Batholith, this complex is intruded by a Mesozoic mafic dyke swarm.

Rb–Sr isochrons obtained in three localities (Reñaca, Algarrobo and Santo Domingo) gave similar ages between 292 ± 2 and 308 ± 15 Ma (Hervé *et al.* 1988). These ages are concordant with two zircon U–Pb ages of 309 and 290 Ma (Godoy & Loske 1988) obtained c. 20 km south of Valparaíso.



Fig. 4.5. Distribution of the Coastal Batholith and associated Mesozoic stratified units between 33°S and 38°S.

Lithologically and geochronologically, this complex is equivalent to the Early Permian Guanta unit of the Elqui–Limarí Batholith.

The granitoids and enclaves form a calcalkaline suite covering a wide compositional spectrum from 50 to 70% SiO_2 and show field relationships and linear trends in variation diagrams for major elements, typical of a suite derived from the mixing of two contrasting magmas (Parada 1990). Both granitoids and enclaves are isotopically (Sr–Nd) enriched. The initial $^{87}\text{Sr}/^{86}\text{Sr}$ ratios fall in a broad range between 0.7057 and 0.7098, the lowest values corresponding to the enclaves. Similar ϵNd values between -2 and -4 were obtained for both granitoids and enclaves (Parada *et al.* 1999).

Table 4.2. Summary of the main features of the Coastal Batholith and Mesozoic volcanic rocks of central Chile based on references given in the text

	Late Palaeozoic plutonism	Triassic–Early Jurassic plutonism	Mid-Jurassic plutonism	Early Cretaceous plutonism	Jurassic volcanism	Early Cretaceous volcanism
Rock type	Hb–Bt tonalites, granodiorites and granites	Leucogranites and Hb–Px gabbros	Px–Hb diorites, Hb–Bt tonalities and granodiorites. Minor amounts of leucogranites	Px–Hb diorites and gabbros, Bt tonalites and granodiorites	Ajial and Horqueta formations: dacites, felsic tuffs and minor amounts of basalts, basaltic andesites and andesites	Ocoite Group: basalts and basaltic andesites. Las Chilcas Formation: rhyolites and andesites
Age of magmatic events	c. 290 Ma	c. 200 Ma	c. 165 Ma	c. 100–95 Ma		119–117 Ma
Textural and structural features	Coarse and tectonically orientated minerals. Microcline megacrysts in granites. Abundant mafic enclaves in tonalities. Commonly intruded by mafic dyke swarms	Coarse-grained to porphyric leucogranites. Isotropic textures. Enclave-free granites. Medium- to coarse-grained gabbros. Mafic dyke intrusions commonly observed	Medium- to coarse-grained rocks. Mineral orientation locally observed. Abundant mafic enclaves in tonalities. Mafic dykes observed locally	Equigranular to porphyric granodiorites. Orthocumulate and mesocumulate equigranular gabbros. Mafic enclaves locally observed. Mafic dykes almost absent	Aphanitic to porphyry rhyolites	Plagioclase phenocryst-rich basalts and basaltic andesites
Geochemical characteristics	Metaluminous calcalkaline suite. Some granite intrusions are peraluminous	Bimodal association of gabbros and granites. Metaluminous to slightly peraluminous granites	Medium- to high-K calcalkaline suite of diorites, tonalities, granodiorites and granites	Calcalkaline suite. High K content and minor amounts of rock with trondhjemitic affinity	Calcalkaline suite	Calcalkaline and shoshonitic affinities
Isotopic signatures	Enriched Sr–Nd isotope values. Sr_i : 0.706–0.710 ϵNd : –1 to –4	Enriched granites: Sr_i : 0.715–0.712 and ϵNd : –0.6, –0.7. Depleted gabbros: Sr_i : 0.7033–0.7035. ϵNd : +3.6, +4.6	Depleted Sr–Nd isotope values. Sr_i : 0.7034–0.7044, ϵNd : +0–9 to +3.7	Depleted to strongly depleted Sr–Nd isotope values. Sr_i : 0.7034–0.7068, ϵNd : +4.3 to +6.5	Depleted signature: Sr_i : 0.7031–0.7050 and ϵNd : c. +2.0 to +4.5	Depleted to strongly depleted isotopic signature. Sr_i : 0.703–0.705. ϵNd : 0 to +6.0
Tectonic regime	Contractional	Extensional	Extensional	Extensional	Extensional	Extensional/contractional

Hb, hornblende; Px, pyroxene; Bt, biotite

Nahuelbuta Complex. This is hosted in the accreted low P–T metasedimentary belt of the Late Palaeozoic subduction complex and is overlain by Late Triassic sedimentary successions. Granite is the most abundant lithology (followed by diorite) and is usually slightly peraluminous, particularly when near metasedimentary host rocks, and has relatively flat REE patterns (Lucassen *et al.* 2001b). Like the Santo Domingo Complex, the Nahuelbuta Complex has ages of about 294 Ma (Hervé *et al.* 1988) and is isotopically enriched: ϵNd values are in the range of –2.5 and –7.5, and initial $^{87}Sr/^{86}Sr$ ratios vary within the range 0.705–0.715, indicating a mixing of at least two isotopically different lithospheric sources, with crust similar in composition to the exposed metasedimentary host rocks being the main contributor (Lucassen *et al.* 2001b).

Late Palaeozoic granitoids have also been identified (based on both radiometric and stratigraphic evidence control, in the Andean Cordillera at about 40°S (Martínez 1998) and, more widely, in the North Patagonian Massif (Cingolani *et al.* 1991), a morphological feature located in Argentina east of the North Patagonian Andes.

Triassic–Early Jurassic bimodal intrusions and associated volcanic rocks

A discontinuous belt of shallow-emplaced leucogranite and gabbro intrusions and associated mafic and felsic dykes is

recognized along the Coastal Batholith. Between 30°30'S and 33°S these mildly peraluminous leucogranites and gabbros have been dated as between 209 ± 4 and 191 ± 4 Ma (Irwin *et al.* 1988; Parada *et al.* 1988) and assembled within the Limarí Complex (Parada *et al.* 1999). The leucogranites are medium- to fine-grained with equigranular to porphyritic textures, and were emplaced passively into both a Late Palaeozoic subduction complex and Late Palaeozoic–Early Mesozoic marine formations (Rivano *et al.* 1985) under an extensional tectonic regime.

The volcanic equivalent of the Limarí Complex is the Pichidangui Formation characterized by the presence of a bimodal association of tholeiitic basalts and rhyolites (Morata *et al.* 2000). Both bimodal associations, the Limarí Complex and the Pichidangui Formation, have similarities and differences in geochemical and isotopic characteristics. The basic plutons have higher MgO contents (8–10%) than the basalts (4–5%), but both types of mafic rocks have ϵNd between +3 and +5 (Parada *et al.* 1999; Morata *et al.* 2000), probably related to an enriched mantle source. All the acidic rocks show compositional evidence of major crustal components in their source, although some isotopic differences between rhyolites and leucogranites are recognized. Initial $^{87}Sr/^{86}Sr$ ratios vary

from 0.7040 to 0.7116 in rhyolites, and two leucogranite samples have values of 0.7154 and 0.7121. ϵNd values between -4.8 and $+2.5$ were determined for the rhyolites, compared with values of -0.6 and -0.7 for the leucogranite samples.

Evidence for Triassic–Early Jurassic plutonism south of 33°S is scattered, with isolated granite bodies distributed along the western margin of the Coastal Batholith. These include the epizonal Topocalma, La Estrella, Pichilemu, Constitución and Hualpén plutons that were emplaced during the 218–202 Ma interval (Hervé *et al.* 1988; Creixell *et al.* 2002) and coevally with a Late Triassic rifting episode in the Chilean continental margin (Charrier 1979). All these plutons are slightly peraluminous granites, although small gabbro intrusions have also been recognized. The Hualpén granite pluton, the only body of the southern segment of the Coastal Batholith that has been studied isotopically, shows evidence of crustal contribution such as ϵNd values of about -2.5 and initial $^{87}\text{Sr}/^{86}\text{Sr}$ ratios of 0.708–0.712 (Lucassen *et al.* 2001b; Creixell *et al.* 2002).

Middle–Late Jurassic and Early Cretaceous plutonic belts

The Middle–Late Jurassic and Cretaceous belts respectively occupy a western and an eastern position and extend southward along the Coastal Cordillera to *c.* 34°S . South of this latitude, only the Cretaceous belt continues, occupying the Andean Cordillera. Numerous Jurassic plutons were emplaced into metasedimentary and metaoceanic rocks of the Late Palaeozoic subduction complex, as well as into Late Palaeozoic granitoids and Early Mesozoic felsic volcanic rocks (Triassic Pichidangui Formation and Early Jurassic Ajial Formation). The Early Cretaceous plutons intruded the Jurassic plutons, but were also emplaced into a thick Early Cretaceous volcanic–sedimentary succession deposited in a subsiding basin (Vergara *et al.* 1995). This succession includes the volcanic-dominated Lo Prado and Veta Negra formations, assembled in the Ocoite Group, and the sedimentary-dominated Las Chilcas Formation.

The main lithologies of the Jurassic plutonic belt are medium-grained two-pyroxene diorites, gabbros and hornblende + biotite tonalites. The tonalites locally have abundant mafic enclaves and synplutonic dykes similar in composition to the diorite and gabbro bodies. Small plutons of leucogranites are also recognized. Whole-rock Rb–Sr isochron ages of 164 ± 2 Ma, hornblende $^{40}\text{Ar}/^{39}\text{Ar}$ of 169 ± 3.6 and 165 ± 2.6 Ma, and zircon U–Pb ages of 157, 160 and 164 Ma are known from this belt (Parada *et al.* 1988; Irwin *et al.* 1987; Godoy & Loske 1988; Gana & Tosdal 1996). Hornblende crystallization pressures of 3–5 kbar were obtained in quartz-diorites and tonalites in localities near Valparaíso (Gana & Tosdal 1996). Despite their wide compositional range, most of the rocks of this belt can be classified as medium- to high-K series and have remarkably similar REE patterns characterized by a $\text{La}_\text{N}/\text{Yb}_\text{N}$ close to 7 and moderate negative Eu anomalies (Parada 1992; Parada *et al.* 1999).

The Cretaceous granitoids constitute the largest Mesozoic plutonic belt of central Chile. They include a wide lithological spectrum from gabbro to granite, defining a typical calcalkaline high-K suite. Abundant geochronological data exist on these granitoids obtained by different methods, with variable precisions (cf. Drake *et al.* 1982b; Parada *et al.* 1988, 2005a; Hervé *et al.* 1988, Gana *et al.* 1996). Recent studies on the Caleu pluton, a good example of the last Cretaceous plutonic event, indicate an age and pressure of emplacement of *c.* 95 Ma and *c.* 2 kbar, respectively (Parada *et al.* 2002, 2005b).

Jurassic and Early Cretaceous volcanism at a rifted continental margin

During the Middle Jurassic–Early Cretaceous interval episodic volcanism took place. At about 33°S these events are represented by the volcanic components of the Mid-Jurassic (Bajocian) Ajial Formation, Late Jurassic Horqueta Formation, and the Early Cretaceous (Valanginian–Barremian) Ocoite Group (Aguirre *et al.* 1989) and (Albian) Las Chilcas

Formation. The Ajial Formation includes a bimodal association of abundant dacitic ignimbrites and interbedded basalts and basaltic andesites. These rocks have a calcalkaline high-K affinity and exhibit poorly fractionated REE patterns (Vergara *et al.* 1995). The Horqueta Formation includes a suite of calcalkaline lavas from basic to acidic composition. The Ocoite Group is represented by a *c.* 15-km-thick succession that includes the Valanginian to Hauterivian Lo Prado Formation and the Hauterivian to Barremian Veta Negra Formation. A minimum effusion rate of about $500 \text{ km}^3/\text{Ma}$ has been calculated during the deposition of the 10-km-thick Veta Negra Formation (Vergara *et al.* 1995). At 30°S the volcanism is represented by the abundant volcanic rocks of the Hauterivian to Barremian Arqueros Formation and Barremian to Albian Quebrada Marquesa Formation.

The rocks of the Ocoite Group, as well as those of the Arqueros and Quebrada Marquesa formations, are subaerial porphyritic basalts and basaltic andesites with high-K to shoshonitic affinity (Levi & Aguirre 1981; Åberg *et al.* 1984; Levi *et al.* 1988; Vergara *et al.* 1995; Morata & Aguirre 2003). Remarkably similar flat REE patterns are recognized among the Early Cretaceous basic and intermediate volcanic rocks. They exhibit low (4–11) $\text{La}_\text{N}/\text{Lu}_\text{N}$ ratios which exclude the presence of garnet as a residual phase in the magma source. Additionally, the REE patterns show a slightly negative Eu anomaly, despite the commonly observed plagioclase-rich porphyritic textures (Morata & Aguirre 2003).

Volcanic rocks are scarce in Las Chilcas Formation, which mainly consists of a lower section of limestone, sandstone and minor amount of andesite and rhyolitic tuffs, and an upper section of thick strata of volcanic–sedimentary breccias and conglomerates with coarse volcanic fragments (molasse-type deposit).

Rifting magmatism and associated subsiding basins are the most outstanding processes developed along the western margin of South America during Jurassic–Cretaceous times. They are probably the result of a trench retreat that led to crustal attenuation, asthenospheric upwelling to fill the gap, bimodal volcanism, burial metamorphism and plutonic activity (Åberg *et al.* 1984; Vergara *et al.* 1995; Aguirre *et al.* 1989). In Chile, between 25°S and 36°S , extensional bimodal volcanic activity developed during Jurassic–Early Cretaceous times, generating a *c.* 1200-km-long belt with an average width of 30 km and thickness of 3 to 13 km. Associated with basin subsidence, very low-grade metamorphism developed, reaching its climax at 93–94 Ma in central Chile (Aguirre *et al.* 1999). These geochronological data show that the very low-grade metamorphism is coeval with the last Cretaceous plutonic event, suggesting that this metamorphism is not the result simply of burial, but also of enhanced regional thermal gradients related to the plutonism.

Unlike the observed temporal and compositional correlations between the Late Palaeozoic–Early Mesozoic plutonic complexes of the High Andes Batholith and its volcanic counterparts, the Middle–Late Jurassic and Cretaceous plutonic events are younger than the spatially related peak in volcanism (Table 4.2). Rhyolites of the Bajocian Ajial Formation are intruded by the Late Jurassic plutons. Similar stratigraphic relationships are observed between the 5–10-km-thick pile of basalts and basaltic andesites of the Early Cretaceous Veta Negra Formation (and equivalent units) hosting the extensive mid-Cretaceous plutonic belt.

The available geochronological data on the Mesozoic volcanism are restricted to the Veta Negra, Arqueros and Las Chilcas formations. $^{40}\text{Ar}/^{39}\text{Ar}$ ages of about 119 ± 2.4 Ma have been obtained on primary plagioclase in basaltic flows of the Veta Negra Formation at $33^\circ 30'\text{S}$, and do not differ substantially from the 117 ± 0.6 and 114 ± 0.7 Ma obtained on primary Ca-plagioclase populations from the Arqueros Formation (30°S).

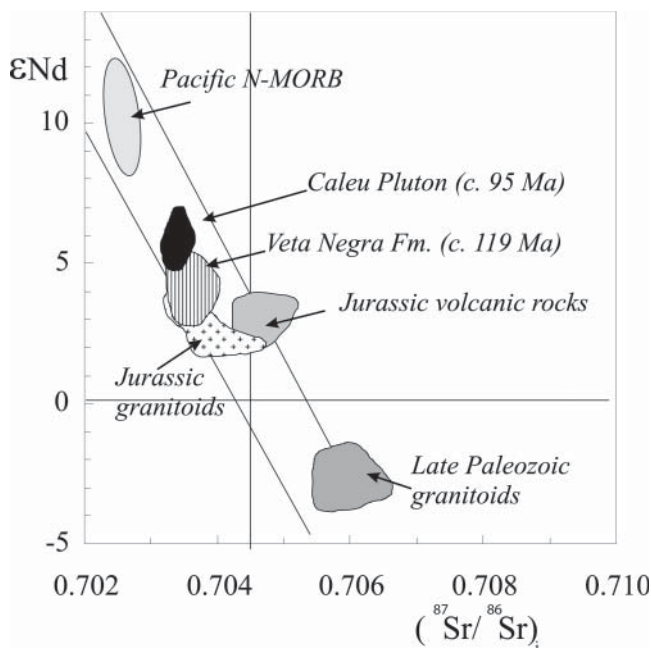


Fig. 4.6. ϵNd versus $^{87}\text{Sr}/^{86}\text{Sr}_i$ initial ratios for the Palaeozoic and Mesozoic components of the Coastal Batholith and associated Mesozoic volcanic units of central Chile, taken from Parada *et al.* (2005a).

Zircon U–Pb ages in the range 109 ± 0.2 to 106.5 ± 0.4 Ma have been obtained in rhyolites of the lower section of the Las Chilcas Formation, whereas its upper section has whole-rock and plagioclase K–Ar ages in the interval 101 ± 3 to 95 ± 3 Ma (Wall *et al.* 1999).

A trend towards MORB isotopic signature with time

Sr–Nd data, obtained from rocks of the Coastal Batholith between 31°S and 34°S (Parada *et al.* 1999, 2002; Morata *et al.* 2001), are plotted in Figure 4.6 and show an abrupt change from an enriched Late Palaeozoic to a depleted Mesozoic source of the magma. This change coincides with the change in the tectonic regime from a compressional subduction associated with the formation of a subduction complex (Hervé *et al.* 1987; Mpodozis & Kay 1992), to extension attributed to arrested subduction related to an episode of slow sea-floor spreading (Larson & Pitman 1972). The absence of a magmatic event older than Late Palaeozoic in central Chile suggests the existence of an old and isotopically enriched lithospheric mantle source for the Late Palaeozoic granitoids and associated volcanic rocks.

Along the central Chilean continental margin, a progressive Mesozoic extension developed, culminating during Early Cretaceous times in an aborted marginal basin (Åberg *et al.* 1984) within which the thick Ocoite Group succession was deposited. This progressive Mesozoic extension correlates with isotopic (Sr–Nd) trends towards MORB signatures (Fig. 4.6) in both plutonic and volcanic rocks (31 – 34°S). This is attributed to a combination of: (i) a continuous asthenospheric upwelling and associated lithospheric removal that accompanied extension (Parada *et al.* 1999, 2005a); (ii) a decreasing participation of the crust due to its increasing refractory nature that resulted from successive extractions of felsic melts or subsolidus dehydration as extension proceeded.

It is interesting to note the more depleted isotopic signatures of the Mesozoic plutonic complex as compared with their host volcanic rocks (Fig. 4.6), confirming the independence between volcanism and plutonism. This situation differs from that described for the Coastal Batholith of Peru (Atherton 1990),

which is considered to be a product of precursor volcanic rocks remelting within a rifted continental margin. The last plutonic event, during which the Caleu pluton formed, would have been generated from the most depleted source during the climax of Cretaceous extension.

Diachronous Mesozoic exhumations of the Coastal Batholith

Fission track dating has revealed an exhumation event in Palaeozoic–Early Cretaceous coastal granitoid rocks ($32^\circ30'\text{S}$ to $33^\circ30'\text{S}$) during the interval 106–90 Ma (Gana & Zentilli 2000; Parada *et al.* 2005a). The magnitude of this Cretaceous exhumation was larger along the present-day coastline at these latitudes where the once deep-seated (c. 3.0–5.0 kbar or c. 11–18 km depth based on Al-in-hornblende geobarometry; Gana & Tosdal 1996; Sial *et al.* 1999) Palaeozoic to Jurassic plutonic–metamorphic belts are now exposed. In the case of the Cretaceous belt, the exhumation would have started at about 7 km depth.

The cause of the exhumation can be attributed to a well-recorded change in tectonic regime in the Coastal Cordillera and along the Chile–Argentina Andes during mid-Cretaceous times. At that time, extensional tectonics ended and a high-stress compressional regime started, giving rise to the Aconcagua fold-thrust belt located in the High Andes (Mpodozis & Ramos 1989; Ramos & Aleman 2000). The age range of the exhumation roughly coincides with the deposition of thick breccias and conglomerates (molasse-type deposits) of the upper section of the Las Chilcas Formation, suggesting a cause-and-effect relationship.

On the other hand, the Late Palaeozoic granitoids of the Nahuelbuta Complex (at about 38°S) were exhumed before the deposition of the Late Triassic sedimentary rocks of the Santa Juana Formation. In fact, basal conglomerates with abundant granitic fragments were deposited over Late Palaeozoic granitoids. Similar stratigraphic relationships have been observed between the pre-Triassic components of the High Andes Batholith and the overlying conglomerates of the Middle–Late Triassic Las Breas Formation.

The Cenozoic plutonic belts: 30 – 38°S

These belts are poorly known, despite the close temporal and spatial relationships with porphyry copper deposits of this segment. The information given here comes mainly from regional mapping and a K–Ar geochronological programme carried out during the 1980s. Two north–south trending Cenozoic plutonic belts with eastward decreasing ages are clearly identified east of the Coastal Batholith, along the Andes of central Chile between 30°S and 38°S . The plutonic rocks of the segment between 30°S and 32°S are those where most of the geological and radiometric data have been obtained (Rivano *et al.* 1985; Parada *et al.* 1988). Stratigraphic relationships and radiometric ages indicate that the western belt is a continuous Palaeogene belt that extends down to 32°S where it abruptly ends. The eastern belt is less continuous and has early and late Miocene ages. Further north of these latitudes the belts are poorly defined by isolated plutons with few radiometric data.

The jump in the locus of plutonism from the Coastal Batholith to the Palaeogene belt and then to the High Andes Neogene belt, corresponds essentially to non-magmatic intervals at 95–70 Ma and 40–26 Ma. During the development of the Neogene belt, a non-magmatic interval is also recognized between 24 and 17 Ma, although no jump in the locus of magmatism exists. The eastward propagation of the locus of plutonism with time correlates with a secular decrease in intensity of the plutonic activity, as suggested by the decreasing area of the respective belt exposures.

The Cenozoic plutons are epizonally emplaced into volcanoclastic successions, in the case of the Palaeogene intrusions, and into deformed Late Jurassic to Palaeogene sedimentary and volcanic formations, in the case of the Miocene bodies.

The Palaeogene belt in the 30–32°S segment includes medium-grained to porphyritic hornblende-pyroxene diorites and quartz-diorites and fine-grained leucogranites assembled in the Cogotí superunit. Eleven K–Ar mineral ages in the range 67–38 Ma have been reported for this superunit (Parada *et al.* 1988). In contrast, only two Miocene events have been identified based on 14 K–Ar mineral ages distributed in the intervals 26–24 Ma and 17–8 Ma. The early Miocene granitoids of this segment correspond to the Rio Grande superunit, exhibit a wide lithologic spectrum from gabbro to granite, and occur as shallow intrusions along the axis of the Andes. The late Miocene granitoids include hornblende–clinopyroxene monzodiorites and dacite porphyries assembled into the Rio Chicharra superunit (Parada *et al.* 1988). As with the early Miocene granitoids, most of the late Miocene granitoids occur as small epizonal bodies located along the highest Andean ranges.

Forming part of the Neogene belt, the late Miocene (*c.* 10 Ma) porphyritic intrusions of the Los Pelambres giant porphyry copper deposit show various features akin to the adakites. These intrusions, located at 31°43'S, 70°29'W, represent an oddity in the late Miocene magmatism of central Chile (Reich *et al.* 2003). In fact, they exhibit distinctly higher Na₂O contents and higher Sr/Y (100–300) and La_N/Yb_N (25–60) ratios than coeval magmatic units such as La Ramada (*c.* 32°S) and Cerro Aconcagua volcanic centres (Kay & Mpodozis 2002) and La Gloria pluton (Cornejo & Mahood 1997), which have typical arc geochemistry with moderate La_N/Yb_N ratios and Eu. The adakitic-like rocks from Los Pelambres, located in the modern flat-slab Andean segment, are closely related in time and space with the subduction of a west–east segment of the Juan Fernández Ridge. This locally restricted scenario has been considered favourable for the partial melting of young and hot rocks of the Juan Fernández Ridge under late Miocene flat-slab conditions and may explain why adakitic rocks have not been found elsewhere along the Neogene belt (Reich *et al.* 2003). It is interesting to note that adakite-like intrusions have also been found associated with late Eocene–early Oligocene porphyry copper systems of northern Chile (Oyarzún *et al.* 2001).

Neogene magmatism in the modern flat-slab Andean segment

The inactive volcanic flat-slab Andean segment (28–33°S) forms a distinctive component of the Chilean Andes, and is located north of the active Andean Southern Volcanic Zone (SVZ; 33–46°S). The subducting slab in this segment presents a relatively smooth northern transition to the north, toward the Central Volcanic Zone (CVZ), and an abrupt southerly transition to segments with a steeper subduction angle (30°) (Cahill & Isacks 1992). Shallow subduction worldwide seems to be associated with the subduction of thickened oceanic crust, particularly seamounts or oceanic plateaux, and with the subduction of ocean ridges. The latter phenomenon is thought to have been responsible for the Chilean flat-slab segment, beneath which has been subducted the aseismic Juan Fernández Ridge (Nur & Ben-Avraham 1981; Pilger 1981, 1984; Kirby *et al.* 1996; Gutscher *et al.* 2000a, b; Yañez *et al.* 2001, 2002).

The relationships between the magmatic history of the Chilean flat-slab, crustal thickening, and subduction of the Juan Fernandez Ridge requires an understanding of the changes in the geochemical signatures of the magmas with time. These signatures can be related to the chemical components of the subducted slab, the overlying mantle wedge, and the crust. Based on a north to south geochemical change of the SVZ as a consequence of crustal thickness variations (Hildreth & Moorbath 1988), several studies have concluded that the temporal geochemical variation of the Cenozoic volcanic successions is related to crustal thickness variations in these three areas (Kay *et al.* 1987, 1988, 1991, 1999; López-Escobar

et al. 1991; Kay & Kurtz 1995; Stern & Skewes 1995; Kay & Mpodozis 2001, 2002; Nyström *et al.* 2003). All these studies have used REE patterns to infer the presence or absence of garnet in the magma source. Accordingly, variations in La/Yb ratios have been used as a tool to determine crustal thickness variations with time. A compilation of the chronostratigraphic characteristics of the volcanic units in the flat-slab segment is presented in Table 4.3.

Although this section deals primarily with the magmatism of central Chile between 28°S and 38°S, the igneous rocks of the Maricunga area in the High Andes between 26°S and 28°S are included because the influence of the flat-slab is recognized down to these latitudes. Accordingly, the following discussion offers a comparison between the magmatic histories of the Cenozoic volcanism in areas along the northern margin (26–28°S), the centre (28.5–32.5°S) and the southern margin (33–34.5°S) of the modern flat-slab segment (Fig. 4.7).

North: Maricunga area (26–28°S)

The magmatic history of the arc in this region during late Oligocene–early Miocene times (24–20 Ma) is recorded in the Maricunga Belt, Andean Cordillera (Fig. 4.8), by the Cerros Bravos, La Coipa and Refugio lava dome complexes (Kay *et al.* 1994, 1999; Mpodozis *et al.* 1995). The volcanic rocks are mainly medium- to high-K calcalkaline andesites and dacites with La/Yb ratios ranging from 7 to 20. The best studied backarc volcanic rocks of this age come from the Segerstrom lavas (*c.* 23 Ma), which are medium-K basalts and basaltic andesites (Kay *et al.* 1999). The trace element characteristics of these arc magmas indicate equilibration with amphibole-bearing residual assemblages. Comparison of the REE patterns of andesites and dacites with similar SVZ rocks suggests a crustal thickness of about 40–45 km during the interval 24–20 Ma.

Volcanic rocks with ages of 21 to 17 Ma are less voluminous than those of late Oligocene–early Miocene age, and correspond to small dacitic dome complexes (21–17 Ma), pyroclastic deposits and dacitic ignimbrites (Kay *et al.* 1994; Mpodozis *et al.* 1995). This magmatic quiescence has been considered as a near-magmatic lull and interpreted as an episode of deformation and crustal thickening (Kay *et al.* 1999; Kay & Mpodozis 2001). After this lull, widespread volcanism developed and produced the Jotabeche Norte centre (27.5°S; *c.* 18–16 Ma) and the Ojos de Maricunga/Pastillos stratovolcanoes (27°S) (McKee *et al.* 1994; Kay *et al.* 1994; Mpodozis *et al.* 1995). The volcanic rocks here are medium- to high-K calcalkaline andesites and have La/Yb ratios up to 26–35 (Kay *et al.* 1994). Comparison of the REE patterns of these andesites with those of the SVZ rocks suggests a crustal thickness of over 50 km during the interval 18–16 Ma (Kay *et al.* 1999; Kay & Mpodozis 2001).

A new volcanic arc started erupting around 16–9 Ma, producing stratovolcano–dome complexes which have been subdivided into two groups (Kay & Mpodozis 2002): (1) Doña Inés volcano, Ojos de Maricunga/Pastillos centre and Cadillal complex, with ages between 16 and 13 Ma (Kay *et al.* 1994; Mpodozis *et al.* 1995); and (2) Copiapó ignimbrite/dome complex and centres near Nevado de Jotabeche, with ages from 11 to 9 Ma (Kay *et al.* 1994). Lavas of group (1) are mostly medium- to high-K calcalkaline andesites with La/Yb ratios between 15 and 26, suggesting a crustal thickness of about 55–60 km. Lavas of group (2) are high-K calc-alkaline andesites and dacites with La/Yb ratios larger than those from group (1). Backarc dacitic ignimbrites erupted at about 15–10 Ma and their geochemical features are similar to those of the western arc rocks (Kay & Mpodozis 2002). Finally, the arc magmatism migrated toward the east after 9 Ma, and high-K calcalkaline andesites were erupted (Mpodozis *et al.* 1997; Kay & Mpodozis 2000).

Late Miocene volcanism is represented by the Copiapó stratocone (8–7 Ma), the rhyodacitic Jotabeche caldera

Table 4.3. Chronostratigraphic compilation of volcanic activity in the Andean flat-slab and bordering segments (26–34.5°S) based on references given in the text

Age (Ma)	26°–28°S Maricunga Transect	28.5°–32.5°S El Indio Transect	33°–34.5°S Los Andes-El Teniente Transect
8–5	Arc: Copiapó stratocone (8–7 Ma)–Jotabeche complex/Pircas Negras (8–5 Ma) Backarc: Farallón Negro (8–5 Ma)–Sierra de Famatina (5 Ma)	Arc: Vacas Heladas ignimbrite/Vallecito Formation (7–5 Ma) Backarc: Cerro Blanco (6 Ma) Pocho field (8–5 Ma)	Arc: Upper Sewell (Teniente Volcanic Complex; 9–7 Ma) Los Bronces/Río Blanco (7–5 Ma)–Braden Breccia (5 Ma)–‘Late Hornblende’ dikes (4–3 Ma) Backarc: Sierra de San Luis (6–2 Ma)
Crustal thickness:	60–65 km	60 km	45 km
11–9	Arc: Copiapó complex (11–9 Ma) Valle Ancho (9 Ma)	Arc: Tambo Formation	Arc: Pirámide (11–9 Ma) Cerro Aconcagua (10–9 Ma) Lower Sewell (Teniente Volcanic Complex; 11–10 Ma) Backarc: Huincán group (14–6 Ma)
Crustal thickness:	55–60 km	> 45 km	30–35 km
16–13	Arc: Doña Inés volcano–Ojos de Maricunga/Pastillos center–Cadillal complex (16–13 Ma) Backarc: Valle Ancho (15–10 Ma)	Arc: Cerro de Las Tórtolas Formation (17–14 Ma) Tambo Formation (13–10 Ma) Backarc: Cerro Ullun (10–11 Ma)	Arc: Cerro Aconcagua (16–15 Ma) Farellones Formation La Ramada (13–11 Ma) Maqui Chico (Teniente Volcanic Complex; 15–11 Ma)
Crustal thickness:	55–60 km	> 45 km	30–35 km
20–17	Reduced volcanism or magmatic lull (20–18 Ma) Arc: Jotabeche Norte center (18–16 Ma)–Ojos de Maricunga/Pastillos stratovolcanoes	Reduced volcanism or magmatic lull (20–18 Ma) Arc: Escabroso Formation (21–18 Ma) Infiernillo unit (18–15 Ma)	Arc: Farellones Formation (25–7 Ma) Intrusives II Backarc: Uspallata/Cerro Colorado (19–16 Ma) Barreal (20 Ma) Ullún (16 Ma)
Crustal thickness:	> 50 km	35–40 km	30–35 km
28–20	Arc: Cerros Bravos–La Coipa–Refugio complexes (24–20 Ma) Backarc: Segerstrom lavas (23 Ma)	Arc: Cerro Pulido (23 Ma)–Cerro Chacay (20 Ma)–Cantarito ignimbrites (22–18 Ma)–Tilito Formation (27–23 Ma)–Escabroso Formation (21–18 Ma) Backarc: Las Máquinas basalts (23 Ma)	Arc: Abanico (= Coya–Machali) Formation (37–15 Ma) Farellones Formation (25–7 Ma) Intrusives I
Crustal thickness:	40–45 km	35–40 km	30–35 km

complex and the Pircas Negras mafic andesite flows. The last two units have ages between 8 and 5 Ma (Mpodozis *et al.* 1995). All these units correspond to medium- to high-K calcalkaline andesites and dacites, and have La/Yb ratios up to 57 (Kay *et al.* 1991), suggesting a crustal thickness of about 60–65 km (Kay *et al.* 1999; Kay & Mpodozis 2001) never attained along the SVZ. Arc volcanism ended around 7.5 Ma and magmatic activity increased in the backarc region, where the Farallón Negro volcanic cluster (27°S; 8.5–5.2 Ma) and the porphyries and domes in the Sierra de Famatina (29°S; 5 Ma) are found.

Centre: El Indio area (28–32°S)

The late Oligocene–early Miocene volcanism near 29°S includes the andesitic Cerro Pulido volcanic complex (23 Ma), the Cerro Chacay andesites (20 Ma), and the rhyolitic Cantarito ignimbrites (22–18 Ma) (Kay *et al.* 1991). The best studied volcanic rocks are from the Doña Ana Group (Maksaev *et al.* 1984; Kay *et al.* 1987, 1991) near 30°S, which comprises two formations: the Tilito Formation (Oligocene: 27–23 Ma) and the Escabroso Formation (Early Miocene: 21–18 Ma). These formations are separated by a mild discordance interpreted as a period of

deformation near 20 Ma (Kay & Mpodozis 2002). Lavas of the Tilito Formation are high-K calcalkaline andesites to rhyolites whereas those of the Escabroso Formation correspond to pyroxene-bearing medium-K calcalkaline basaltic andesites and andesites. Trace element features are consistent with pyroxene- and amphibole-bearing mineral residues. La/Yb ratios of both formations range generally between 6 and 15, suggesting a crustal thickness of about 35–40 km. Small amounts of olivine basalt flows, Las Máquinas basalts (23 Ma), erupted in a backarc position with respect to the arc volcanic rocks of the Doña Ana Group. Their trace element characteristics are OIB-like suggesting backarc extension over a steeply dipping subduction zone (Kay *et al.* 1991).

The initial shallowing of the subduction zone has been timed at *c.* 18 Ma based on the eastward broadening of the arc (Kay *et al.* 1987, 1988, 1991, 1999; Kay & Abbruzzi 1996), the occurrence of high-angle thrusting in the Main Cordillera (Maksaev *et al.* 1984), the inception of deformation in the Precordillera close to 18 Ma (Jordan *et al.* 1993), and the end of backarc volcanism (Kay & Mpodozis 2002). Thus, as in the Maricunga area, the magmatic activity corresponds to a near lull during

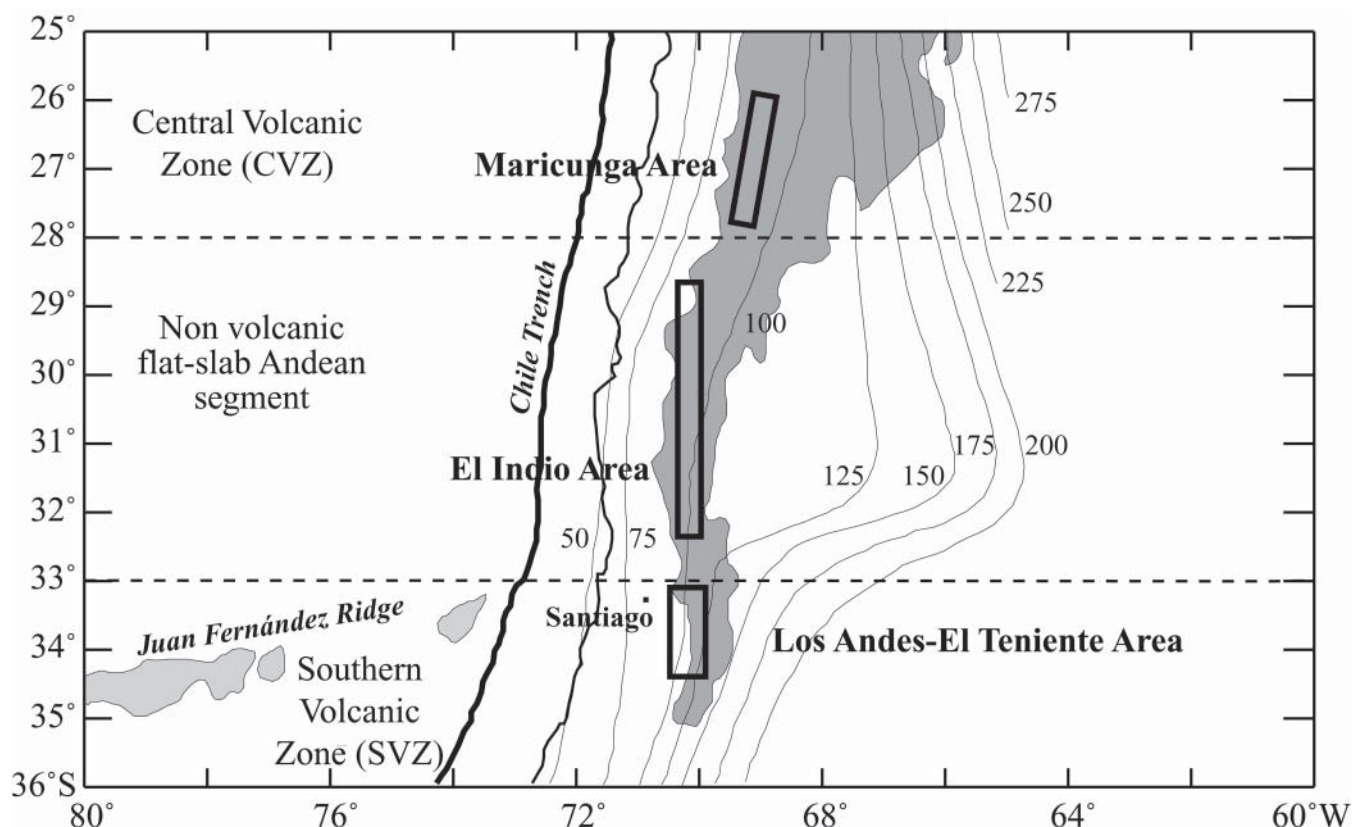


Fig. 4.7. Map of the Central Andes showing the three areas used to analyse the magmatic development in the modern flat-slab segment. Modern depth contours (in km) of the Wadati-Benioff seismic zone (Cahill & Isacks 1992), regions > 3 km in elevation (dark grey) and Juan Fernández Ridge are also shown.

20–18 Ma and is manifested by the Escabroso Formation (Early Miocene: 21–18 Ma) and the intrusion of subvolcanic plutons and porphyritic stocks from the Infiernillo unit (18–15 Ma; Makshev *et al.* 1984; Kay *et al.* 1987). Lavas of the Escabroso Formation consist of pyroxene-bearing medium-K calcalkaline basaltic andesites and andesites with geochemical characteristics consistent with a crustal thickness of about 35–40 km. The Infiernillo unit is composed of high-K calcalkaline andesites and their geochemical features are poorly understood; their relationship with the crustal thickness is difficult to interpret (Kay *et al.* 1987, 1991).

Arc volcanism during middle Miocene times (17–14 Ma) is represented by the Cerro de Las Tórtolas Formation (Martin *et al.* 1997a). Lavas of this formation are mainly amphibole-bearing medium- to high-K calcalkaline andesites and dacites, and have La/Yb ratios up to 25, suggesting a crustal thickness of over 45 km (Kay *et al.* 1991, 1999; Kay & Mpodozis 2001). The Tambo Formation (middle-late Miocene: 12.7–10 Ma; Martin *et al.* 1997a) is composed of medium- to high-K calcalkaline intermediate to felsic tuffs with La/Yb ratios higher than those from the Cerro de Las Tórtolas Formation (Kay & Mpodozis 2002). At about 8 Ma the volcanism ended in this region and its final activity is recorded further east in Argentina, where andesites with La/Yb ratios up to 25 are found. Toward the east of these andesites, in the Argentine Precordillera, the ignimbrite/dome complex at Cerro Ullun and a dacitic porphyry east of Rodeo, with ages from 10 to 11 Ma, are found (Leveratto 1976; Kay *et al.* 1988; Kay & Abbruzzi 1996).

Continued flattening of the subduction zone resulted in cessation of the andesitic volcanism at about 9 to 8 Ma in the Main Cordillera (Kay *et al.* 1991). The dacitic Vacas Heladas

ignimbrite of the Vallecito Formation (late Miocene: 7–5 Ma; Martin *et al.* 1997a) represents the only significant arc activity (Makshev *et al.* 1984; Ramos *et al.* 1989; Kay *et al.* 1991). These rocks correspond to high-K calcalkaline rhyodacites and have La/Yb ratios as high as 35, suggesting a crustal thickness of about 60 km (Kay *et al.* 1999; Kay & Mpodozis 2001). In the Precordillera and the Sierras Pampeanas, in the backarc environment, the Cerro Blanco centre (31.5°S; c. 6 Ma; Kay *et al.* 1988; Kay & Abbruzzi 1996) and the Pocho volcanic field in the Sierra de Córdoba (32°S; 7.9–4.5 Ma; Kay & Gordillo 1994) are found.

South: Los Andes–El Teniente area (33–34.5°S)

Unlike volcanism in the Maricunga and El Indio areas, the late Oligocene–early Miocene magmatic history of this region is recorded in the Central Valley, which is a graben with eroded volcanic centres (López-Escobar & Vergara 1997), and in the Andean Cordillera (Fig. 4.9). Most of the studies carried out south of 32°S indicate that the Late Oligocene–Early Miocene volcanic and volcanoclastic deposits that crop out in the Central Valley and Principal Cordillera between 32°S and 36°S can be included in the Abanico (37–15 Ma; Wyss *et al.* 1993; Rivera & Falcón 2000) and Farellones (25–7 Ma; Munizaga & Vicente 1982; Vergara *et al.* 1988) formations (Vergara & Drake 1979; Vergara *et al.* 1988; Rivano *et al.* 1990; Charrier *et al.* 1996; Fuentes *et al.* 2002). In addition to the Abanico and Farellones formations, other Oligocene–Miocene magmatic units exist and correspond to intrusive bodies, mainly stocks, dykes, sills and volcanic necks, which occur within and to the east of the Central Valley. These bodies are called here Intrusives I (34–20 Ma) and correspond to a range of microgabbros, dolerites, basalts and pyroxene andesites (Drake *et al.* 1976; Gana & Wall

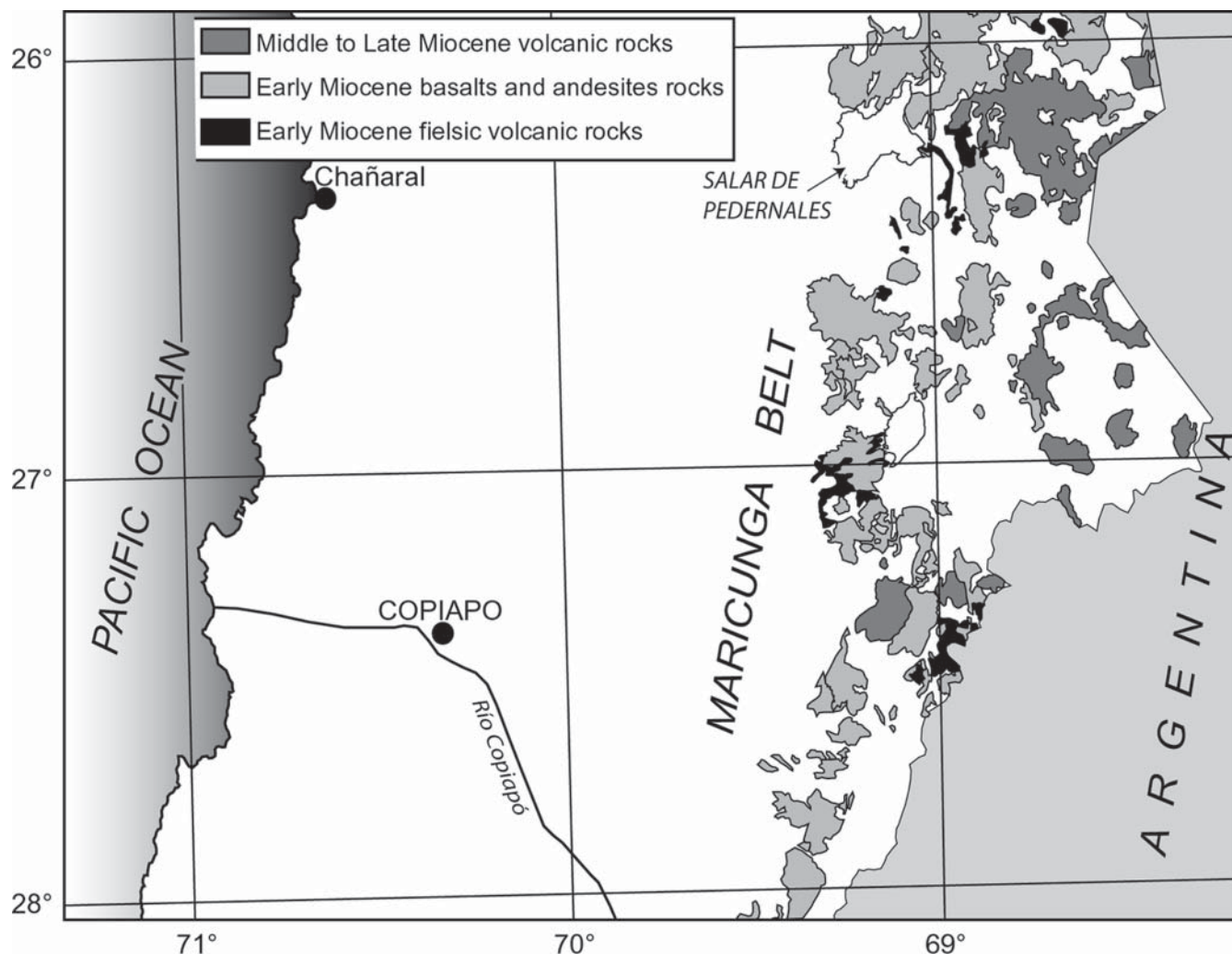


Fig. 4.8. Distribution of the Miocene volcanic rocks of the Maricunga Belt, high Andes Cordillera taken from Mapa Geológico de Chile (Sernageomin 2002).

1997; Wall 1997). Volcanic rocks between 37 and 20 Ma define tholeiitic to calcalkaline series, whereas those between 20 and 16 Ma show mainly calcalkaline affinities. The rocks range between basalts and rhyolites, showing a broad compositional range. Trace element features are consistent with pyroxene-dominated mineral residues. La/Yb ratios of rocks from the Abanico Formation range between 2 and 7, whereas those of rocks from the Farellones Formation range between 4 and 9, suggesting a crustal thickness of about 30–35 km during the 37–20 Ma interval (Kay & Kurtz 1995; Kay *et al.* 1999; Fuentes *et al.* 2000; Nyström *et al.* 2003). It would appear that a backarc setting did not exist during this time range, but instead there was a wide volcanic arc comprising two volcanic chains.

During the interval 20–16 Ma, magmatic activity is mainly represented by the Farellones Formation and equivalents (Fig. 4.9) with lavas ranging from medium- to high-K basalts to rhyolites, and with La/Yb ratios from 5 to 14. Their REE patterns suggest a crustal thickness of about 30–35 km (Nyström *et al.* 2003). However, some lavas from this formation, as well as amphibole-bearing andesitic to rhyolitic porphyries called here Intrusives II (*c.* 21 and 14 Ma), show chemical features distinctive of adakites (Vatin-Perignon *et al.* 1996; Sellés 1999a, b; Fuentes *et al.* 2000) with La/Yb ratios up to 28. Two possible mechanisms and sources can be invoked for the generation of these rocks: (1) melting of mixtures of

subducted metabasalt and sediments followed by extensive interaction of these melts with mantle wedge peridotite; and (2) melting of forearc continental crust tectonically removed by subduction erosion and incorporated into the oxidized, hydrated mantle wedge, followed by extensive interaction of these melts with mantle wedge peridotite.

To the east, in Argentina, amphibole-bearing andesitic lavas with ages of about 16 to 15 Ma, and La/Yb ratios of 19–22, are found at 32°40'S in the Cerro Aconcagua region (Kay *et al.* 1991; Ramos *et al.* 1996). Even further east, amphibole-bearing isolated subvolcanic bodies occur in the Uspallata Valley, Cerro Colorado (18.9–16.2 Ma; Kay *et al.* 1991) and other Argentinian localities. La/Yb ratios for these bodies are below 15 suggesting a crustal thickness of about 30–35 km, like that of the Farellones Formation. In summary, unlike the volcanism in the Maricunga and El Indio areas, no magmatic lull is recorded at *c.* 33°S during the interval 20–16 Ma. However, further south, at 34°S, a magmatic lull occurred at 19–16 Ma (Kay & Mpodozis 2002) and has been interpreted as a period of uplift and crustal thickening associated with compressional deformation (Kurtz *et al.* 1997).

During the interval 15–9 Ma, volcanic activity concentrated in Argentina, although the upper levels of the Farellones Formation are found in Chile, near the Argentinian border. Around 32–33°S, in Argentina, the La Ramada stratovolcano

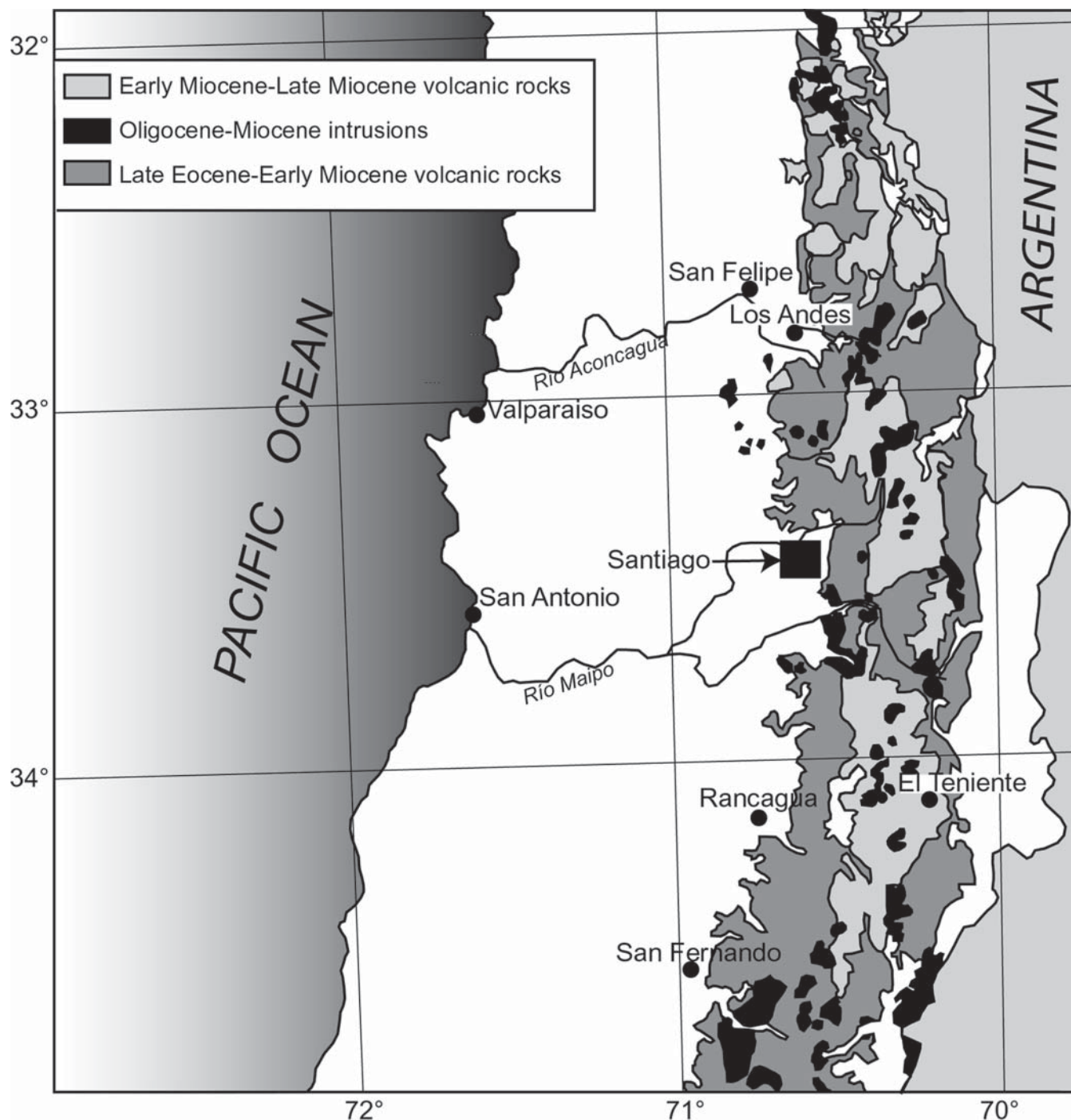


Fig. 4.9. Map showing the distribution of the Tertiary volcanic and plutonic rocks of the Andes of central Chile between 32°S and 35°S.

complex (12.7–10.7 Ma), the Pirámide region centres (11.4–9 Ma) and the Cerro Aconcagua stratovolcano complex (10.3–9 Ma) occur. Lavas from these centres are generally amphibole-bearing medium- to high-K calcalkaline andesites and dacites with La/Yb ratios less than 15, suggesting a crustal thickness of 30–35 km (Kay *et al.* 1991). Near 34°S, the Teniente Volcanic Complex (15–7 Ma; Godoy *et al.* 1999) can be divided into three subgroups (Kay & Kurtz 1995; Kay *et al.* 1999; Kurtz *et al.* 1997; Kay & Mpodozis 2002): (1) the Maqui Chico subgroup, composed of medium- to high-K calcalkaline basalts to rhyolites with highly variable La/Yb ratios that range from 4 to 22, suggesting an amphibole (and titanite)-based residual mineralogy; (2) the Lower Sewell (11–9.5 Ma)

subgroup; and (3) the Upper Sewell (9.3–7 Ma) subgroup. These last two subgroups correspond to medium- to high-K calcalkaline basalts to rhyolites with La/Yb ratios from 7 to 13, but with higher Sm/Yb ratios than those from subgroup (1). Kay *et al.* (1999) suggested that these subgroups originated in a progressively higher pressure magmatic environment in a thickening crust.

At about 34°S, in the Malargüe fold and thrust belt of Argentina, backarc volcanic rocks from the Huincán group (13.9–5.6 Ma) were erupted (Baldauf 1997; Baldauf *et al.* 1997). Their geochemical features correspond to typical backarc lavas and have similar REE patterns to those from the Maqui Chico and Lower Sewell subgroups.

At 33–34°S, the late Miocene magmatic activity in the Teniente Volcanic Complex waned at *c.* 7 Ma (Kay *et al.* 1999; Kurtz *et al.* 1997). The Los Bronces/Rio Blanco tourmaline breccias (7–4.9 Ma; Warnaars *et al.* 1985; Stern & Skewes 1995), the El Teniente region Braden Breccia (4.7 Ma; Cuadra 1986), and the ‘Late Hornblende’ dykes (3.8–2.8 Ma; Kay & Mpodozis 2002) represent the final phase of magmatism in the Main Cordillera. These units mostly comprise medium- to high-K calcalkaline andesites and dacites with La/Yb ratios as high as 77. Although these high ratios suggest a crustal thickness larger than 65 km, Kay *et al.* (1999) and Kay & Mpodozis (2001) have proposed a more conservative estimate of over 45 km. Additionally, source contamination resulting from forearc tectonic erosion has been invoked for the El Teniente rocks (Stern 1991a; Kay *et al.* 2005). In the Sierras Pampeanas, in the backarc, centres with ages of 6.4–1.9 Ma in the Sierra de San Luis (33°S; Ramos *et al.* 1991) are found.

Tectonic controls on magmatic events in central Chile

The spatial, temporal and geochemical patterns of Cenozoic magmatism over the flat-slab segment outlined above were presumably controlled by the composition and state of stress of the lithosphere and the crust through which the magmas erupted, by changes in the convergence parameters, and by changes in the physical nature of the subducted slab. In the flat-slab segment, this latter control corresponds to the subduction of the Juan Fernández Ridge, which arrived at this segment around 14 Ma (Yañez *et al.* 2001, 2002).

Tectonic reconstructions of the convergence between the Nazca (Farallon) oceanic and South American plates are given by Pilger (1984), Pardo-Casas & Molnar (1987) and Somoza (1998). Although these authors examine only the convergence area farther north than 32°S, other studies indicate that the convergence parameters of Somoza (1998) can be assigned to the entire zone from 30°S to 40°S (Jordan *et al.* 2001).

From about 38 to 28 Ma convergence between the plates was 6 cm/year and with a high degree of obliquity (55°) relative to the South American Plate margin. At about 28 Ma the rate of convergence increased to *c.* 9 cm/year, and by around 26 Ma it was even faster (15 cm/year), with the degree of obliquity dropping to *c.* 10° (Somoza 1998). This change in convergence rate at 28–26 Ma was due to the increase in the rate of motion of the subducting plate caused by the break-up of the Farallon Plate (Pardo-Casas & Molnar 1987). Consequently, no change in age or buoyancy of the oceanic lithosphere subducting in the Chile Trench occurred at 28–26 Ma. This period of fast, nearly orthogonal convergence continued until around 20 Ma (Pardo-Casas & Molnar 1987; Somoza 1998).

Along the flat-slab segment, magmatic and tectonic indicators suggest a more compressional Oligocene–Early Miocene (28–20 Ma) tectonic regime in the north than in the south (Kay & Mpodozis 2002). As shown above, calcalkaline arc and backarc magmas were associated with a thicker crust in the Maricunga area (Kay *et al.* 1994; Mpodozis *et al.* 1995) than in the Los Andes–El Teniente area (Kurtz *et al.* 1997; Kay *et al.* 1999; Godoy *et al.* 1999; Nyström *et al.* 2003; Fuentes *et al.* 2000). Charrier *et al.* (2002b) have pointed out that during this period the South American active continental margin between 32°S and 36°S experienced a long-term extensional episode. Volcanic, volcanoclastic and sedimentary deposits accumulated in a north–south orientated, strongly subsident, extensive basin system that can be assigned to an intra-arc basin (Charrier *et al.* 2002b). Extensional basins have been suggested as far south as 42°S (Muñoz *et al.* 2000; Jordan *et al.* 2001).

Concerning the period between approximately 20 and 16 Ma, disagreements exist in the convergence models of the Nazca–South American plates, arising from uncertainties in sea-floor spreading histories. Three different convergence models have been proposed: (a) the rate of convergence increased from 15 to

c. 18 cm/year and had only a small obliquity increase (Pardo-Casas & Molnar 1987); (b) the rate of convergence decreased from 15 to 13 cm/year and the degree of obliquity increased from *c.* 10° to *c.* 30° relative to the plate margin (Somoza 1998); and (c) the dextral obliquity of convergence slightly decreased (Cande & Leslie 1986; Kay & Mpodozis 2002).

The change in the convergence parameters at about 20 Ma marked the beginning of the long period of Miocene compressional deformation and tectonic inversion along the flat-slab segment (Kay & Mpodozis 2002). The reduced magmatic activity during the interval 20–17 Ma recorded in some regions could be explained by a mechanical adjustment between the two converging plates due to the change in convergence parameters. Evidence for this compressional regime comes from: (1) tectonic inversion and uplift at 20–18 Ma at 34°S, suggested by Kurtz *et al.* (1997) and Godoy *et al.* (1999); (2) high-angle reverse faulting at 30°S (Maksaev *et al.* 1984) and inception of Precordillera thrusting (Jordan *et al.* 1993) at 18 Ma; (3) eastward expansion of the magmatic arc into the Calingasta/Uspallata Valley and western Precordillera (Kay *et al.* 1988). Additionally, from 32°S to 36°S during the interval 20–16 Ma, contractional conditions prevailed with the tectonic inversion of pre-depositional extensional faults taking place (Charrier *et al.* 2002b). Nevertheless, Nyström *et al.* (2003) have indicated that, at least near 33°S, extensional conditions continued until *c.* 18 Ma, an age that in accordance with Kay *et al.* (1987, 1991, 1999) marks the initial shallowing of the subduction zone beneath the flat-slab segment. From 32°S to 34°S the frontal arc moved toward the east and an eastward broadening of the arc occurred, which widened the Central Depression as far as the western Precordillera in Argentina (Kay & Mpodozis 2002). Evidence for this eastward migration extends from 30°S to 36°S (Kay & Abbruzzi 1996; Kay *et al.* 1987), but is not recorded in the Maricunga area where vigorous arc volcanism reinitiated there at 16 Ma (Kay *et al.* 1994).

High La/Yb ratios in some lavas erupted during this time, although indicative of high pressure mineral residuals, cannot be explained by crustal thickening (Sellés 1999b; Kay & Mpodozis 2002). The use of lower crustal contamination models like the MASH (melting, assimilation, storage, homogenization) model of Hildreth & Moorbath (1988) allows an explanation for long-term systematic REE changes in the Miocene flat-slab magmas (Kay *et al.* 1987, 1991; Kay & Abbruzzi 1996), but transient variations require unreasonable changes in crustal thickness over a short period of time (Kay & Mpodozis 2002). Therefore, Kay & Mpodozis (2002) have related such high La/Yb ratios to the melting of forearc continental crust tectonically removed by subduction erosion and incorporated into the oxidized, hydrated mantle wedge (von Huene & Scholl 1991; Stern 1991a; Kay & Mpodozis 1999). However, melting of mixtures of subducted metabasalt and sediments cannot be discarded.

At 14 Ma, the arrival of the Juan Fernández Ridge occurred. The subsequent period (14–9 Ma) is characterized by thrusting related to compressional shortening and andesitic arc volcanism along the entire flat-slab segment. All convergence models indicate a rate faster than 10 cm/year and a degree of obliquity of *c.* 12°. Kay & Mpodozis (2002), assuming that the Juan Fernández Ridge affected a region of about 150–200 km, suggested that the passage of the ridge through the Maricunga area at 14 Ma correlates with the transition from a stratovolcanic chain to an isolated ignimbrite complex at about 11 Ma, producing magmas with high La/Yb ratios (e.g. Copiapó Complex). Ignimbrites erupted in the backarc at 15–14 Ma when the ridge arrived, and other similarly felsic volcanic units were formed as the ridge migrated south. At 12–10 Ma, the ridge arrived at the El Indio area, coinciding with the change from the andesite-dominated Cerro de Las Tórtolas Formation to the dacite-dominated Tambo Formation. As in the Maricunga area, lavas of this latter formation have high La/Yb ratios.

Ridge subduction cannot explain coeval events in the Los Andes–El Teniente area, because this region is located south of the area affected by the ridge. The increase in La/Yb ratios from 14 to 10 Ma in this area coincides with crustal thickening associated with compressional shortening (Kurtz *et al.* 1997; Kay *et al.* 1999; Godoy *et al.* 1999). Deformation at 14–9 Ma in this region (Baldauf *et al.* 1997) is similar in age to that inferred for the Precordillera in the north (12–10 Ma) by Jordan *et al.* (1993). Therefore, crustal shortening and thickening have been associated with a regional compressional regime that extended beyond the region affected by the subduction of the Juan Fernández Ridge (Kay & Mpodozis 2002). Overall, this situation suggests that the Oligocene–early Miocene extensional basin between 33°S and 36°S could have been developed as far as 30°S and that processes of crustal thickening may be associated with tectonic inversion of the extensional basin, between 30°S and 36°S, in addition to the subduction of the Juan Fernández Ridge (Charrier *et al.* 2005a).

The subduction of the NE arm of the Juan Fernández Ridge changed around 10 Ma due to the subduction of the east–west segment of the ridge. In the Maricunga area, the arc front shifted eastward at 7–5 Ma, coinciding with the passage of the NE-trending arm. The magmas in this new arc (Copiapó stratocone and Jotabeche complex) have very high La/Yb ratios, suggesting a high pressure residual mineralogy. The chemistry of these magmas has been interpreted as the result of an episode of forearc subduction erosion as the slab shallowed and the front migrated eastward (Kay & Mpodozis 1999, 2000, 2002). At 4 Ma, the NE-trending ridge segment had passed the Maricunga area, allowing the modern CVZ to be stabilized before 2 Ma.

In the El Indio area, arc volcanism ceased at 5 Ma and the eruption of the backarc Cerro Blanco centre at 7 Ma appears to be related to the passage of the bend in the ridge below the eastern Precordillera (Kay & Mpodozis 2002). In contrast in the Los Andes–El Teniente area, arc volcanism ceased at 9 Ma with the last eruptions of the La Ramada/Cerro Aconcagua/Pirámide centres, coinciding with the arrival of the bend in the ridge beneath the frontal arc (Kay & Mpodozis 2002). Further south, at 34°S, magmatic patterns cannot be explained by ridge subduction, because this region is outside of the influence of the ridge. However, again the magmatic and tectonic evolution in this region is similar to that of the north. The arc front migrated eastward at 7 Ma, coinciding with a major compressional deformation event (Kurtz *et al.* 1997; Godoy *et al.* 1999). Although the end of volcanism in the modern flat-slab frontal arc and the arc migration events at 8–4 Ma in the Maricunga and Los Andes–El Teniente areas coincide with the subduction of the kink of the ridge axis and the arrival of the east–west ridge segment, the ridge was only a perturbation in a much larger set of driving forces affecting the Andean margin (Kay & Mpodozis 2002). Such forces appear to be related to variations in the Nazca–South American plate convergence parameters.

The Central Depression and Coastal Cordillera late Oligocene–early Miocene volcanism (37–44°S) (J.M.B., R.T.V. & C.R.S.)

In south-central Chile between 37°S and 44°S, late Oligocene–early Miocene volcanic and subvolcanic rocks are locally exposed both to the east and within the Main Andean Cordillera, as well as within the Central Depression and along the coast on the western slope of the Coastal Cordillera (Fig. 4.10). Particularly good exposures of these partially eroded Oligocene–Miocene volcanic complexes have been identified in the Los Angeles–Temuco segment within the Central Depression and along the coast on the western slope of the Coastal Cordillera at Bahía Capitanes, Caleta Estaquilla, Caleta Parga,

Ancud and Guapi Quilan islands, the latter to the SW of Quellón town (Fig. 4.10). These exposures represent remains of individual volcanic complexes previously grouped together as the Coastal Cordillera Volcanic Belt (Vergara & Munizaga 1974), the Eocene–Miocene Central Depression Volcanic Belt (López-Escobar *et al.* 1976), the Central Depression Upper Oligocene–Miocene Volcanic Belt (Stern & Vergara 1992) and/or the Coastal Magmatic Belt (Muñoz *et al.* 2000). Both Central Depression and Coastal Cordillera volcanic complexes define a NNE-trending belt interpreted by Muñoz *et al.* (2000) as the late Oligocene–early Miocene volcanic front (Fig. 4.10).

Central Depression and Coastal Cordillera Oligocene–Miocene volcanic complexes were emplaced upon Palaeozoic–Triassic metamorphic basement and the effusive products underlie, cover or are interbedded with late Oligocene to early Miocene continental and/or marine sedimentary sequences. These relationships indicate that this magmatic activity was synchronous with the opening and/or subsidence of forearc and intra-arc continental and/or marine sedimentary basins (i.e. Temuco-Labranza, Valdivia, Osorno-Llanquihue and Chiloé basins; Fig. 4.10) (Cisternas & Frutos 1994; Martínez & Pino 1979; Muñoz *et al.* 1997, 2000; Elgueta *et al.* 2000b). Other Oligocene–Miocene intra-arc continental or marine sedimentary basins were also open along and to the east of the Main Cordillera between 37°S and 44°S, for example the Curmallin continental basin (Niemeyer & Muñoz 1983; Suárez *et al.* 1992; Suárez & Emparan 1995), Lago Ranco marine basin (Campos *et al.* 1998) and Nirihaio marine and continental basin (Spalletti & Dalla Salda 1996). These Main Cordillera and extra-Andean sedimentary basins were also temporally related to Oligocene–Miocene volcanism, (i.e. Lago Ranco volcanics (Campos *et al.* 1998) and El Maitén Volcanic Belt east of the Main Cordillera (Rapela *et al.* 1988).

K–Ar geochronology

All available whole-rock K–Ar ages and cited localities for the Oligocene–Miocene volcanic complexes between 37°S and 44°S are shown in Figure 4.10. Most of K–Ar determinations in the Los Angeles–Temuco segment are in the range 29–20 Ma (Vergara & Munizaga 1974; Rubio 1993; Stern & Vergara 1992; Troncoso 1999; Elgueta *et al.* 2000b; Muñoz *et al.* 2000). Muñoz *et al.* (2000) reported K–Ar ages from 28 to 25 Ma for samples in the Los Angeles–Temuco segment and from 29 to 22 Ma in the Guapi Quilan Islands Complex, SW of Quellón. García *et al.* (1988) and Muñoz *et al.* (2000) obtained ages of 21 and 24 Ma for samples from the volcanic neck at Punta Polocué, and 20 to 23 Ma for samples in the vicinity of Ancud, both belonging to the Ancud Volcanic Complex. Stern & Vergara (1992) and Muñoz *et al.* (2000) determined ages of 25 and 23 Ma, respectively, for glassy compacted fragments separated from a rhyolitic pyroclastic flow cropping out within Ancud city. Also, a conventional U–Pb age determination for zircons separated from a 10 cm ashfall deposit separating two coal layers interbedded in a continental sedimentary sequence within the Catamutún coal mine in the western portion of the Central Depression, north of Osorno city, yielded an age at the Oligocene–Miocene boundary (23.5 ± 0.5 Ma; Elgueta *et al.* 2000b), in good agreement with the K–Ar data. Similar late Oligocene to early Miocene ages have been reported in the western slope of the Main Cordillera in the Colbún area (36°S; Vergara *et al.* 1988, 1999) and north, west, east and SE of Santiago (33–34°S; Wall & Lara 2001; Nyström *et al.* 2003; Fuentes *et al.* 2002; Muñoz *et al.* 2006), confirming the prolongation of the Oligocene–Miocene volcanism north of 37°S.

Two K–Ar ages for a basaltic andesite and a dacite from Bahía Capitanes Complex gave ages of 32.9 and 27.5 Ma (Muñoz *et al.* 2000), the former older than most of the other dated samples. Due to alteration assemblages indicative of

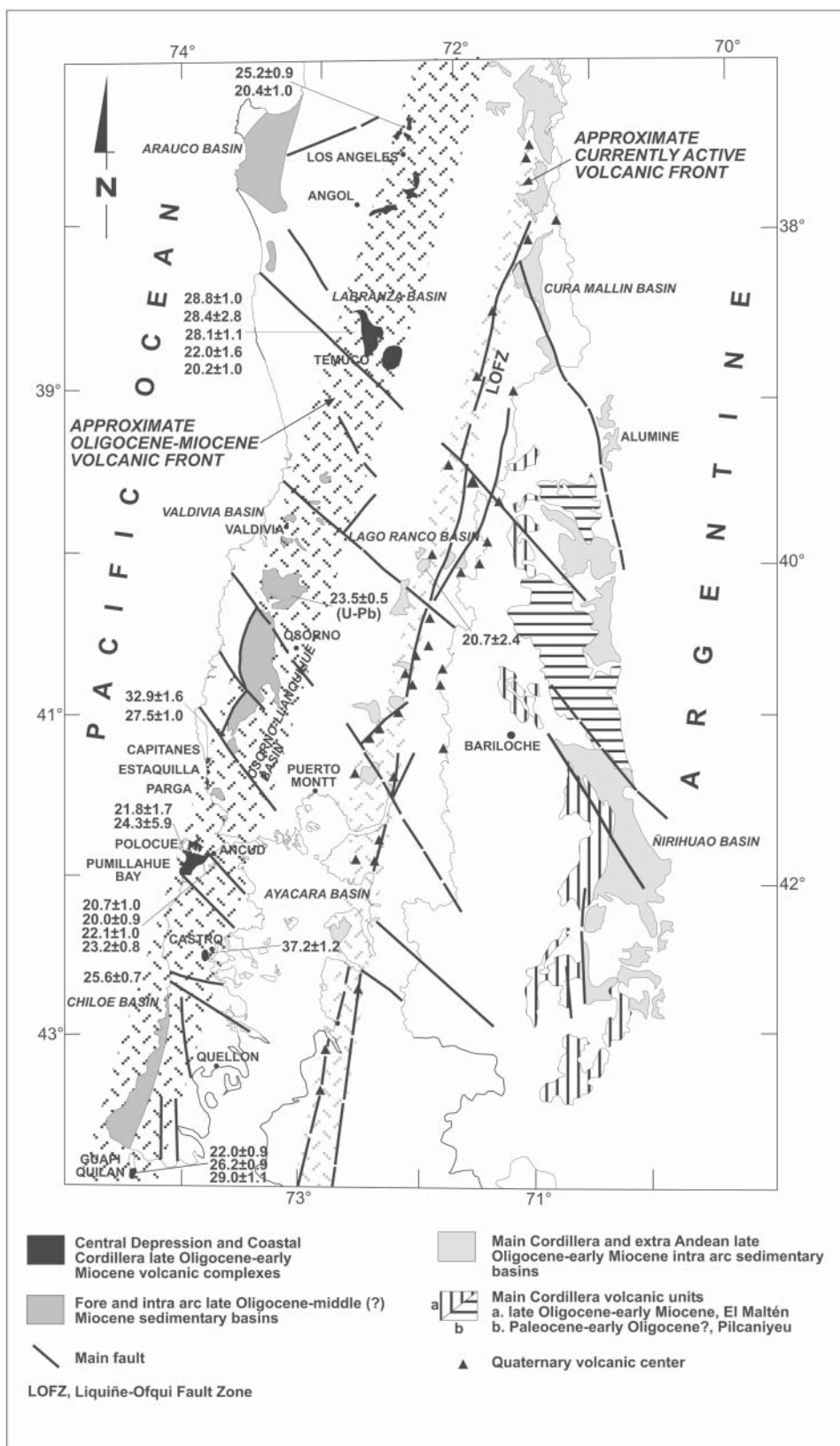


Fig. 4.10. Distribution and K-Ar ages for the Central Valley and Coastal Cordillera late Oligocene-early Miocene volcanic complexes, and related sedimentary basins between 37 and 44°S, including contemporaneous sedimentary basins and volcanic units within and east of the Main Cordillera (modified after Muñoz *et al.* 2000). Also shown are the approximate location of the Oligocene-Miocene and current active CSVZ volcanic fronts.

magma–seawater interaction, no viable K–Ar ages have been determined yet for samples from the Parga and Estaquillas complexes. Available K–Ar data between 37°S and 44°S suggest an older Coastal Cordillera Tertiary magmatic pulse in Eocene–early Oligocene times, represented by dacitic biotite- and quartz-bearing sills cropping out near Castro city (37.2 ± 1.2 Ma; Valdivia & Valenzuela 1988; Muñoz *et al.* 2000), altered dacitic porphyry at Río Futa (52.7 Ma in sericite; Peri & Rivera 1991), and tonalitic bodies at Metalqui locality south of the Ancud Volcanic Complex (39.6 ± 0.3 Ma; Arenas & Duhart 2003). Similar Eocene–early Oligocene ages have been reported in the western slope of the Main Cordillera at the lower part of the volcanic sequence in the Colbún area (36°S; Vergara *et al.* 1988, 1999) and north and SE of Santiago (Fuentes *et al.* 2002; Muñoz *et al.* 2006), confirming the existence of this older pulse. Whether the older early Oligocene age obtained at Capitanes belongs to this earlier pulse is still unresolved. Unfortunately, the alteration assemblage does not permit reliable ages for the Parga, Capitanes and Estaquillas complexes.

Petrography

Oligocene–Miocene Central Valley and Coastal Cordillera partially eroded volcanic complexes include porphyritic to aphanitic lava and pyroclastic flows, ashfall tuffs, hydrothermal and hyalopilitic breccias, glassy domes or bodies, columnar jointed volcanic necks, sills and dykes. Most of the lava flows, sills, necks and dykes range from basaltic to andesitic in composition, although dacitic and rhyolitic members are also represented at some localities (e.g. Los Angeles, Capitanes, Estaquillas and Ancud complexes). Although there is not a clear north–south petrographic or mineralogical trend, orthopyroxene phenocrysts are common in andesites of the Los Angeles–Temuco (37–39°S) segment and in the Guapi Quilan complex (43°30'S), but they are rare or absent in basalts and basaltic andesites in the Caleta Parga, Capitanes, Estaquilla and Ancud complexes (41–42°S), which show mostly clinopyroxene and olivine as phenocrysts and microcrysts.

Plagioclase, clinopyroxene, orthopyroxene (\pm hornblende) porphyritic subalkaline andesitic lava flows, necks, stocks and dykes, and quartz \pm K-feldspar dacites dominate in the Los Angeles–Temuco segment, with trachytic or glassy groundmass (Vergara 1982; Rubio 1993; López-Escobar & Vergara 1997; Troncoso 1999). No olivine basalts have been reported in this segment and red-coloured hornblende phenocrysts are common in the vicinity of Temuco.

Necks and lavas in the Capitanes, Estaquilla and Caleta Parga volcanic complexes are porphyritic to aphanitic plagioclase, clinopyroxene, olivine basalts and basaltic andesites, with trachytic, interstitial, ophitic or intergranular groundmass (Troncoso *et al.* 1994; Troncoso 1999; Muñoz *et al.* 2000; Vargas 2001). Dacitic domes and subvolcanic bodies, which occur east of the coastline and to the south of Estaquilla, have porphyritic textures and show trachytic groundmass. Pyroclastic rocks including accretionary lapilli and pyroclastic flows interbedded with volcanoclastic marine sandstones and polymictic conglomerates are also common in the Caleta Parga and Estaquillas complexes.

The Ancud Volcanic Complex (Vergara & Munizaga 1974; Valenzuela 1982, García *et al.* 1988; Stern & Vergara 1992; Muñoz *et al.* 1997, 2000) includes basaltic to andesitic lava flows and volcanic necks (Fig. 4.11), rhyolitic pyroclastic flows, and black-coloured obsidian bodies. Basaltic andesite necks and lava flows have fine-grained and porphyritic textures with labradorite plagioclase, clinopyroxene and olivine in a glassy groundmass. Pyroclastic rocks are abundant at Pumillahue bay and are mainly represented by white, glassy, lithic-rich rhyodacitic pyroclastic flows (Figs 4.12 & 4.13) with fresh plagioclase, orientated fragments of both white and compacted



Fig. 4.11. Columnar jointing in basaltic andesitic neck at Punta Polocue, Ancud Volcanic Complex (photo by J. Muñoz).

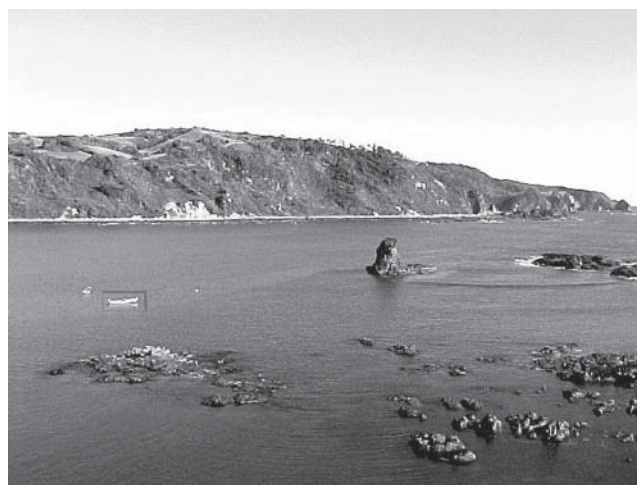


Fig. 4.12. Panoramic view to the south of the Pumillahue bay showing mafic dark volcanic rocks and white coloured pyroclastic flows, Ancud Volcanic Complex (photo by J. Muñoz).



Fig. 4.13. Lithic-rich rhyodacitic pyroclastic flow at Pumillahue bay, Ancud Volcanic Complex (photo by J. Muñoz).

black pumice, partially altered volcanic lithics, rounded clastic sedimentary fragments and carbonized wood, within a recrystallized perlitic, silicic glass.

The secondary alteration assemblage (mainly calcite, silica, chlorite and/or zeolites, with silica, calcite and zeolites filling amygdaloids, veins and/or as disseminations) is well represented in all the volcanic complexes along the present-day coastline (Capitanes, Parga, Estaquillas and Ancud volcanic complexes) and has been suggested to represent magma–seawater interaction during eruptions (Muñoz *et al.* 2000). Also, hyalopilitic breccias in the Capitanes Complex have been interpreted as the centre of a submarine volcanic system (Alfaro *et al.* 1994). Clear evidence of hydrothermal alteration (e.g. infilled vesicles, chalcedony, calcite and/or limonite veins, hydrothermal breccias and supergene clay minerals) and Au and As geochemical anomalies have been detected in most of the late Oligocene–early Miocene Central Valley and Coastal Cordillera volcanic complexes, but have been described in detail only in the Parga Complex (Vargas 2001).

Petrochemistry

Although most of the samples from the Oligocene–Miocene Central Valley and Coastal Cordillera volcanic complexes are arc-type subalkaline rocks in terms of silica, total alkalies, TiO_2 , Ba, Nb and REE contents, an important number of samples from volcanic complexes along the coastline on the western slope of the Coastal Cordillera (Capitanes, Estaquillas, Parga and Ancud complexes) show alkaline affinities and Ba/La, La/Nb and/or La/Yb ratios similar to oceanic island basalts (Muñoz *et al.* 2000).

In the Los Angeles–Temuco segment, low TiO_2 subalkaline orthopyroxene-bearing arc-type andesites show moderate LREE enrichment relative to HREE ($\text{La/Yb}=4\text{--}7.3$), LIL enrichment relative to LREE ($\text{Ba/La}=24\text{--}31$) and HFSE depletion relative to REE ($\text{La/Nb}>2.3$), compared to oceanic island basalts (López-Escobar *et al.* 1976; López-Escobar & Vergara 1997; Muñoz *et al.* 2000; see Fig. 4.14A & B). These ranges for La/Yb, Ba/La and La/Nb ratios are all similar to those reported from stratovolcanoes and minor eruptive centres (MEC) along the current volcanic front at a similar latitude (37°S to 43°S , Hickey *et al.* 1986; Hickey-Vargas *et al.* 1989; López-Escobar & Vergara 1997), confirming the subalkaline affinities shown by petrographic and mineralogical observations.

As noted by Muñoz *et al.* (2000), not all basalts and basaltic andesites from the Capitanes, Parga, Estaquillas and Ancud volcanic complexes have clear geochemical signatures indicative of the incorporation of components derived from the dehydration of subducted oceanic lithosphere. Some basalts from Caleta Parga and some basaltic andesites from Bahía Capitanes have relatively high TiO_2 ($\geq 2\text{ wt\%}$) compared to typical arc-type calcalkaline or tholeiitic mafic rocks, indicating a more alkaline composition. Also, REE contents in these complexes are higher than those in andesites from the Los Angeles–Temuco complexes, although their La/Yb ratios (4.5–5.2) are similar. In contrast, Ba/La (8.8–21.2) and La/Nb (1.4–2.1) ratios (Fig. 4.14A & B) of these mafic samples are more similar to oceanic island basalts and extend to significantly lower values than the samples from the Los Angeles–Temuco segment and the basalts from stratovolcanoes and MEC along the volcanic front of the active Central Southern Volcanic Zone (CSVZ) of the Andes.

Similarly, some basaltic andesite samples from the Ancud Complex have high TiO_2 ($> 2\text{ wt\%}$) and more alkaline affinities, similar to the samples from Caleta Parga, whereas other basalts and basaltic andesites are clearly subalkaline. La/Yb ratios (4.6–5.9) of basalts and basaltic andesites from Ancud are similar to those from the Bahía Capitanes, Caleta Parga, and the Los Angeles–Temuco segment. In contrast, Ba/La ratios (12.5–19.2) are similar to the samples from Bahía Capitanes and

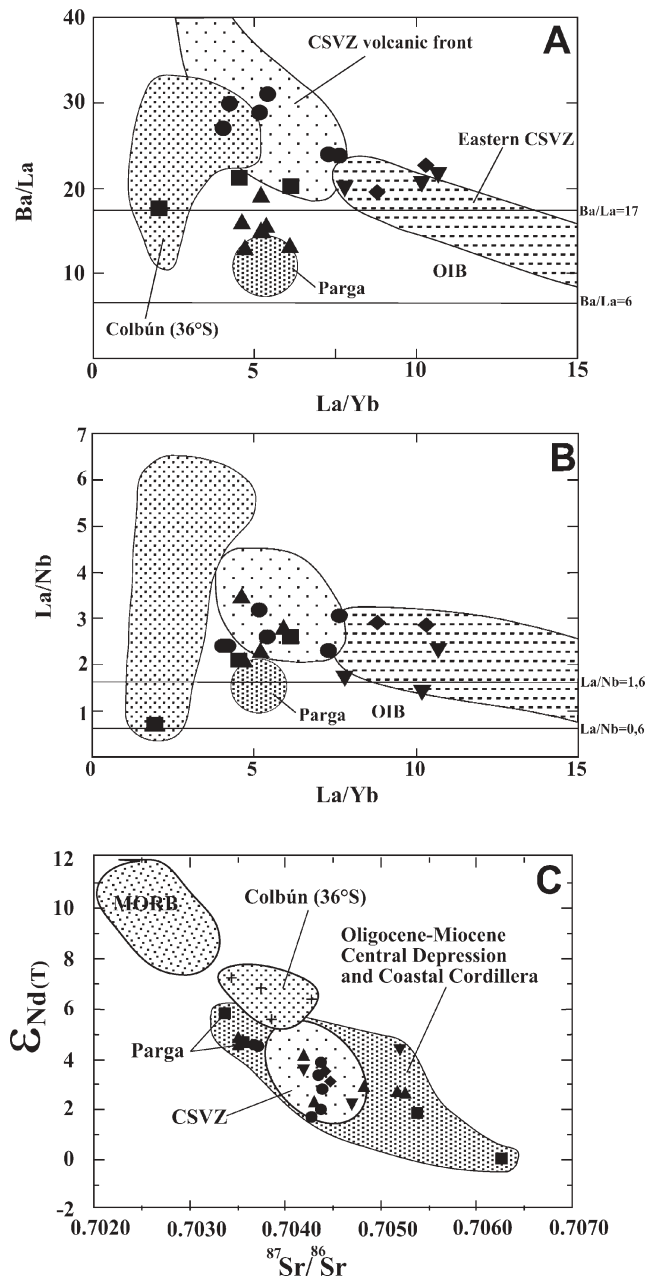


Fig. 4.14. (A) Ba/La versus La/Yb ratios, (B) La/Nb versus La/Yb ratios and (C) initial $^{87}\text{Sr}/^{86}\text{Sr}$ ratios versus ϵ_{Nd} , for late Oligocene–early Miocene Central Valley and Coastal Cordillera volcanic complexes between 37°S and 44°S : Los Angeles and Temuco (circles), Capitanes and Estaquilla (squares), Ancud and Polocue (triangles), Gamboa and (diamonds), Guapi Quilan (inverted triangles). Also shown are fields for the Parga Volcanic Complex, Colbún area (Vergara *et al.* 1999) and CSVZ (data in Hickey *et al.* 1986; Hickey-Vargas *et al.* 1989; Muñoz & Stern 1989; Stern *et al.* 1990; López Escobar & Vergara 1997). Modified after Muñoz *et al.* (2000).

Caleta Parga, but lower than those from Los Angeles–Temuco, and from stratovolcanoes or MEC basalts of the current volcanic front of the CSVZ, while La/Nb ratios (1.6 to > 3.5) are transitional between the values for samples from the Bahía Capitanes–Caleta Parga and the Los Angeles–Temuco segment. The silicic pyroclastic rocks from Ancud have high REE contents and a significant negative Eu anomaly, but similar La/Yb, Ba/La and La/Nb ratios to the associated mafic rocks.

Sr, Nd and Pb isotopes

In addition to petrochemical alkaline affinities and trace element similarities to ocean island basalts, basalts from Parga have initial Sr and Nd isotopic compositions (Fig. 4.14C) more primitive than most other samples determined for the Oligocene–Miocene Central Valley and Coastal Cordillera complexes (Muñoz *et al.* 2000) and the current volcanic front of the active CSVZ, including MEC basalts (López-Escobar & Vergara 1997). On the other hand, basaltic andesites, dacites and rhyolitic members from Capitanes and Estaquillas have higher initial $^{87}\text{Sr}/^{86}\text{Sr}$ ratios and lower initial $^{143}\text{Nd}/^{144}\text{Nd}$ isotopic ratios, with the higher Sr and lower Nd values represented by rhyolitic members, suggesting possible assimilation of Palaeozoic–Triassic crust. Some basaltic andesites from the Ancud Complex have primitive initial Sr and Nd isotopic compositions similar to basalts from Caleta Parga, while other mafic samples from this complex are similar to CSVZ and MEC along the present-day volcanic front (Fig. 4.14C). One basaltic sample from Los Angeles–Temuco complexes shows an Sr and Nd isotopic composition similar to that of the Caleta Parga complex, whereas other mafic samples from these complexes are similar to CSVZ and MEC along the present-day volcanic front (as is the Guapi Quilan complex).

As reported by Muñoz *et al.* (2000), Pb isotopic composition of the more mafic rocks at Parga are similar to magmas erupted from the active CSVZ, whereas dacites and rhyodacites show higher values of the Pb isotopic ratios, again possibly due to crustal assimilation. In contrast, the glassy rhyodacitic pyroclastic flow in the Ancud Complex is isotopically similar to more mafic rocks from the same complex.

Petrogenesis

The Central Valley and Coastal Cordillera volcanic complexes between 37°S and 44°S represent the late Oligocene–early Miocene volcanic front located between 80 and 100 km to the west of the current Andean volcanic front at a similar latitude (Fig. 4.10). Alteration assemblages, especially those in the Coastal Cordillera complexes, indicate magma–seawater interaction and submarine volcanism, suggesting that part of this volcanic front formed as an island arc built on the Palaeozoic–Triassic continental crust.

The Oligocene–early Miocene volcanism, the opening of sedimentary basins and the initiation of development of the present-day Central Valley in south-central Chile (37–44°S) all occurred during a widespread regional episode of crustal extension (Muñoz *et al.* 2000; Jordan *et al.* 2001; Muñoz & Stern 2003). This regional episode of late Oligocene to early Miocene extension, the related volcanism and the opening and subsidence of sedimentary basins have also been reported along and in the western slope of the Main Cordillera north of 37°S to the north, east and south of Santiago (Nyström *et al.* 1993, 2003; Thiele *et al.* 1991; Vergara *et al.* 1999; Godoy *et al.* 1999; Charrier *et al.* 2005a). Evidence for Oligocene–Miocene crustal extension includes low-angle normal faulting bounding the western edge of the present-day Central Valley (Muñoz *et al.* 2000) and the Cura Mallin sedimentary basin on the eastern flank of the Main Andean Cordillera (Spalletti & Dalla Salda 1996; Jordan *et al.* 2001). Also, regional negative gravity and positive magnetic anomalies (Muñoz & Arana 2000) and interpretation of seismic reflection profiles (McDonough *et al.* 1997) suggest a thin crust (33 km) below the Central Valley and the Main Cordillera as a consequence of crustal thinning during late Oligocene–early Miocene extension. The late Oligocene (± 29 Ma) initiation of the Central Valley and Coastal Cordillera volcanism and sedimentary basin opening were coeval with plate reorganization in the SE Pacific (Cande & Leslie 1986; Tebbens & Cande 1997), resulting in an increase in plate convergence rate below the southern Andes that changed

the geometry of plate subduction from oblique to almost orthogonal (Pardo-Casas & Molnar 1987; Somoza 1998).

No obvious chronological, petrographic, chemical or isotopic north–south trend may be defined for the Oligocene–Miocene Central Valley and Coastal Cordillera volcanic rocks (Muñoz *et al.* 2000). However, subalkaline orthopyroxene andesites predominate in the Los Angeles–Temuco segment and the Guapi Quilan complexes, the northern and southern representatives of the Central Valley and the Coastal Cordillera volcanism between 37°S and 44°S. Primitive basalts and basaltic andesites with alkaline affinities are important in the Capitanes, Parga, Estaquillas and Ancud volcanic complexes along the Pacific coastlines of the Coastal Cordillera.

All Oligocene–Miocene mafic volcanic rocks have Pb isotopic compositions similar to the samples from the current volcanic front of the CSVZ at the same latitude, but this is not always true for trace element ratios and Sr and Nd isotopic compositions. The occurrence at some localities of mafic rocks with alkaline affinities, low La/Yb, Ba/La (< 17) and La/Nb (< 1.6) ratios and primitive Sr and Nd isotopic compositions (e.g. Parga and Ancud complexes), suggest local absence or at least lowered input of slab-derived hydrous fluids into the mantle source region. Also, Central Valley and Coastal Cordillera Oligocene–Miocene volcanism does not exhibit a negative correlation between either Ba/La or La/Nb and La/Yb, as do the current volcanic arc magmas at the same latitude. Trace element geochemical data suggest that dehydration of subducted slab may not have been the fundamental mechanism driving magma genesis for some Coastal Cordillera volcanic complexes. The fact that all the samples have similar Pb isotopic compositions and many have Ba/La and La/Nb ratios similar to those of the modern Andean arc magmas has been interpreted as the effects of source region contamination of the subcontinental mantle during earlier episodes of subduction of oceanic lithosphere below this portion of the southern South American continent (Muñoz *et al.* 2000).

Geochemical data suggest not all late Oligocene–early Miocene Central Valley and Coastal Cordillera magmatism was directly related to slab dehydration, but that chemically heterogeneous mantle sources were also involved, some resembling the sources of oceanic basalts and being apparently free of slab-derived components. Muñoz *et al.* (2000) suggested that some of these magmas (e.g. Parga, Capitanes and Ancud volcanic complexes) resulted from an asthenospheric slab window which developed in association with changes in convergence rate and direction, and with slab-rollback of the subducting Nazca Plate. This scenario is envisaged to have developed in response to a transient episode of invigorated asthenospheric wedge circulation caused by the three-fold increase in late Oligocene trench-normal convergence rates between the Nazca and South American plates. Thus, during the late Oligocene, more rapid (10 cm/year) subduction at a steeper angle resulted in the opening of a slab window and upwelling and melting of asthenospheric mantle uncontaminated by slab-derived components. This led in turn to interaction of these melts with subcontinental mantle lithosphere containing stored slab-derived components, and to crustal extension and subsidence (see model in Fig. 4.15).

The ending of Central Valley and Coastal Cordillera volcanism between 37°S and 44°S during the early Miocene (± 20 Ma) did not coincide with any obvious change in plate convergence rates. It did, however, broadly coincide with closure of the Central Valley and Coastal Cordillera sedimentary basins (e.g. Osorno–Llanquihue basin) which occurred during early (Martínez & Pino 1979) or middle Miocene (Elgueta *et al.* 2000b) due to tectonic inversion that gently folded the sedimentary sequences. Early Miocene tectonic inversion also produced the closure and folding of the continental sedimentary basins and related sedimentary sequences along the Main Cordillera

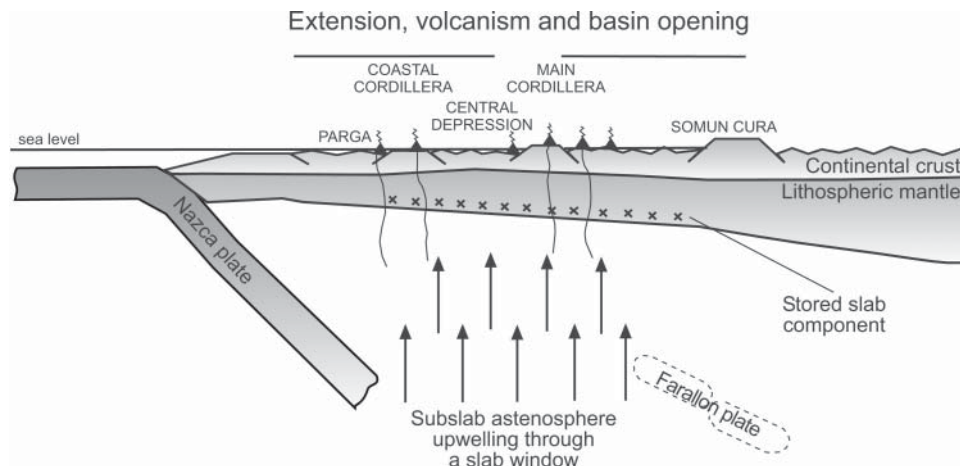


Fig. 4.15. Proposed schematic tectonic cross-section across the western margin of southern South America, at approximately the latitude of the Parga Volcanic Complex (41°S), during late Oligocene–early Miocene times.

north and south of Santiago (Godoy *et al.* 1999; Charrier *et al.* 2005a). During the early to middle Miocene, westward extension of the continental margin and a decreasing angle of subduction returned the arc to its current position in the Main Cordillera and caused deformation, uplift and exposure of the late Oligocene–early Miocene volcanic and sedimentary rocks.

Magmatism in the North Patagonian Andes (40–47°S) (M.A.P., D.M. & F.E.)

The North Patagonian Andes, developed between the North Patagonian Massif and the Coastal Cordillera, extend from about 40°S to 47°S, where the triple-junction between the Nazca, South America and Antarctic plates is located. The North Patagonian Andes is mainly the result of intensive subduction-related magmatism active since mid-Jurassic time. Evidence for this magmatism is provided by the Early Cretaceous–late Cenozoic North Patagonian Batholith (Pankhurst *et al.* 1999), the Jurassic–Eocene arc and backarc volcanism (Parada *et al.* 2001b), and the Holocene volcanoes of the southern segment of the Southern Volcanic Zone. One of the most striking structural features of the North Patagonian Andes is the north–south Liquiñe–Ofqui Fault Zone, a dextral strike-slip fault system recognized for *c.* 900 km from 39°S to 47°S (Thiele *et al.* 1986), that played a key role in the emplacement of Neogene–Holocene magmatic rocks.

The North Patagonian Batholith

The magmatic evolution of the North Patagonian Andes has been mainly documented in the arc domain, particularly in the North Patagonian Batholith, where distinct plutonic events have been identified (Fig. 4.16) by using different radiometric methods (Rb–Sr isochrons, K–Ar and ⁴⁰Ar/³⁹Ar; Halpern & Fuenzalida 1978; Bartholomew 1984; Pankhurst *et al.* 1999; Suárez & De La Cruz 2001). This batholith occupies the axis of the North Patagonian Andes and constitutes, together with the South Patagonian Batholith, one of the largest batholiths on earth. Identification of individual plutons within the batholith is difficult due to their similar lithology and the dense forest cover. The western margin of the batholith is defined by intrusive contact with low-grade metasedimentary rocks of the Late Palaeozoic subduction complex, whereas the eastern margin is marked by an intrusive contact with the Jurassic Ibáñez Formation.

The North Patagonian Batholith was formed episodically from Early Cretaceous to late Tertiary times. Based on recently published geochronological data (Pankhurst *et al.* 1999; Suárez & De La Cruz 2001; Cembrano *et al.* 2002) it is possible to recognize three main plutonic events: Cretaceous, early Miocene and late Miocene–Pliocene. Unlike the Mesozoic–Cenozoic plutonic development in central Chile, the locus of the North Patagonian Batholith components does not change significantly with time. For example, along the northern (40–42°S) segment of the batholith, two north–south plutonic belts are recognized occupying the axis of the Cordillera: an eastern Early Cretaceous belt and a western early to late Cenozoic belt (Carrasco 1995). The boundary between the two belts roughly coincides with the Liquiñe–Ofqui Fault Zone. Further south (44–47°S) the batholith is, in a broad sense, formed by western plutons forming a poorly defined Early Cretaceous belt, a central Miocene to Pliocene belt of isolated plutons, and eastern Early to mid-Cretaceous intrusions forming the widest plutonic belt of the batholith (see Pankhurst *et al.* 1999; Suárez & De La Cruz 2001).

The batholith as a whole exhibits a wide lithological spectrum with a typical calcalkaline affinity. The Cretaceous granitoids include mainly metaluminous granodiorites and tonalites, whereas the Miocene–Pliocene granitoids are composed of different lithologies that cover a wide spectrum from gabbro to granite (Parada *et al.* 1987; Pankhurst *et al.* 1999). Peraluminous granites have been found as part of the late Miocene plutonic event closely related to the Liquiñe–Ofqui Fault Zone (Parada *et al.* 1987, 2000).

The North Patagonian Batholith shows progressive variation in Sr and Nd isotopes with time, from enriched Early Cretaceous granitoids to depleted late Cenozoic rocks (Pankhurst *et al.* 1999). This isotopic evolution, which is similar to that shown by the Late Palaeozoic–Early Cretaceous evolution of the Coastal Batholith in central Chile, has been attributed to mixed sources, in different proportions, of mafic crustal underplate and lower crust (Pankhurst *et al.* 1999). An alternative explanation, however, based on thermochronological and geobarometric evidence, has been invoked for the origin of the late Cenozoic rocks, such as the Queulat Complex in the vicinity of the Liquiñe–Ofqui fault Zone at 44°30'S. This complex includes 18–16 Ma deep-seated (19–24 km) quartz-diorites and tonalites (Parada *et al.* 2000) and 10 Ma peraluminous shallow (<10 km) granitoids (Hervé *et al.* 1993), that would have been formed by partial melting of a lower crust that underwent modifications in its thermal structure. Such modifications would have been derived from rapid exhumation events along

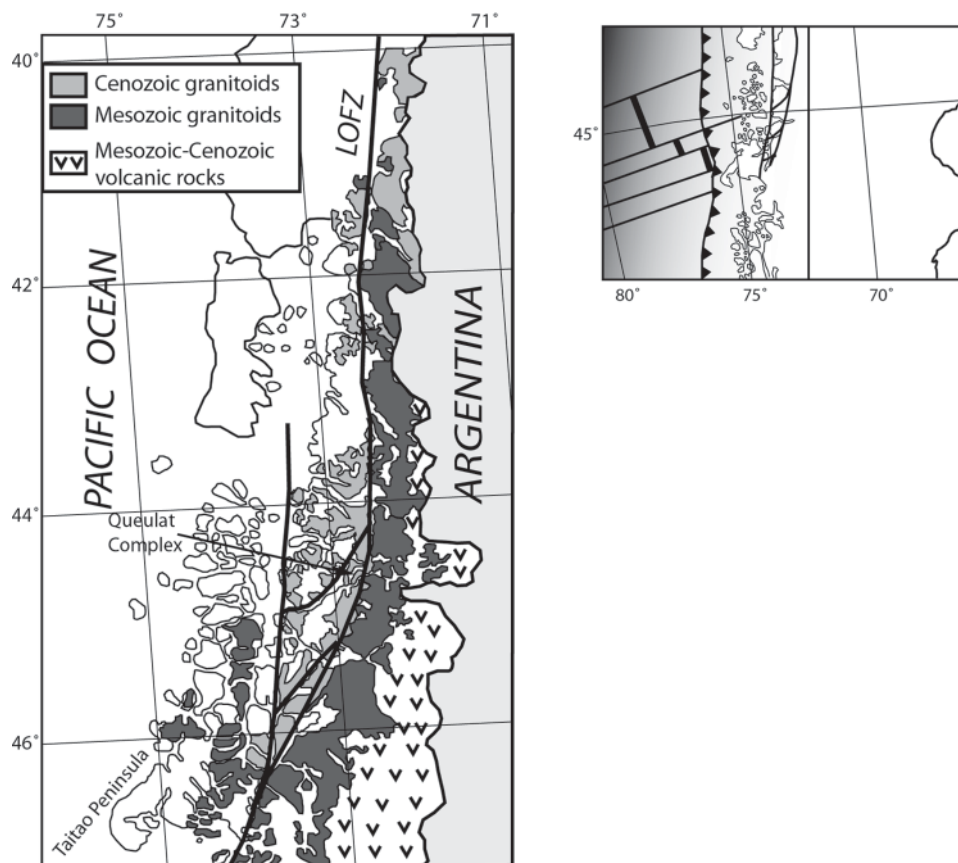


Fig. 4.16. Distribution of the plutonic components of the Northern Patagonian Batholith.

the Liquiñe–Ofqui Fault Zone (Hervé *et al.* 1993; Parada *et al.* 2000) during a contractional deformation generated from a nearly orthogonal subduction episode.

The Mesozoic–Eocene backarc volcanism of the North Patagonian Andes

The volcanic rocks located to the east of the North Patagonian Batholith are the result of a Meso-Cenozoic backarc extensional regime (Bartholomew & Tarney 1984). The area where these rocks are continuously exposed corresponds to the eastern flank of the North Patagonian Andes of the Aysén Region between 45°S and 47°S.

The products of the Mesozoic volcanism, erupted over highly deformed Late Palaeozoic metamorphic rocks cropping out south of 46°S, have been placed into a Jurassic Ibáñez Formation and a Cretaceous Divisadero–Ñirehuao Formation. The Eocene volcanism is represented by the Balmaceda basalts, the rhyolitic tuffs of the Chile Chico Formation (Niemeyer 1975), and the lower section of the Meseta Buenos Aires plateau basalts (Charrier *et al.* 1979; Petford *et al.* 1996).

The Ibáñez Formation includes felsic to intermediate volcanic rocks underlying an Early Cretaceous marine succession (Bell & Suárez 1997) of the Coyhaique Group, and is part of the Jurassic Large Igneous Province of Patagonia associated with the break-up of Gondwana (Féraud *et al.* 1999; Pankhurst *et al.* 2000). K-feldspar and biotite $^{40}\text{Ar}/^{39}\text{Ar}$ ages and U–Pb zircon data indicate an age interval between 130 and 160 Ma for the deposition of this formation (Pankhurst *et al.* 2000; Parada *et al.* 2001b). The integration of field, radiometric, geochemical and scarce isotopic data available for these Jurassic volcanic rocks and related plutons indicates a significant crustal

participation in the origin of these magmas (Parada *et al.* 1997; Pankhurst *et al.* 2000).

The Divisadero–Ñirehuao Formation, which represents the most intensive event of the backarc volcanism, overlies the Ibáñez Formation and marine rocks of the Coyhaique Group. It is composed mainly of felsic tuffs and rhyolites, although flat-lying basalts are also found in the eastern exposures of this unit. Available radiometric data for this formation indicate that Cretaceous volcanism in this region developed during the interval 115–75 Ma, slightly after the Cretaceous plutonic event of the North Patagonian Batholith (Parada *et al.* 2001b). Following this, after a period of magmatic quiescence lasting about 20 Ma, an Eocene volcanic event developed during the interval 46–55 Ma (Parada *et al.* 2001b) giving rise to olivine flood basalts and felsic tuff components of the volcanic-sedimentary Chile Chico Formation (Niemeyer 1975).

Rocks belonging to the Jurassic–Neogene successions in Chilean Patagonia between 43°S and 46°S have been affected by very-low to low-grade metamorphism (Aguirre *et al.* 1997). Differences in grade are related to the age of the rock successions, with the youngest metamorphosed to zeolite and the oldest to greenschist facies. In addition, in the case of the Jurassic Ibáñez Formation, a thermal input by Cretaceous granitoids has almost completely obliterated an earlier low-grade metamorphic event.

Based on geochemical and isotopic compositions, the backarc volcanic rocks between Coyhaique and Cochrane have been divided into two magmatic units (Parada *et al.* 2001b) referred to as the Northern and Southern magmatic domains. The Southern Magmatic Domain begins at about 46°30'S, and is composed of basalts and intermediate-composition volcanic rocks. They are typically calcalkaline and have enriched Sr–Nd

isotopic values that are compatible with a lithospheric mantle source. In contrast, basalts from the Northern Magmatic Domain have alkaline affinities and depleted to slightly depleted Sr–Nd signatures, suggesting an asthenosphere-dominated source. With regard to the felsic rocks, those in the Southern Magmatic Domain are more isotopically (Sr–Nd) enriched than the equivalent rocks of the Northern Magmatic Domain. These isotopic distinctions between the two domains are attributable to: (i) the participation of Palaeozoic metamorphic basement in the origin of the volcanic rocks of the Southern Magmatic Domain; and (ii) a greater degree of tectonic extension in the Northern Magmatic Domain and, consequently, only minor participation of a thinner lithosphere (Parada *et al.* 2001b).

The Patagonian Plateau Basalts at about 47°S: the role of Chile Ridge subduction

The Cenozoic geodynamic evolution of the western margin of South America has been dominated by the subduction of different lithospheric plates and various oceanic spreading ridges (e.g. Cande & Leslie 1986). A particularly prominent event in the recent history of the margin has been the oblique subduction of the South Chile Spreading Ridge (SCR) beneath the South American Plate, a process that began at 14–15 Ma. At this time a segment of the ridge collided with the Chile Trench near Tierra del Fuego (c. 55°S; Cande & Leslie 1986), generating the Chile triple-junction. The northward migration of the Chile triple-junction involved the subduction of various fracture zone–ridge segments (orientated c. N160), the last of which started subducting at c. 0.3 Ma (SCR1; Cande & Leslie 1986; Bourgois *et al.* 2000) at the Taitao Peninsula (46°12'S; Guivel *et al.* 1999). According to palaeo-tectonic reconstructions (Cande & Leslie 1986), another active ridge, the Farallon–Aluk ridge, collided with the western border of South America during Palaeocene–Eocene times (c. 55–53 Ma). This triple-junction migrated southward reaching Patagonian latitudes at c. 50 Ma.

The subduction of divergent mid-ocean ridges below continental plates is thought to produce a gap between the two subducting plates under the continental backarc region, the so-called slab window, which allows the decompressional melting of upwelling asthenosphere from sub-slab regions (Dickinson & Snyder 1979; Thorkelson 1994, 1996) and subsequent generation of mafic plateau volcanism in the backarc domain. Magmas generated under these conditions are expected to reproduce the chemistry of the asthenospheric mantle beneath the subducting plate (Stern *et al.* 1990; Gorrington *et al.* 1997; D'Orazio *et al.* 2000; Gorrington & Kay 2001), together with the probable occurrence of contamination during their trip to the surface.

The Patagonian flood basalts form an extensive basaltic province east of the Andean Cordillera (Patagonian Plateau Lavas; Fig. 4.17A & B) and extend from approximately 34°S to 52°S (Baker *et al.* 1981). Around 46°S the flood basalts are mostly located south of Lago General Carrera (Fig. 4.17C) and on both sides of the Chile–Argentina international border. In this area, the flood basalts, which overlie Mesozoic–Cenozoic sedimentary and volcanic rocks, have been divided (Baker *et al.* 1981; Charrier *et al.* 1979) into four age and genetically related groups: (i) Late Cretaceous (c. 80 Ma) mainly tholeiitic basalts, with some calcalkaline affinities, related to subduction; (ii) Eocene (c. 57–43 Ma) olivine tholeiites to alkaline basalts emplaced in a backarc domain; (iii) Late Oligocene to Late Miocene (c. 25–9 Ma) dominantly alkali basalts; and (iv) Pliocene to Quaternary (c. 4–0.2 Ma) highly undersaturated basanites. The Tertiary magmatic events are of continental intraplate type and were probably developed in an extensional

regime as an indirect response to the subduction of various active ridges, which would have induced the opening of different slab windows beneath the continent during Eocene and Mio-Pliocene times (Ramos & Kay 1992; Petford *et al.* 1996; Gorrington & Kay 2001; Gorrington *et al.* 1997, 2003; Espinoza *et al.* 2005).

The Chilean Patagonian flood basalts at this latitude form the Meseta Chile Chico, which is located south of Lago General Carrera (46°30'S to 47°S; Fig. 4.17C), c. 300 km east of the present-day position of the Chile triple-junction and slightly eastward of the inferred location of the subducted Chile Ridge Segment 1 (SCR–1; Fig. 4.17B) that collided with the South American Plate c. 6 million years ago. K–Ar ages define two main basaltic sequences in the Meseta Chile Chico: the Lower Basaltic Sequence (57–40 Ma) and the Upper Basaltic Sequence (16–3 Ma) (Charrier *et al.* 1979; Baker *et al.* 1981; Petford *et al.* 1996; Petford & Turner 1996; Flynn *et al.* 2002b; Espinoza 2003; Espinoza *et al.* 2003, 2005). Both sequences are separated from each other by late Oligocene–early Miocene calcareous sandstones of the Guadal Formation (Niemeyer *et al.* 1984; Frassinetti & Covacevich 1999).

The Lower Basaltic Sequence is a 500–550-m-thick pile of basaltic lava flows and some peridotite xenolith-bearing basanitic necks (Espinoza & Morata 2003b). These late Palaeocene–Eocene basalts can be correlated with the 57–45 Ma Posadas Basalt (Baker *et al.* 1981; Kay *et al.* 2002) and with the c. 42–49 Ma Balmaceda Basalts (Baker *et al.* 1981; Demant *et al.* 1996; Parada *et al.* 2001b), located further east and north of the Meseta Chile Chico basalts, respectively.

The Upper Basaltic Sequence comprises a 400-m-thick pile of basalts, with minor rhyolites, covering an area of about 300 km². This Mio-Pliocene upper series can be correlated with similar volcanic rocks at the Meseta del Lago Buenos Aires (Fig. 4.17B). Taking into account all the published K–Ar ages, a magmatic gap of 24 ± 4 Ma (between 38 ± 2 and 14 ± 2 Ma), is defined in this Patagonian sector during the Tertiary (Espinoza *et al.* 2005).

Petrology and geochemistry of the flood basalts

Olivine, clinopyroxene and plagioclase plus minor Fe–Ti oxides are the main phenocrysts in intergranular, pilotaxitic, rarely intersertal or ophitic to subophitic basalts from both the lower and upper sequences. A major petrographic difference is the presence in basalts of the upper sequence, of rounded quartz xenocrysts (1–3 mm) rimmed by clinopyroxene (<0.5 mm), the composition of which is similar to those of clinopyroxene phenocrysts of the host basalts (Espinoza *et al.* 2005).

Basalts of the lower sequence are mainly ne-normative olivine basalts and scarce hy-normative olivine tholeiites ranging in composition from basanites to trachybasalts, whereas those of the upper sequence classify as basalt, basanite, trachybasalt, basaltic trachyandesite (rocks with quartz xenocrysts) with alkaline affinities (mainly ne- and minor hy-normative olivine basalts) and high-K calcalkaline rhyolites. The basic and acid terms of the upper sequence define a bimodal distribution with a distinctive lack of intermediate compositions between 54 and 72 wt% SiO₂. In both, the lower and upper series, the high [Mg#] number, together with high Ni, Cr and Co contents are consistent with those of mantle-derived primitive melts. Major, trace and rare earth element geochemistry of both lower and upper series basalts are indicative of an OIB-like signature of magmas.

According to Espinoza *et al.* (2005), the lower-series-basalts have initial ⁸⁷Sr/⁸⁶Sr ratios of 0.70385 to 0.70311 and εNd values from +5.1 to +4.9. These values are generally consistent with previous analyses for the Eocene basalts (Hawkesworth *et al.* 1979; Baker *et al.* 1981; Parada *et al.* 2001). Moreover, the lower series basalts display similar initial ⁸⁷Sr/⁸⁶Sr ratios and εNd

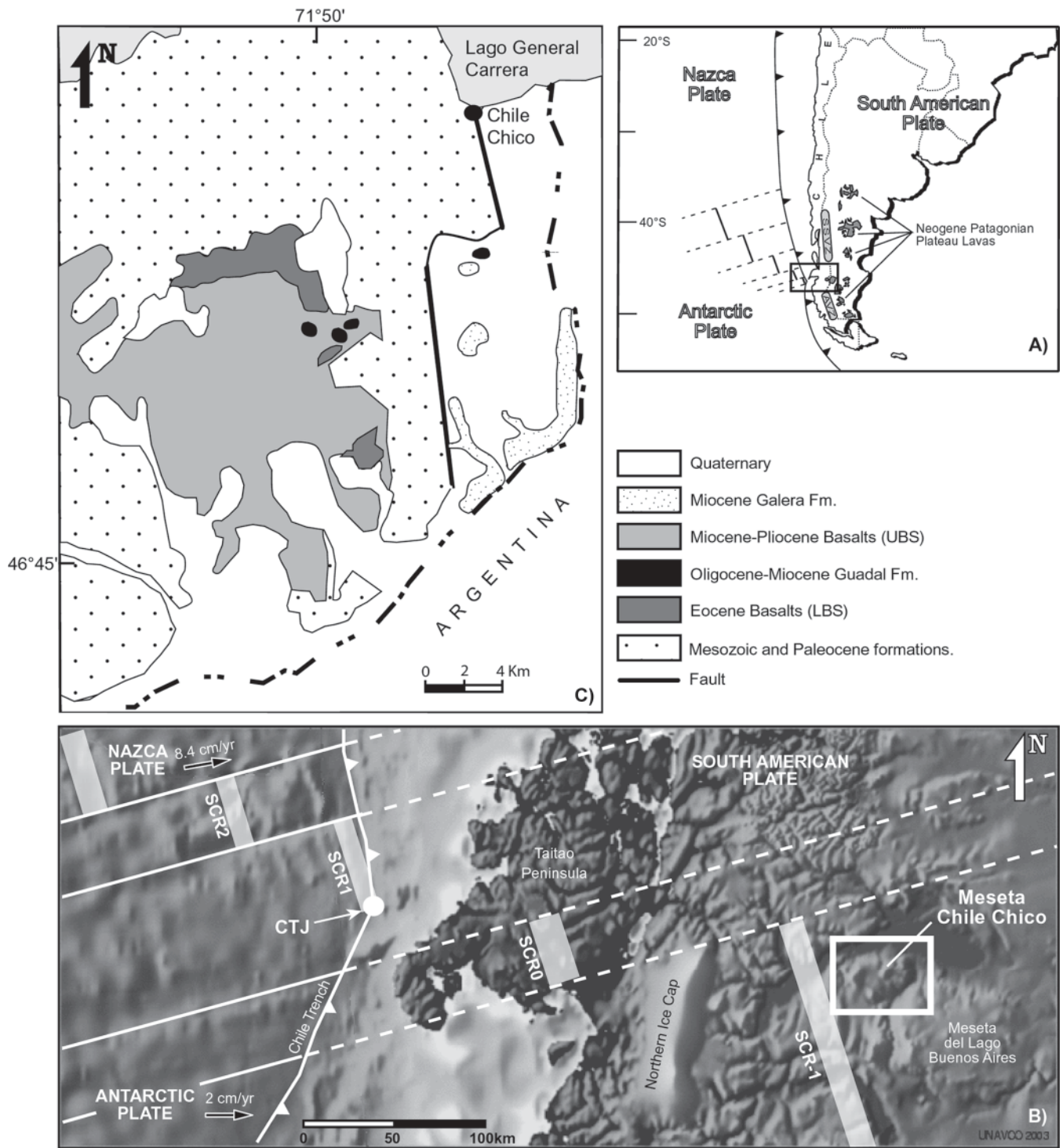


Fig. 4.17. (A) General view of South America showing the distribution of the Patagonian Neogene Plateau Lavas together with the location of the study area and of the Southern South (SSVZ) and Austral Volcanic Zone (AVZ) in the Southern Andes. (B) Tectonic setting of southern South America between 45.8–47.4°S and 75.8–76.6°W, in the area of Lake General Carrera, showing location of present-day Chile triple-junction, Meseta Chile Chico and Meseta del Lago Buenos Aires, relative to fracture zones and Southern Chile Ridge (SCR2, SCR1, SCR0 and SCR-1) segments (Cande & Leslie 1986). Black arrows indicate relative sense of motion of Nazca and Antarctic plates with respect to the South American Plate, numbers are plate average velocity. C) Simplified geological map of the Meseta Chile Chico (46°35′–46°47′S; 71°46′–72°02′W), south of Lake General Carrera (modified from Espinoza *et al.* 2005).

values compared with the coeval Posadas Basalts (Ramos & Kay 1992; Kay *et al.* 2002). An andesitic sample from the upper series has an initial $^{87}\text{Sr}/^{86}\text{Sr}$ ratio of 0.70414 and an ϵNd value of +4.7. A Miocene rhyolite has an initial $^{87}\text{Sr}/^{86}\text{Sr}$ ratio of 0.70449 and ϵNd value of +0.7, very similar to those obtained in a coeval pluton (Paso de la Llavas granite; Pankhurst *et al.* 1999) located in a neighbouring locality.

Petrogenetic model and geodynamic implications

Using trace element ratios, REE and isotopic modelling, Espinoza *et al.* (2005) suggested that lower- and upper-series intermediate and primitive basaltic magmas were generated at approximately similar pressures by equivalent degrees of partial melting of similar mantle sources, characterized by the presence of garnet as a residual phase (Yb_N 6.6–9.5).

The genesis of the Patagonian flood basalts in the Meseta Chile Chico may be integrated within a model based on the opening of two different slab windows below South America during the Eocene and Pliocene epochs, respectively (Ramos & Kay 1992; Espinoza *et al.* 2005). This kind of model is based on the temporal evolution of ridge–trench collision and slab window development under southern South America and has been proposed for other Patagonian basaltic sequences deposited during Pliocene–Recent events (Gorring *et al.* 1997, 2003; D’Orazio *et al.* 2000).

Despite several uncertainties concerning the related geodynamic evolution, a slab window model for Eocene magmatism is strongly supported by the deep mantle geochemistry (OIB-like signature) of the Eocene lavas (Ramos & Kay 1992; Kay *et al.* 2002). The geotectonic reconstruction for early Tertiary times proposed by Cande & Leslie (1986) shows that around 50 Ma one segment of the active Farallon–Aluk ridge would have collided with the Chile Trench at Patagonian latitudes (*c.* 46°S). This collision would have induced the opening of a slab window beneath the South America continental margin, with subsequent melting and ascent of subslab asthenosphere.

The basaltic episode of the upper series would have begun between 12 and 10 Ma, prior to the arrival of the slab window beneath the Lago General Carrera basalts. At *c.* 5 Ma, the partially opened slab window may have been located beneath this area. Consequently, as proposed for the Eocene period, together with a new extensional tectonic event (and uplift as a consequence of late Miocene compression; Ramos 1989; Flint *et al.* 1994; Morata *et al.* 2003), decompressional melting would occur in the subslab asthenosphere. The Meseta Chile Chico is characterized by the occurrence of long-lived magmatism since Eocene to Pliocene times, as a consequence of some kind of thermal and compositional anomaly responsible for the input of primitive OIB-like asthenospheric melt.

Magmatism in the southernmost Andean segment (47–56°S) (M.C.)

The present-day geodynamic situation of the southernmost segment of the Patagonian Andes, a 4000-m-high mountain belt with only rare volcanism and a complex fold and thrust belt to the east, is dominated by the subduction of the Antarctic oceanic lithosphere beneath the South American continental plate. Along the convergent margin several spreading-centre segments have been subducted during the Miocene epoch. This phenomenon is temporally and spatially related to pauses in arc volcanism and the eruption of large volumes of backarc plateau basaltic lavas (Ramos & Kay 1992; Gorring *et al.* 1997). The northern limit of the convergent margin is given by the subduction of the Chile Ridge, resulting in the Pliocene obduction of the Taitao ophiolite (47°S) in the forearc region (Forsythe *et al.* 1986; Hervé *et al.* 2003b).

South Patagonian Batholith

The composite South Patagonian Batholith and the Fuegian Batholith, which extends to around 1200 km long and 50–100 km wide between 47°S and 55°S, is flanked to the east and west by metamorphic complexes with protoliths of Palaeozoic ages (Fig. 4.18), and which record diachronous metamorphic events associated with the evolving continental margin of Gondwana and South America (Hervé *et al.* 2003a; see chapter 2). The composite Southern Patagonian Batholith consists of hypidiomorphic and medium- to coarse-grained mafic (diorite, gabbro), intermediate (tonalite, quartz-diorite, quartz-monzodiorite) and felsic (granite, monzogranite, granodiorite) lithologies. Layered gabbros containing pyroxene and olivine,

often with coronitic texture, are commonly found, whereas the dominant intermediate and felsic rocks contain hornblende and/or biotite. Accessory minerals in intermediate and felsic rocks include magmatic epidote (allanite), titanite and Fe–Ti oxides, among others (Weaver *et al.* 1990; Ureta 2000). The eastern side of the batholith is composed mainly of biotite granites (Nelson *et al.* 1988; Weaver *et al.* 1990) spatially related with migmatites and high-grade metasedimentary rocks and minor biotite–muscovite leucogranites with garnet and tourmaline (*c.* 49°S; Calderón *et al.* 2003). In general, between 48°S and 50°S intermediate and felsic compositions predominate in the western and eastern margin of the batholith, respectively, whereas mafic rocks are more abundant along the central part (Ureta 2000).

Hornblende geobarometry indicates that the components of the batholith were emplaced in the upper crust between 2 and 4 kbar (50–52°S; Dzogolyk *et al.* 2003), which is consistent with widespread andalusite–sillimanite in metapelitic rocks along a diachronous regional aureole at the eastern margin of the batholith (48–50°S; Calderón & Hervé 2000). Deeper levels of emplacement, equivalent to *c.* 5.5 kbar, have been estimated from the celadonite content of magmatic muscovite in garnet-bearing granites east of the Southern Patagonian Batholith (*c.* 51°40′S; Massonne *et al.* 2004).

The ages of the plutonic components of the Southern Patagonian Batholith range from 151 to 16 Ma (Bruce *et al.* 1991; Martin *et al.* 2001) and are distributed in a zoned pattern. Jurassic plutons occur along the eastern margin (*c.* 151–141 Ma), Early Cretaceous plutonic units have been identified in the west (*c.* 137 Ma), and Late Cretaceous to Tertiary granitoids are concentrated near the central axis of the SPB (U–Pb conventional and SHRIMP zircon ages; Martin *et al.* 2001). This age distribution, which is also revealed by K–Ar and ⁴⁰Ar/³⁹Ar methods, has been considered as the result of an ‘inflating’ batholith, where younger intrusions are hosted in older granitoids within an extending magmatic arc (Bruce *et al.* 1991).

Low-temperature cooling ages of the batholith have been revealed by zircon and apatite fission track thermochronology along a southern NW–SE transect, at *c.* 50°S. Reset zircon fission track ages reveal a progressive decrease from 18 to 14 Ma (Thomson *et al.* 2001), which are similar to ⁴⁰Ar/³⁹Ar (in hornblende) and K–Ar (biotite) ages (*c.* 18 to *c.* 13 Ma) of Miocene satellite plutons located to the east of the Southern Patagonian Batholith (at *c.* 51°S; Bruce *et al.* 1991).

Whole-rock major and trace element compositions of the Southern Patagonian Batholith plutons indicate calcalkaline metaluminous affinities (Stern & Stroup 1982; Weaver *et al.* 1990). The batholith has been divided into a tonalitic and a granodioritic series, suggesting that differentiation of two distinct parental magmas occurred during batholith formation (Nelson *et al.* 1988; Weaver *et al.* 1990). Initial ⁸⁷Sr/⁸⁶Sr ratios range from 0.7036 to 0.7074 and initial εNd values from +7 to –7 (Fig. 4.19). The older plutonic rocks have the highest initial ⁸⁷Sr/⁸⁶Sr ratios and lowest εNd values (48°S; Weaver *et al.* 1990). These isotope compositional variations have been interpreted as evidence for magma contamination by Palaeozoic metasedimentary rocks. An origin from mantle-derived magmas, with crustal melts that progressively decrease in importance with time, has been inferred (Weaver *et al.* 1990).

At Puerto Edén (*c.* 49°S), the easternmost biotite granites (assumed to be Jurassic) have initial ⁸⁷Sr/⁸⁶Sr ratios of *c.* 0.7075 and negative εNd of *c.* –7, which are considered to reflect a contribution from Palaeozoic metasedimentary rocks in their genesis, during low-pressure and high-temperature anatexis (Calderón *et al.* 2003; Hervé *et al.* 2003a). Western plutonic rocks of Early Cretaceous ages (*c.* 130–137 Ma) in the Archipiélago Madre de Dios (*c.* 50°S) have initial ⁸⁷Sr/⁸⁶Sr ratios ranging from 0.7046 to 0.7050 and low positive εNd from 0 to +1. The magma source of this pluton is thought to lie at the base of the continental crust (Duhart *et al.* 2003).

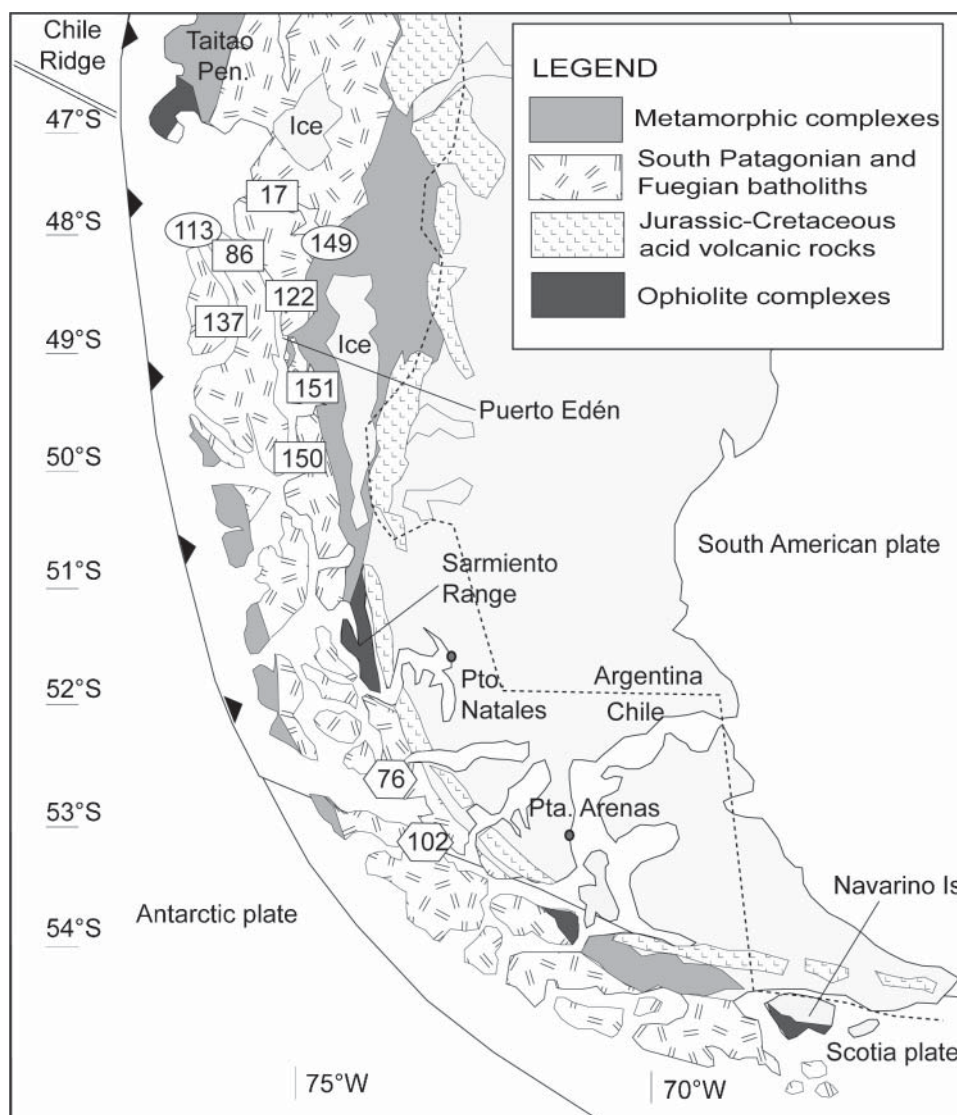


Fig. 4.18. Sketch map of the southernmost segment of the Patagonian Andes of southern Chile, modified from Pankhurst *et al.* (1998) and Mapa Geológico de Chile (Sernageomin 2002). Selected zircon U-Pb ages (in Ma) of the South Patagonian batholith: in ellipses, from Weaver *et al.* (1990); in hexagons, from Bruce *et al.* (1991); and in boxes, from Martin *et al.* (2001).

Mesozoic volcanic rocks

Jurassic felsic volcanic rocks

Along the eastern side of the Patagonian and Fuegian Andes, Jurassic and Cretaceous supracrustal and plutonic rocks (Fig. 4.18), formed during continental rifting, gave rise to the Rocas Verdes backarc marginal basin succession (Bruhn *et al.* 1978; Dalziel 1981; Stern & de Wit 2003). These units have subsequently been deformed by several thrusting episodes. The closure of this marginal basin began after 100–120 Ma (Dalziel 1981), with a later development of the Magallanes foreland basin after the Turonian (*c.* 92 Ma; Fildani *et al.* 2003).

Silicic volcanic rocks of the El Quemado and the Tobífera formations form the westernmost components of the Jurassic Chon Aike Large Igneous Province, which is considered to be the product of extensive crustal anatexis (Pankhurst & Rapela 1995; Pankhurst *et al.* 1998). The Tobífera and El Quemado formations have SHRIMP zircon ages of *c.* 172–173 Ma and *c.* 153 Ma, respectively (Pankhurst *et al.* 2000). The plutonic equivalent of these formations is the S-type biotite–garnet granite suite (of *c.* 160 Ma; U–Pb zircon age) of the Darwin Cordillera, interpreted as a product of the anatexis of upper

crustal metasedimentary rocks during the earliest stages of backarc basin formation (Hervé *et al.* 1981*c*; Mukasa & Dalziel 1996).

Thrust sheets of foliated silicic rocks of the Tobífera Formation (Galaz *et al.* 2005), cropping out to the north and south of the southern Patagonian ice field, are correlated with subsurface silicic rocks in southeastern Patagonia, seen in boreholes in the Magallanes basin (Fuenzalida & Covacevich 1988; Pankhurst *et al.* 2000). However, this correlation is not supported by recent data of the Andean components which yield a Late Jurassic age of crystallization (*c.* 148 Ma; Calderón 2006) considerably younger than previously constrained. A sub-aquatic depositional environment has been proposed for at least part of the Tobífera Formation, preceding the formation of the ocean mafic floor of the Rocas Verdes marginal basin (Dalziel 1981; Fuenzalida & Covacevich 1988; Hanson & Wilson 1991).

Late Jurassic–Early Cretaceous mafic rocks

Discontinuous and incomplete ophiolite complexes crop out along the Sarmiento Cordillera (Sarmiento Complex; *c.* 52°S), Navarino Island (Tortuga Complex; *c.* 55°S) (Fig. 4.18) and the

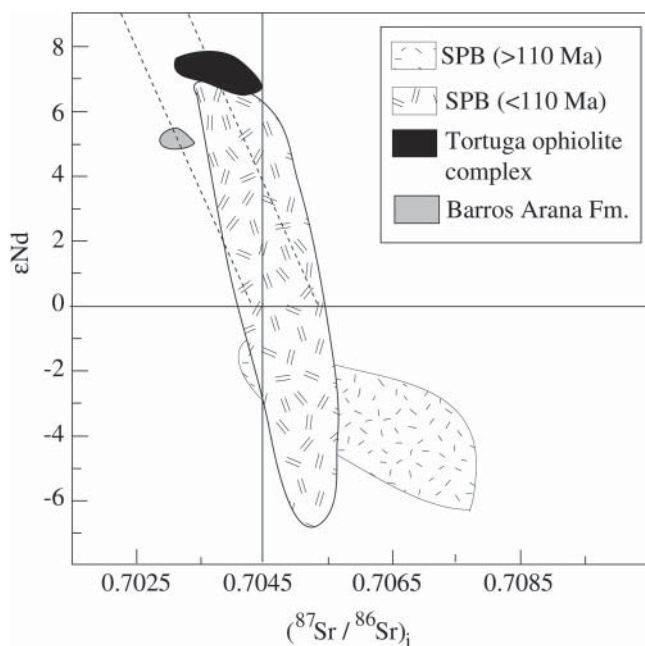


Fig. 4.19. ϵ_{Nd} versus initial $^{87}\text{Sr}/^{86}\text{Sr}$ ratios for rocks in the SPB (Weaver *et al.* 1990), Tortuga ophiolite complex (Stern 1991b) and Barros Arana Formation (Stern *et al.* 1991).

island of South Georgia. They consist of submarine mafic extrusives, sheeted dykes, gabbros and local plagiogranites, flanked on both sides by successions of silicic volcanic rocks. They are interpreted as ophiolites formed at a mid-ocean-ridge-type spreading centre during Late Jurassic and Early Cretaceous times (Dalziel 1981; Stern *et al.* 1992; Mukasa & Dalziel 1996; Stern & de Wit 2003). The mafic rocks of the Tortuga Complex have tholeiitic trends, low initial $^{87}\text{Sr}/^{86}\text{Sr}$ ratios (0.70323 to 0.70429) and high ϵ_{Nd} values (+6.8 to +7.6) (Fig. 4.19), indicating that they were derived from a depleted MOR-type asthenospheric mantle source (Stern 1991b). REE compositions and ϵ_{Nd} values from +0.8 to +2 were obtained in the Sarmiento complex, suggesting a slightly enriched E-MORB-type magmatic source. The age of the ophiolite complexes has been inferred from U–Pb zircon ages of 136–142 Ma (Sarmiento Complex; Stern *et al.* 1992) and 150 ± 1 Ma (South Georgia island; Mukasa & Dalziel 1996) obtained in plagiogranites. The observed diachronism of the ophiolite emplacement is considered indicative of a northward ‘unzipping’ mode of marginal basin formation (e.g. Stern & de Wit 2003).

Early Cretaceous (*c.* 104 Ma) spilitized clinopyroxene–amphibole-bearing mafic dykes and lavas with mildly alkaline shoshonitic affinities, occur *c.* 20 km east of the Sarmiento Complex. These rocks have low initial $^{87}\text{Sr}/^{86}\text{Sr}$ ratios (*c.* 0.7030) and ϵ_{Nd} values (*c.* +5.0), which are considered to reflect a contribution from the subcontinental lithospheric mantle in their magma genesis (Stern *et al.* 1991).

Pleistocene to Holocene volcanism in the Chilean Andes (L.L.-E., H.M. & O.F.)

The most recent Andean magmatism has produced three prominent volcanic belts in Chile, situated (i) in the far north, (ii) south from Santiago as far as 46°S , and (iii) in the far south. Volcanism in northern Chile extends into NW Argentina, SW Bolivia and southern Peru, north of which there is another major gap before a fourth major volcanic belt is reached (in the

far NW of South America: see Fig. 5.1 in Chapter 5). Thus Andean volcanism in South America has been divided, from north to south, into four zones: Northern (NVZ), Central (CVZ), Southern (SVZ) and Austral (AVZ); only the last three of these crop out in Chile. These volcanic zones are separated by flat-slab segments where Pleistocene–Holocene volcanism is absent. The following description sets the scene for the more detailed examination of Chilean volcanism presented in Chapter 5.

Northern Chilean volcanoes

Miocene to Recent volcanic activity in the CVZ of northern Chile has produced stratovolcanoes, monogenetic centres and ignimbrites. The stratovolcanoes are the highest volcanic edifices (up to 2000 m above their base). Since they are built on the Altiplano–Puna, their altitude can reach over 6000 m a.s.l. (e.g. Ojos del Salado, 6887 m a.s.l.). They are mainly composed of andesitic lava flows (Déruelle 1979; Wörner *et al.* 1992a), and minor amounts of pyroclastic deposits, some with volcanic avalanche deposits generated by collapse of the central edifice. Domes comprise either dacites or rhyolites, and have either rounded forms and abrupt edges or consist of lateral flows, as illustrated by the Chao flow (22.1°S ; de Silva *et al.* 1995). The monogenetic cones are products of single eruptions. They are small (about 100 m high) and their lavas are less differentiated (basaltic andesites) than those of the stratovolcanoes.

The ignimbrites cover most of the topography of this volcanic zone and, taken together, they constitute the world’s largest late Tertiary–Recent ignimbritic province. They are mainly early Miocene in age in the northernmost part of Chile ($<21^\circ\text{S}$) and late Miocene–late Pliocene between latitudes 21°S and 24°S (Wörner *et al.* 2000b, and references therein). The abundant ignimbrites between 21°S and 24°S have been designated as the Altiplano–Puna Volcanic Complex (de Silva 1989a), which covers more than 70 000 km² and represents $>30\,000$ km³ (Lindsay *et al.* 2001b). Most sources of ignimbrites correspond to calderas, identification of which has been revealed by satellite imagery. These calderas are generally located in the backarc zone, aligned parallel to the actual chain of stratovolcanoes. Some of them, such as the Pacana caldera, have huge dimensions (60 km \times 35 km; Gardeweg & Ramírez 1987; Lindsay *et al.* 2001b).

Beneath this volcanic belt the crust–mantle boundary has a broad transitional character due to active processes such as hydration of mantle rocks, magmatic underplating and intraplate under and into the lowermost crust, and partial melting (ANCORP Working Group 2003). Seismic studies also show a pronounced low-velocity zone in the mid-crust (Wigger *et al.* 1994; Yuan *et al.* 2000; ANCORP Working Group 2003), which together with other geophysical observations (such as bright reflectivity, high conductivity, high heat flow values, negative anomaly in the residual gravity field), has been interpreted as a zone of partial melting (for a review see Babeyko *et al.* 2002; ANCORP Working Group 2003). The low velocities of the P waves ($V_p = c.$ 6 km/s) and the anomalous low Poisson ratio (0.25) would imply that the crust has a felsic composition down to 50–55 km depth (Swenson *et al.* 2000, and references therein), being predominantly mafic at greater depths (Yuan *et al.* 2002).

Petrography and geochemistry

The stratovolcano lavas vary from basaltic andesite to rhyolite with a predominance of andesites and dacites. Plagioclase is the most abundant phenocryst, although olivine, orthopyroxene and clinopyroxene phenocrysts are also found in the basaltic andesites, whereas amphibole can be observed in andesites. The dacitic–rhyolitic domes are highly porphyritic (up to 50 vol%), presenting phenocrysts of amphibole, biotite, and two feldspars, with little or no quartz and pyroxenes. Disequilibrium

textures, such as sieve textures in plagioclase, are common. Most of the Altiplano–Puna Volcanic Complex ignimbrites are crystal-rich and compositionally homogeneous (95% dacites and 5% rhyolites).

Most of the rocks erupted from the CVZ centres have a medium-K calcalkaline character. Generally, TiO_2 , Al_2O_3 , Fe_2O_3^* , MnO and CaO decrease, and K_2O increases, as SiO_2 increases; such patterns are consistent with the fractionation of plagioclase, pyroxenes and Fe–Ti oxides. In comparison with the lavas of SVZ, CVZ lavas are enriched in incompatible elements and have higher $^{87}\text{Sr}/^{86}\text{Sr}$ and lower $^{143}\text{Nd}/^{144}\text{Nd}$, implying a greater amount of crustal contamination (for a review of Andean magma genesis see Stern 2004). The increase in the La/Yb ratio as the Yb contents decrease suggests that this contamination took place deep in the crust, where garnet is a stable phase (e.g. Hildreth & Moorbath 1988; Feeley & Davidson 1994). At this level, mantle-derived magmas evolve by contamination and crystal fractionation to basaltic andesitic composition, which decreases its density and permits the magmas to migrate to shallow crustal levels, where they accumulate at the bases of dominantly andesitic magma chambers. These chambers must be stratified and periodically refill with basaltic andesite magmas (Feeley & Davidson 1994; Matthews *et al.* 1999).

Based on isotopic composition, two types of magma differentiation are recognized (Davidson *et al.* 1991): (a) closed system, e.g. in Nevados de Payachata (Davidson *et al.* 1990, and references therein) and San Pedro–San Pablo (O’Callaghan & Francis 1986), where in spite of their wide variation in elemental composition, they exhibit only minor variations in Sr-, Nd- and Pb-isotopic composition; and (b) open system, e.g. Ollagüe (Feeley & Sharp 1995, and references therein), Licancabur (Figuerola 2001) and Lascar (Matthews *et al.* 1994), where isotopic compositions change with indices of magma differentiation, which is interpreted as the result of assimilation plus fractional crystallization (AFC).

Fractional crystallization played an important role in the origin of dacites from andesitic (or basaltic andesitic) magmas. Magma mixing commonly occurred in addition to fractionation processes, as evidenced by disequilibrium textures (plagioclase resorption), mineralogical disequilibria (inverse zonations) and geothermometric considerations. The latter indicate, for example, higher equilibrium temperatures in the rims of orthopyroxenes than in their cores. In the specific case of Lascar volcano, such heterogeneities have been interpreted to result from the remobilization of crystallized or semicrystallized shallow intrusions of andesitic composition during the injection of basaltic andesite magma (Matthews *et al.* 1999).

The isotopic compositions of the large Altiplano–Puna Volcanic Complex ignimbrites ($^{87}\text{Sr}/^{86}\text{Sr} > 0.709$ and $^{143}\text{Nd}/^{144}\text{Nd} < 0.5123$) are considered to reflect large-scale mid-crustal melting (e.g. de Silva 1989a), which is supported by geophysical studies (see above). Therefore ignimbritic magmas are hybrid but the proportion of crustal to mantle-derived material is difficult to identify because of the heterogeneity of pre-Andean basement (Lindsay *et al.* 2001b). Mixing calculations indicate that compositions of Purico ignimbrites could be produced by adding *c.* 70% crustal components to *c.* 30% mantle-derived basaltic andesite (Schmitt *et al.* 2001), although small ignimbrites that erupted in the immediate vicinity of stratovolcanoes have less crustal influence (Dérulle *et al.* 2000, and references therein).

Southern Chilean Volcanoes

The Southern Volcanic Zone (SVZ)

Volcanic activity in Chile between 33°S and 46°S (SVZ) has been continuous and very active (one eruption per year on average) during post-glacial times (last 15 000 years). The Holocene volcanic front, whose axis is located about 280 km from the

Chile–Peru Trench, has an average width of 40 km, although it is almost 80 km wide around 39°S. The volcanic activity is expressed as numerous composite stratovolcanoes, megacalderas (Diamante, Calabozos, Copahue), domes, and hundreds of minor eruptive centres consisting of scoria cones \pm lava flows and maars. Lahars, ashfalls and lava flows have been the main volcanic hazards within historical times, although pyroclastic flows and surges, together with voluminous debris avalanches, have also occurred during the latest Pleistocene and Holocene. Among the 46 main stratovolcanoes between 33°S and 41.5°S, about 30 of them have erupted in post-glacial times and 18 of them have historical records. On the other hand, most minor eruptive centres are post-glacial, and three of them (Riñinahue, Carrán and Mirador) erupted during the twentieth century. Individual stratovolcano elevations generally vary between *c.* 700 and 2100 m above the base, although further south they reach up to 2500 m.

Field and seismic evidence suggests that the tectonic regime within the SVZ arc has been dextral strike-slip for the last few million years (Cembrano 1992, and references therein). The fact that the direction of maximum horizontal stress ($\sigma_{H_{\max}}$) is roughly N50–70°E may reflect a transpressional tectonic regime, resulting from a combination of dextral strike-slip and shortening across the arc. Following the fracture propagation model of Shaw (1980), rapid ascent of magma should be expected along inherited or newly created NE-trending tensional fractures and faults within the volcanic arc. This agrees with geochemical interpretations based on U–Th disequilibrium considerations (Tormey *et al.* 1991b).

Tectonism seems to control whether or not basaltic magmas either reach the surface or evolve to more differentiated products within the crust. In fact, most young volcanic centres (Late Pleistocene–Holocene), define NE-trending alignments erupting magmas of mainly basaltic to basaltic andesite composition (e.g. Osorno–Puntiagudo–Cordón Cenizas volcanic chain). This is consistent with an extensional regime that allows a short residence time of magmas in the crust, resulting in limited contamination and fractionation of mantle-derived magmas. On the other hand, volcanic edifices controlled by NW-trending fractures and faults (e.g. Villarrica–Quetupillán–Lanín and Puyehue–Cordón Caulle volcanic chains) may be under a combination of shortening and strike-slip deformation, which will cause a longer intracrustal magma residence, yielding more differentiated compositions, including rhyolite.

Basaltic rocks erupted from either N50–60°W or N50–70°E transverse fractures tend to increase their incompatible elements abundances and La/Yb and $^{87}\text{Sr}/^{86}\text{Sr}$ ratios and decrease their Ba/La, and $^{143}\text{Nd}/^{144}\text{Nd}$ ratios from west to east. These geochemical characteristics seem to be independent of the orientation of fractures and faults where those centres are emplaced, suggesting that they are controlled mainly by subduction-related processes.

Even the most primitive basalts of the Andean segment between 37°S and 46°S show evidence of having undergone fractional crystallization. They have $\text{MgO} < 11\%$, and both Ni and Cr are lower than those expected in mantle-derived primary magmas. Olivine and plagioclase phenocrysts are present within the whole suite (basalts to rhyolites), with even a few rhyolites containing fayalitic olivine. Plagioclase phenocrysts vary in abundance from about 1–10% in minor eruptive centres volcanic rocks to 20–50% in stratovolcano products.

Isolated young andesitic stratovolcanoes, such as the Calbuco and Huequi volcanoes, lie on NW-trending lineaments tens of kilometres long. Lanín (Lara & Moreno 1994a) and Tronador (Mella *et al.* 2005) volcanoes are emplaced on an uplifted block, east of the LOFZ main trend. Calbuco was also emplaced on an uplifted block (López-Escobar *et al.* 1995a, and references therein). Unlike other centres, Mocho-Choshuenco, a basaltic andesite to dacitic stratovolcano, located at 40°S

(McMillan *et al.* 1989), is emplaced on a basement that, in addition to Jurassic igneous rocks and Triassic metasediments, contains Palaeozoic metasedimentary rocks of the coastal Western Series.

Two main types of basaltic rocks, one K-depleted ($K_2O < 1\%$; also depleted in other incompatible elements such as Rb, La, Th) and the other K-enriched ($K_2O = 1\text{--}1.5\%$), have been distinguished in places (López-Escobar *et al.* 1995a, and references therein), as well as in stratovolcanoes and minor-eruptive-centre basalts. Only in the K-rich group are minor-eruptive-centre basaltic rocks significantly richer in MgO than stratovolcano basaltic rocks. K-poor basaltic rocks tend to have higher Ba/La and lower La/Yb ratios than K-rich ones. Some of the highest Ba/La and lowest La/Yb ratios are presented by basalts from the Pichihuínco maar (one of the westernmost minor eruptive centres of this Andean region). In contrast, one of the lowest Ba/La and highest La/Yb ratios are exhibited by the Puyuhuapi minor-eruptive-centre basalts (Demant *et al.* 1994; Lahsen *et al.* 1994; López-Escobar & Moreno 1994). In fact, the latter basalts have La/Yb ratios as high as those presented by andesites from the northernmost part of the SVZ (33–34.5°S) (López-Escobar 1984; López-Escobar *et al.* 1995a), where the thickness of the continental crust is 55–60 km. The relatively low Ba/La ratios of the Puyuhuapi and, in general, of K-rich basaltic rocks have been explained by subduction-related processes (López-Escobar *et al.* 1993). These processes could also explain the enrichment of these magmas in incompatible elements and their relatively high La/Yb ratios. The extremely high La/Yb ratio of the Puyuhuapi basalts, which is mainly due to their low Yb contents, also suggests that their parental magmas were in equilibrium with garnet at their mantle source or at lower crustal levels. In both groups of basalts high $^{87}\text{Sr}/^{86}\text{Sr}$ ratios are generally accompanied by low $^{143}\text{Nd}/^{144}\text{Nd}$ ratios, a trend commonly interpreted as evidence of contamination with crustal material.

The Austral Volcanic Zone (AVZ)

The southernmost Andean volcanic segment, located between latitudes 49°S and 55°S, has only six volcanic centres (Chapter 5), and these have erupted andesites and dacites, lacking the basalts and basaltic andesites commonly seen elsewhere in Chile (Kilian *et al.* 1991; Stern & Kilian 1996; Stern 2004). Unlike the CVZ and SVZ volcanoes, the AVZ volcanic centres are the result of subduction of the oceanic Antarctic plate below the South American plate. Relatively low base and summit elevations, and the presence of garnet-free granulitic lower crustal xenoliths, indicate a relatively thin crust (Stern & Kilian 1996).

The essential mineralogy of all the AVZ andesites and dacites involves pyroxenes, amphibole and plagioclase (Stern 1984; Kilian *et al.* 1991; Stern & Kilian 1996). Both a greater proportion of crustal xenoliths and larger, more complexly zoned phenocrysts are observed from south to north, suggesting increasing importance of near-surface magma chamber processes such as slow cooling and crystallization, magma mixing, wall-rock assimilation, and volatile degassing.

In comparison with typical orogenic andesites and dacites, the AVZ eruptive rocks have high Al, low Ti and relatively high [Mg#]. They also show adakitic chemical features (Stern & Kilian 1996), with $\text{SiO}_2 > 56 \text{ wt}\%$, $\text{Al}_2\text{O}_3 > 15 \text{ wt}\%$, low HREE ($\text{Yb} < 1.9 \text{ ppm}$) and $\text{Y} < 18 \text{ ppm}$, high $\text{Sr} > 400 \text{ ppm}$ and $\text{Sr}/\text{Y} > 40$, and positive Sr and Eu anomalies. These characteristics have been interpreted to reflect the presence of residual garnet, amphibole and pyroxene, but with little or no olivine and plagioclase, in the source region.

AVZ andesites and dacites also have low concentrations of HFSE, which is a common feature of both adakites and typical convergent plate boundary magmas. However, other chemical characteristics, such as LREE content, LREE/HREE, LILE/

LREE, LREE/HFSE and isotopic composition, which may reflect source composition rather than source mineralogy, vary significantly between, but not within, individual centres (Stern & Kilian 1996).

Geothermal models indicate that partial melting of the subducted oceanic crust is probable below the AVZ due to the slow subduction rate (2–3 cm/year) and the young age ($< 24 \text{ Ma}$) of the subducted oceanic lithosphere. The source of AVZ adakites is thus likely to be subducted oceanic basalt, recrystallized to garnet-amphibolite or eclogite (Stern 1984; Ramos & Kay 1992; Stern & Kilian 1996; Kilian & López-Escobar 2000). To explain the origin and evolution of these adakitic andesites and dacites, Stern & Kilian (1996) propose a multi-stage, four-component (MORB, subducted sediment, mantle wedge and crust) model in which the proportions of the different source materials involved in the genesis of AVZ magmas vary significantly from south to north. Thus, andesites from Cook Island volcano, where subduction is more oblique, have MORB-like isotopic and trace-element ratios. These can be modelled by small degrees (2–4%) of partial melting of eclogitic MORB, yielding a tonalitic primary magma, followed by limited interaction of this magma with the overlying mantle (*c.* 90% MORB melt, *c.* 10% mantle), and very little (*c.* 1%) or no participation of either subducted sediments or continental crust. In contrast, models for the magmatic evolution of AVZ andesites and dacites located between 49°S and 52°S require melting of a mixture of MORB (35–90% MORB-derived mass) and subducted sediment (*c.* 4% sediment-derived mass), followed by interaction of this primary melt with the overlying mantle (10–50% mass contribution) and the continental crust (0–30% mass contribution). AFC processes and the mass contribution from the continental crust become more significant northwards in the AVZ as the angle of convergence becomes more orthogonal.

Concluding remarks on recent magmatism

The main sources that are involved in the geochemical characteristics of the Andean Pleistocene to Holocene volcanism are as follows. (1) The subducted oceanic crust which in the CVA and SVZ provides aqueous fluid solutions, enriched in alkaline and alkaline-earth elements, that contaminate the mantle wedge. In the AVZ, melts from the Antarctic plate seem to be the main source of magmas. (2) The asthenospheric part of the mantle wedge is the main source of magmas in the CVZ as well as in the SVZ. (3) The lithospheric part of the mantle wedge has been proposed as a source of contaminants of magmas coming from below. (4) The lower crust, especially in those places where crust is thick, seems to play an important role in modifying the geochemical characteristics of mantle-generated magmas. (5) The upper crust is an important source of meteoric water and is a place where important geochemical processes take place. Many different processes have been proposed to explain the geochemical characteristics of Andean magmas: dehydration of the subducted slab (CVZ and SVZ), melting of the subducted slab (AVZ), fractional melting of the asthenosphere, contamination at mantle lithosphere and lower crust, magma mixing at crustal level, assimilation of crustal material, fractional crystallization at low and high pressures, differentiation along the conduits, and various combinations of the above. These processes, their eruptive products, and the hazards associated with specific volcanic centres, are examined further in Chapter 5.

Most of the results presented here have been obtained thanks to the following research projects: Fondecyt projects 1990980, 1031000, 1000125, 1990050 and 8000006; CNRS-Conicyt projects 1999, 2000 and 2001, ECOS-Conicyt project C01U01. This paper benefited from constructive comments from S. Kay and N. Petford.